

**Master Thesis in Geosciences**

# **Development of a 1D-2D coupled hydrodynamic model for the Øyeren Delta in southern Norway.**

**Nils Charles PRIEUR**



**UNIVERSITY OF OSLO**

**FACULTY OF MATHEMATICS AND NATURAL SCIENCES**



# **Development of a 1D-2D coupled hydrodynamic model for the Øyeren Delta in southern Norway.**

**Nils Charles PRIEUR**



Department of Geosciences

Discipline: Hydrology

University of Oslo

Blindern, Norway

01.06.2011

© Nils Charles PRIEUR, 2011

Tutor(s): **Lena Tallaksen (UiO) – Peter Borsány (NVE)**

This work is published digitally through DUO – Digitale Utgivelser ved UiO

<http://www.duo.uio.no>

It is also catalogued in BIBSYS (<http://www.bibsys.no/english>)

The picture in the front page is an aerial photo of the Øyeren delta by Gjerde<sup>1</sup> (2006).

All rights reserved. No part of this publication may be reproduced or transmitted, in any form or by any means, without permission.

---

<sup>1</sup> <http://www.naturfotograf.info>

# Abstract

In this study a coupled 1D-2D hydrodynamic model, MIKE FLOOD was used to simulate flood inundation extent, water levels and water velocities in the delta region of Lake Øyeren in southern Norway. The objective was to evaluate the improvement gained using a more complex framework. In addition, the credibility of existing flood zone maps made for Lillestrøm by Norges Vassdrag- og Energidirektorat (NVE) in 2005 was assessed. They were based on the assumption that the water levels predicted for Fetsund were applicable for the construction of flood zone maps at Lillestrøm. The model was set up and calibrated from historical hydrometric data as well as newly measured data. A methodology to correctly integrate the data required for flood inundation modeling was put forward. In addition, an assessment of the model sensitivity to various factors such as interpolation method, mesh resolution and model parameters was performed. The model performance seems to be greatly influenced by the quality of the digital elevation model (DEM), and hence also influenced by methods used to interpolate bathymetry, and mesh resolution. According to the results from the model, the assumption behind flood zone maps was determined to be conservative, overestimating water levels at Lillestrøm. The simulations also show a model capable of representing the hydraulic conditions of the delta, and demonstrate that the use of advanced numerical methods is now feasible, being an efficient way to obtain flood information.

**Keywords** MIKE FLOOD●Delta●Flood Management●Numerical methods●Model responses

# Acknowledgments/Remerciements

This work was made possible by the collaboration of NVE (Norges vassdrags og energidirektorat) and UiO (University of Oslo). I would like to thank my supervisors Lena Tallaksen and Peter Borsány for their input, ideas, feedback, support and mentorships throughout the course of this study.

In addition, I would like to thank Statkraft for giving me the opportunity to have a job related to hydrology this past year, where I have learned a lot.

I would also like to thank MIKE by DHI (Danish hydraulic Institute), which provided me with a free student license for MIKE 11, MIKE 21 and MIKE FLOOD packages for a period of one year.

I would like to say that I appreciate the infinite support and love from my parents Dominique and Bente Prieur, my brother Johan Prieur and Siri Birkeland that have helped me to advance every day through this study.

Finally, I will now write some words to my friends in French.

Je voudrais remercier tous mes amis qui ont participé à la relecture du mémoire et saluer tous les amis du basket à Oslo et à La Ciotat. Finalement je voudrais terminer cette belle aventure d'un an par les paroles d'un groupe de musique français, originaire du sud de la France :

J'aurais pu vivre au Pôle Nord, du côté d'Aix ou d'Avignon,

J'aurais pu vivre au Pôle Sud, habiter Bandol ou Toulon,

J'aurais pu vivre en Alaska, à Katmandou, à Bornéo,

Oui, mais j'habite à La Ciotat avec la mer et les bateaux

Moussu T

Que je sois en Norvège, en France ou à l'autre bout du monde, La Ciotat aura toujours une grande place dans mon cœur.

Nils, franco/norvégien et comme on le dirait dans le sud de la France: fier de l'être.

# Table of contents

Abstract .....	
Acknowledgments/Remerciements .....	
1. Introduction .....	1
1.1 Motivation and background .....	2
1.2 Thesis objectives .....	3
1.3 Outline .....	3
2. Study area .....	4
2.1 Climate and hydrology .....	5
2.2 Delta geomorphology .....	9
2.3 Vegetation .....	10
3. Data and Instrumentation .....	12
3.1 Data .....	12
3.1.1 Gauging stations .....	12
3.1.2 Collected data .....	13
3.1.3 GIS data .....	14
3.2 Instrumentation .....	15
3.2.1 ADCP .....	15
4. Flood extent modeling .....	17
4.1 Model theory .....	17
4.1.1 Saint Venant's equations .....	17
4.1.2 Hydraulic roughness .....	19
4.2 Review of floodplain modeling methods .....	20
4.3 Modeling methodology .....	22
4.3.1 MIKE 11 .....	22
4.3.2 MIKE 21 .....	23
4.3.3 MIKE FLOOD .....	24
5. Methodology .....	28
5.1 Input parameters .....	28
5.1.1 Topography .....	28
5.1.2 Resistance .....	30

5.1.3	Mesh resolution.....	31
5.1.4	Boundary conditions .....	36
5.1.5	Eddy viscosity .....	36
5.2	Calibration methodology.....	36
5.3	Statistical tools .....	37
5.4	Model setup .....	38
5.4.1	Computer properties.....	38
5.4.2	MIKE FLOOD .....	38
5.5	Creation of scenarios inputs .....	39
5.5.1	Scenarios description .....	39
6.	Results.....	41
6.1	Interpolation methods.....	41
6.2	Verification.....	42
6.3	Model responses .....	45
6.4	Scenario simulations .....	49
6.5	Uncertainties.....	61
6.5.1	Uncertainties in flood management .....	61
6.5.2	Uncertainty results .....	61
7.	Discussion .....	67
7.1	Interpolation methods.....	67
7.2	Verification.....	68
7.3	Model responses .....	68
7.3.1	Mesh resolution.....	69
7.3.2	Hydraulic roughness .....	69
7.3.3	Eddy viscosity and dX .....	70
7.4	Scenario simulations .....	70
7.4.1	Flood extent .....	70
7.4.2	Water level .....	70
7.4.3	Velocity .....	71
7.5	Summary of the scenario simulations .....	72
8.	Conclusion .....	73



9.	Notation.....	74
10.	References.....	75
11.	Appendix.....	80
11.1	Project.....	80
11.2	ADCP measurements.....	83
11.3	Flood zone map .....	84

## Table of Figures

Figure 1.	Location map of Øyeren delta, Norway; Source: Statkart.no (2011).....	4
Figure 2.	Simulated and Observed discharge series from 1995 to 2000, with "Nittelva+Leira" and Rånåsfoss respectively; Source: NVE (2011). .....	7
Figure 3.	Water level series for 1999 and 2000, at Fetsund's Bridge (blue), Øyeren 2 (green) and Mørkfoss (red); Source: NVE (2011). .....	8
Figure 4.	Sketch of a delta; Source : earthscience.org (2011). .....	9
Figure 5.	Vegetation and bank erosion process along the main river channel at Øyeren delta; Source: NVE (2011). .....	11
Figure 6.	Photos of the instrumentations used during the fieldwork conducted in July 2010. (a) GPS device; (b) The acoustic device was mounted at the front of the boat; (c) Bluetooth connection to the computer allowed real time measurements; (d) The speed of the boat was limited to avoid waves interaction; Source: NVE (2011). .....	14
Figure 7.	The acoustic doppler current profilers, Rio Grande; Source: ADCP.com (2011).....	16
Figure 8.	MIKE 11 set-up from Bingsfoss to Fetsund's bridge, cross sections are marked with white rectangles and red lines; Source: Statkart.no (2011) (background photo).....	22
Figure 9.	MIKE 21 set-up of the delta, the mesh is composed of elements corresponding to the topography of the area. ....	23
Figure 10.	Sketch representing the application of a standard link; Source: DHI (2011c). .....	24
Figure 11.	Sketch representing the application of lateral links; Source: DHI (2011c). .....	25
Figure 12.	Chart presenting the methodology followed during this study. ....	29
Figure 13.	The lowest mesh resolution, MESH 1. ....	32
Figure 14.	The default mesh resolution, MESH 2. ....	33
Figure 15.	The highest mesh resolution with triangular elements, MESH 3. ....	34
Figure 16.	The highest mesh resolution with triangular and rectangular elements, MESH 4. ....	35
Figure 17.	Difference in meters of the bathymetry created in this study minus the test bathymetry, Øyeren delta; Source: Statkart.no (2011) (background map).....	43
Figure 18.	Calibrated data for the MIKE FLOOD model compared with runoff data from Nordhagan; Source: NVE (2011). .....	44

Figure 19. Model's responses to change in Manning's n values are quantified with the help of the RMSE statistical tool. ....	47
Figure 20. Model's responses to change in mesh resolution are quantified with the help of the RMSE statistical tool. ....	47
Figure 21. Model's responses to change in Smagorinsky parameter values are quantified with the help of the RMSE statistical tool. ....	48
Figure 22. Model's responses to change in dX values are quantified with the help of the RMSE statistical tool. ....	48
Figure 23. Observation points in the Øyeren area where simulated water levels were looked at; Source: Statkart.no (2011) (background map). ....	49
Figure 24. Water level comparison at the observation points in the model area (Scenario 1,3,5 and 7). ....	52
Figure 25. Water level comparison at the observation points in the model area (Scenario 2,4,6 and 8). ....	52
Figure 26. Simulated current speed (m/s) at Øyeren delta for scenario 1; Source: Statkart.no (2011) (background map). ....	53
Figure 27. Simulated current speed (m/s) at Øyeren delta for scenario 2; Source: Statkart.no (2011) (background map). ....	54
Figure 28. Simulated current speed (m/s) at Øyeren delta for scenario 3; Source: Statkart.no (2011) (background map). ....	55
Figure 29. Simulated current speed (m/s) at Øyeren delta for scenario 4; Source: Statkart.no (2011) (background map). ....	56
Figure 30. Simulated current speed (m/s) at Øyeren delta for scenario 5; Source: Statkart.no (2011) (background map). ....	57
Figure 31. Simulated current speed (m/s) at Øyeren delta for scenario 6; Source: Statkart.no (2011) (background map). ....	58
Figure 32. Simulated current speed (m/s) at Øyeren delta for scenario 7; Source: Statkart.no (2011) (background map). ....	59
Figure 33. Simulated current speed (m/s) at Øyeren delta for scenario 8; Source: Statkart.no (2011) (background map). ....	60
Figure 34. Location of the two different interpolated areas, areas with good and poor density sampling are enlarged respectively in Figure 35 and Figure 36; Source: Statkart.no (2011) (background map). ....	63
Figure 35. Interpolation of the bathymetry with Natural Neighbor, Topo to Raster, IDW, and Spline with barriers interpolation methods in an area with good sampling density. ....	64
Figure 36. Interpolation of the bathymetry with Natural neighbor, Topo to Raster, IDW, and Spline with barriers interpolation methods in an area with poor density sampling. ....	65
Figure 37. Representation of the delta with a coarse mesh composed of elements describing the topography of the delta. ....	66

Figure 38. Overview of collected ADCP measurements during the fieldwork conducted by NVE in 2010; Source: Statkart.no (background map). .....	83
Figure 39. Flood zone map at Fetsund, the gray color corresponds to the 200-year return period inundated area. ....	85
Figure 40. Flood zone map at Øyeren delta, the gray color corresponds to the 200-year return period inundated area. ....	86
Figure 41. Flood zone map at Lillestrøm, the gray color corresponds to the 200-year return period inundated area. ....	87
Figure 42. Flood zone map at the northern part of Svellet, the gray color corresponds to the 200-year return period inundated area. ....	88
Figure 43. Flood zone map at the meeting point of Leira and Nittelva, the gray color corresponds to the 200-year return period inundated area. ....	89

Table 1. Seasonal monthly average discharge and water level above the sea level for a period from 1990 to 2000; Source: NVE (2011). ....	6
Table 2. Average monthly temperature (in °C) at Lillestrøm (1961-1990); Source: eklima.no (2011). ....	6
Table 3. Summary descriptions of gauging stations used in this study. ....	13
Table 4. List of GIS database prepared and used in this study. ....	15
Table 5. Manning's n values estimated at the start of the study with the help of Manning's table (Chow 1959). ....	30
Table 6. Description of various mesh resolution. ....	36
Table 7. List of various scenarios used in MIKE FLOOD model. ....	40
Table 8. Discharge and water level values corresponding to $Q_M$ , $Q_H$ , $H_M$ and $H_{200}$ at the three boundaries of MIKE FLOOD model. ....	40
Table 9. Optimum values for parameters and statistical analysis of different interpolation methods (N= number of closed points selected to interpolation, p= exponential power, S= smoothing parameter). ....	41
Table 10. Average observed and simulated water level at Nordhagan gauging station, during the verification of the model. ....	42
Table 11. Model responses, with observation of the average observed and simulated water levels, the root mean square error and the Nash-Sutcliffe efficiency coefficient. Bolded values correspond to optimized values. ....	46
Table 12. Summary of results from scenario simulations with: the type of velocities and the difference of water levels at Fetsund and Lillestrøm. ....	51

# 1. Introduction

The Glomma River and the Øyeren delta have unfortunately a rich flood history. Flood observations started as early as in the 18<sup>th</sup> century, due to the high and severe impacts on human welfare. Flood stones were erected in different places in Norway, along the main rivers, and also along the Glomma River. In the last century, two major floods with important return period, occurred in 1967 and 1995. These floods caused considerable damage on vegetation and wild life, and made important modifications in the Øyeren delta. But they also drew attention to the need of predicting flood inundation in floodplains caused by floods of different magnitudes.

Floods are one of the most severe natural disasters in Norway. They frequently occur in spring and autumn, and result in damage to property, crops and other negative impacts on human society. It is of great value in the planning process at a regional and local scale, to be able to predict, prevent and remedy the effects of flooding in an efficient way (Yang et al. 2002). Recent years have witnessed a growing concern over the frequency and extent of overbank flood events and their relationship to climate change, hydraulic engineering and floodplain land use (Nicholas and Mitchell 2003). The understanding of the processes behind floods is required to provide a good and efficient way to protect areas at risk.

Different types of methods can be adopted to avoid severe damages, such as structural and non-structural measures (Patro et al. 2009). Structural measures (embankments, levees, spurs) have proved to be helpful at a short time scale. Nevertheless, non-structural measures may be more efficient at a longer timescale. The use of flood maps, to map and predict the possible hazards of flood inundation in an area, is now common and widely used to avoid and limit risk due to flood inundation. However, modeling of flood extent is difficult due to the complexity of hydraulic processes during flood events. The use of numerical methods is required to simulate processes correctly. The application of simple numerical methods can over-simplify complex processes happening during flood events, especially turbulent exchange between the channel and floodplains. Recently, progresses in computational resources, data collection and development of several numerical codes have enhanced the use of hydrodynamic modeling approaches to simulate the flood extent in the floodplains (Werner 2004, Bates et al. 2005, Patro et al. 2009).

## 1.1 Motivation and background

Norges Vassdrag- og Energidirektorat (NVE) developed in 2005 a one-dimensional unsteady hydraulic model (1D). The 1D model simulates water levels and discharges over several cross sections in the area of Fetsund (see Figure 1). However, it is known that water levels at Fetsund are controlled by the Øyeren Lake, which was not incorporated into this model. Development and creation of flood level maps at Fetsund therefore resulted in a somewhat simplified model with a reduced length reach. Lillestrøm is situated at the north-west of Fetsund, at an approximate distance of 10 km. Creation of flood level maps at Lillestrøm were also realized in 2005, but due to the limited amount of data on flood measurements, it was assumed that the water levels predicted for Fetsund were applicable for the construction of flood zone maps at Lillestrøm. Therefore, these flood level maps were created on a questionable assumption.

In order to account for the influence of the Lake Øyeren, NVE continued to develop the model in 2010, extending the model from Bingsfoss to Mørkfoss (Figure 1). Even if a new version was developed, it was only a simplified representation of the delta. In an attempt to reproduce correctly the hydraulic processes within the delta, the use of a more advanced numerical method was considered. The main objective of this study was therefore to develop a 1D-2D coupled hydrodynamic model, using the one-dimensional model created by NVE in 2010, to simulate hydraulic processes between Bingsfoss and Fetsund. The area downstream of Fetsund, and the Øyeren delta was simulated with the help of a two-dimensional hydraulic model. Both models were connected together, forming a 1D-2D coupled hydrodynamic model. Simulation of hydraulic processes in the delta with the help of a more complex dimensional modeling code will here be assessed to test the validity of the simplifications and the assumption behind flood zone maps created in 2005.

This study is part of a larger research and development project conducted by NVE with the collaboration of the University of Oslo (UiO). The main project aims to introduce more advanced flood inundation modeling techniques, in order to use new high-resolution bathymetry data, collected in Norway. As a part of this project, the introduction of a methodology to correctly integrate data required for flood inundation modeling will be performed in this study. A development of a one to two-dimensional coupled unsteady hydraulic model (MIKE FLOOD) for the area of Øyeren delta will give us an idea of the application of this method in the future.

## 1.2 Thesis objectives

The main objective of this thesis is the development of a 1D-2D coupled hydrodynamic model for the Øyeren delta in order to improve the quality of flood inundation map and elucidate the performance and the potential limits to it.

Special focuses are:

- Calibration of the hydraulic model from limited available data and quality analysis of results.
- Estimation and mapping of flooding areas for different type of scenarios and return periods (e.g. simultaneous extreme events for Glomma, Leira and Nittelva).
- Evaluate the uncertainty in the estimation by a model sensitivity analysis.
- Assessment of the validity of the assumption behind flood zone maps at Lillestrøm.

Eight different flood management scenarios will be created with discharge and water levels corresponding to 200-year and median return period flood. Observation of the hydrological processes between the delta and Lillestrøm for the different scenarios will provide information on the assumption made. In addition, the quality of the model results will be verified according to hydrometric data and earlier observations made in different studies.

## 1.3 Outline

**Section 2** starts with the description of the area of study, and related work concerning the Øyeren delta. **Section 3** gives an overview of existing and collected data for the study and a description of the instrumentation used for data collection. In **Section 4**, the modeling theory behind MIKE 11 and MIKE 21 are elaborated in order to help the reader. Then a review of different classes of numerical models used in floodplain modeling, and additional information on MIKE FLOOD is also provided. **Section 5** introduces the methodology used in this paper, presenting the different steps followed in the set up of the model. In **Section 6**, results from the estimation of the best methods to interpolate data collected from acoustic measurements are presented. Results from the verification of the model are then given, with the comparison of simulated and observed water levels for a period of two months. In addition the sensitivity of the results with respect to the model set-up is also evaluated, including the optimization of i) mesh resolution, ii) resistance, iii) eddy viscosity and iv) the distance between the discharge's and water level's calculation points in MIKE 11 set up (dX). Finally, results for scenario simulations and uncertainties are outlined. In **Section 7**, discussion about the results presented in Section 6 will be carried out. In **Section 8**, the conclusion for the study will be given. **Section 9** provides a description of variables and units used throughout this thesis. **Section 11** contains the appendix. Here it is possible to find the original objectives for this study, permitting the reader to have an overview of the starting points of this study. Finally, a map showing the location of measurements made in the delta, and flood zone maps of the study area, created in 2005 by NVE, are supplied.

## 2. Study area



Figure 1. Location map of Øyeren delta, Norway; Source: Statkart.no (2011)

The main focus will be the Øyeren delta, which is the largest freshwater delta in Northern Europe (Zinke et al. 2010). The Øyeren delta is situated in southern Norway and is a reservoir managed for hydropower use and flood regulation (Figure 1). The regulated Lake Øyeren reaches 87.4 km<sup>2</sup> and has a normal water level of 101 m above sea level (Eilertsen and Hansen 2008). In addition, the delta is a nature protected area with important wildlife presence (Zinke et al. 2010). Øyeren is part of the Glomma river system which is the largest river in the country with history of demolishing floods. (e.g. with the 1967 and 1995 floods). The delta is located at the meeting point of three rivers: Glomma, Leira and Nittelva. The main inflow in the delta is provided by the Glomma River (Figure 2), since its basin represents 97% of the delta's total catchment area of 40055 km<sup>2</sup> (Bogen and Bønsnes 2002). Nittelva and Leira contribute less to the total discharge of the delta, as their basins are much smaller than Glomma's (Figure 2). North-west of this area, Nittelva and Leira are flowing into the shallow lake Svellet which is considered as a pond with less importance during low and mean water level. But during flood events, Svellet may have an important role, and thus greatly influence water processes and water levels within the Øyeren delta.

## 2.1 Climate and hydrology

In general Øyeren has a humid continental climate, with cold winters and warm, often humid summers. Monthly averaged temperatures at Lillestrøm are ranging from 16.5°C in July, to -7.4°C in January (Table 1). The area has a mean annual precipitation and temperature of respectively 820 mm and 4.1 °C (MET.no<sup>2</sup>2011, see also Eilertsen and Hansen 2008). Due to low temperatures from October to April, precipitation falls mainly as snow. Snow accumulates during this period, forming a snowpack. Discharge and water levels at this period of the year, are often low due to snowfall storage (Table 2). When spring and warm temperatures come, the snowpack is slowly warmed up, until water contained in the snowpack is released as run-off. This run-off is called the snowmelt run-off. This snowmelt contributes considerably to the total run-off, with usually high observed discharges and water levels in May, June and July (Table 1). Precipitation is moderate throughout the year, with slightly higher precipitation in August and September. Flood events may also occur in autumn, but will only be generated by rainfall runoff. Floods observed in 1967 and 1995 are results of the combination of several factors such as i) high unusual snow storage, ii) rapid snowmelt and iii) important rain precipitation.

Even though the hydrological regime is affected by seasonal variation, water regulation minimizes differences between low and high water levels, variations being less pronounced than in natural water channels. The delta was affected by water level regulation as early as 1862. The need for control and a constant water level for navigation and timber transport were the main

---

<sup>2</sup> <http://www.met.no>



incentives (Bogen and Bønsnes 2002). During the twentieth century further regulations of the Glomma River and Lake Øyeren were realized at Bingsfoss, Rånåsfoss and Solbergfoss. Bingsfoss and Rånåsfoss are both located upstream the delta, along the Glomma River (Figure 1). Solbergfoss hydropower station is situated downstream of the Lake Øyeren. If the water levels between 1852 and 1862 are compared with present water levels, major changes can be reported. Water level fluctuated between 96 and 104 m a.s.l. between 1852 and 1862. Nowadays water levels are constrained between 99.5 and around 102 m a.s.l. (Figure 3). These modifications in water levels have an impact on the different sedimentation processes within the delta and have been source of several studies conducted by NVE (Bogen and Bønsnes 2002, Bogen et al. 2002).

*Table 1. Seasonal monthly average discharge and water level above the sea level for a period from 1990 to 2000; Source: NVE (2011).*

	Water level [m]			Discharge [m <sup>3</sup> /s]	
	Fetsund's bridge	Mørkfoss	Rånåsfoss	Nittelva+Leira	Solbergfoss
January	101.45	100.66	425.82	7.87	464.48
February	100.97	100.31	375.68	7.16	419.22
March	100.30	99.89	322.88	9.17	375.51
April	100.79	99.82	451.57	36.46	510.03
May	102.08	101.61	1159.89	40.80	1234.28
June	101.91	101.99	1178.55	13.22	1227.36
July	101.98	101.62	864.63	11.13	899.87
August	101.76	101.53	692.93	12.71	702.60
September	101.60	101.46	586.64	14.13	617.33
October	101.62	101.38	575.85	22.33	649.14
November	101.64	101.16	473.07	24.91	571.65
December	101.55	100.96	434.15	13.98	495.26

*Table 2 Average monthly temperature (in °C) at Lillestrøm (1961-1990); Source: eklima.no (2011).*

Jan.	Feb.	Mar.	Apr.	May	Jun.	Jul.	Aug.	Sept.	Oct.	Nov.	Dec.
-7.4	-7.0	-2.3	3.2	10.0	14.4	16.5	14.5	9.5	5.4	-1.1	-6.0

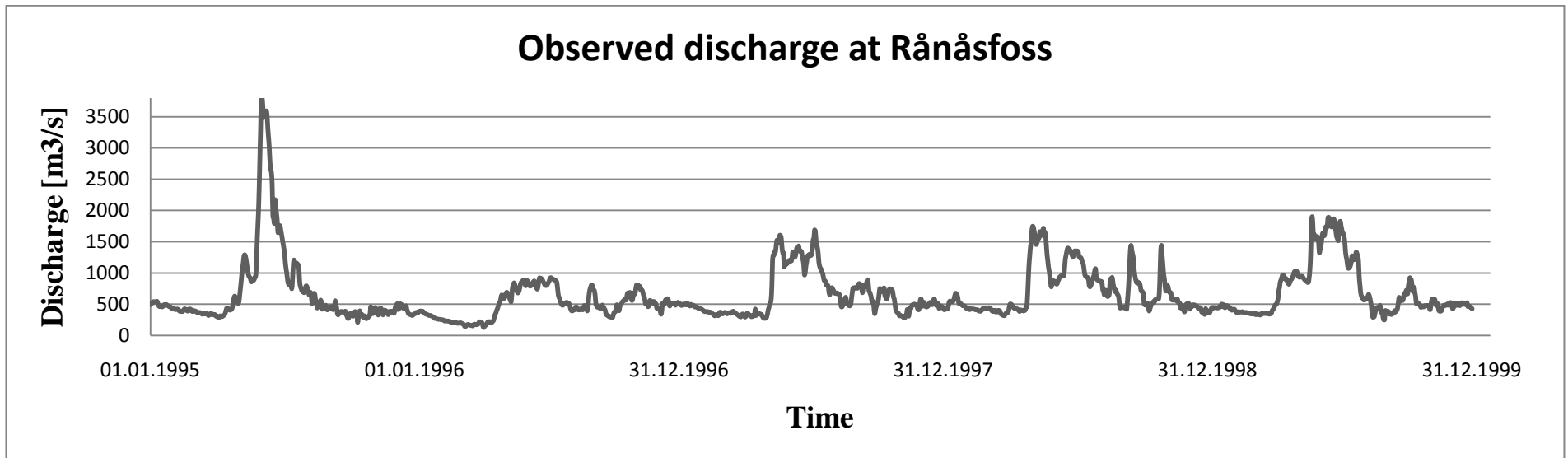
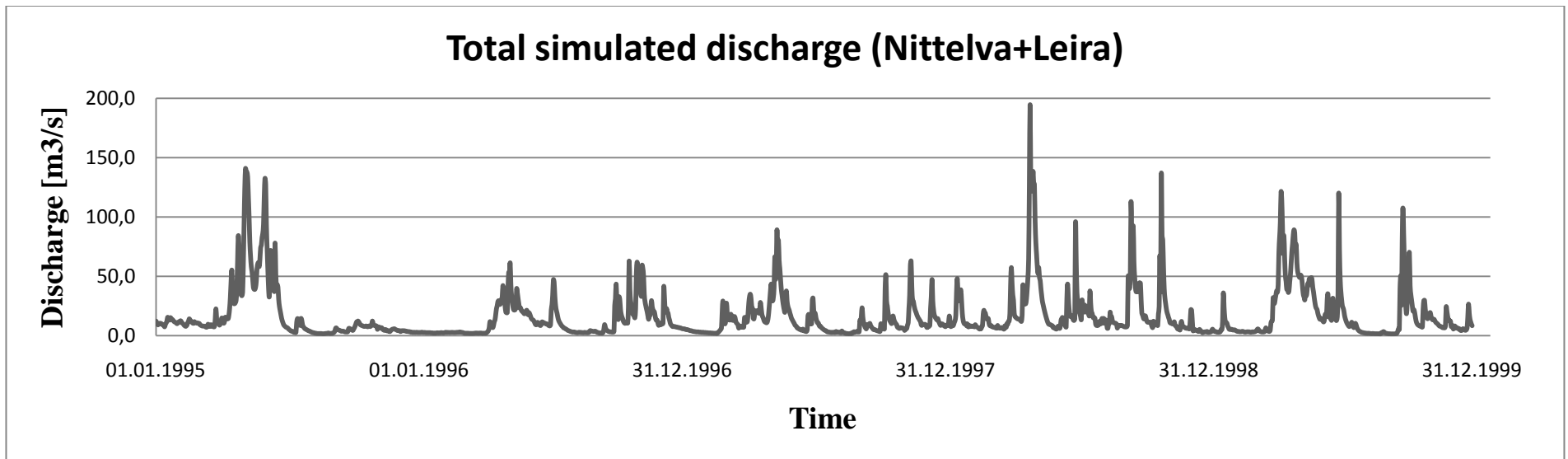


Figure 2. Simulated and Observed discharge series from 1995 to 2000, with "Nittelva+Leira" and Rånåsfoss respectively; Source: NVE (2011).

## Water levels

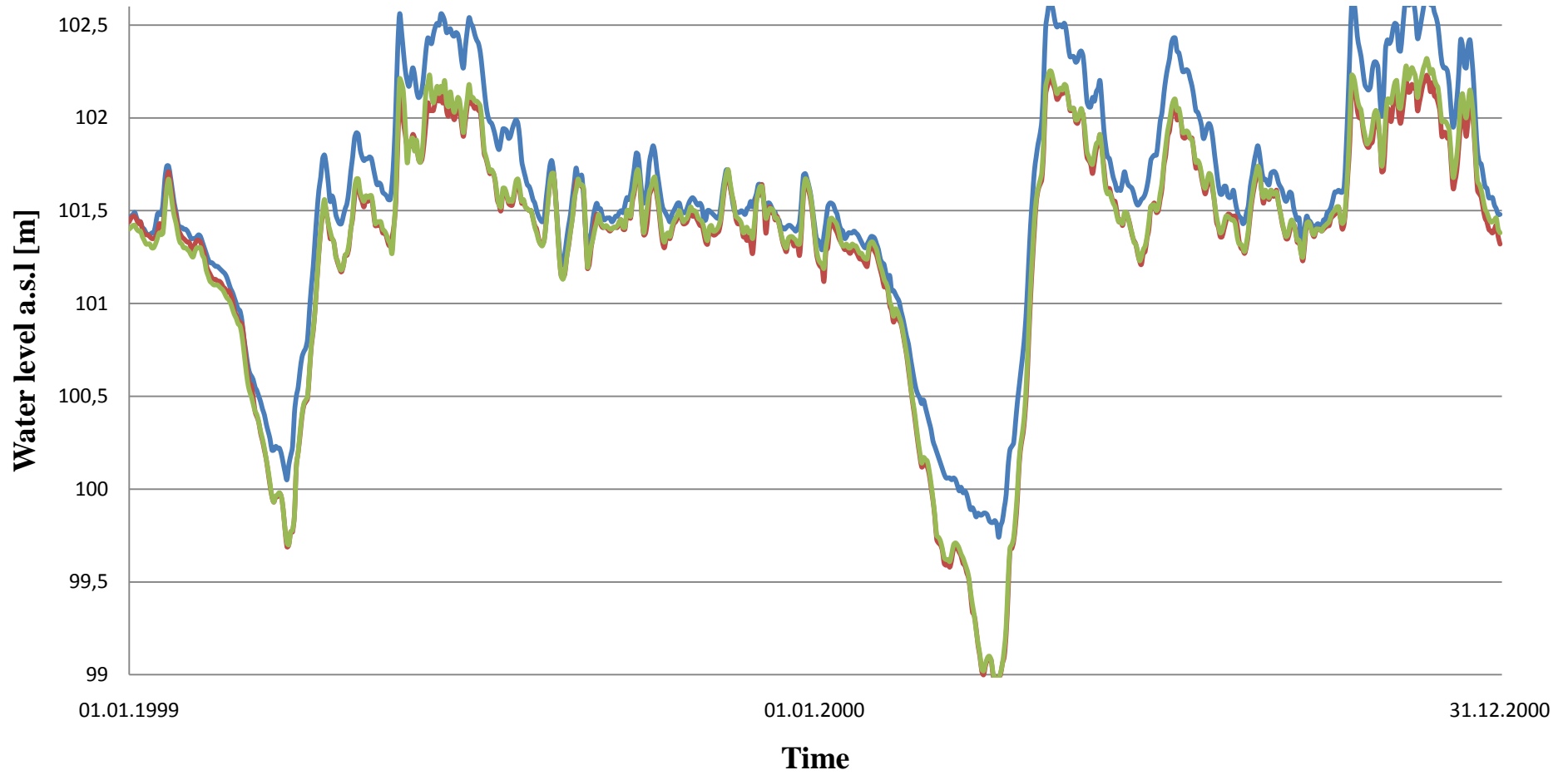


Figure 3. Water level series for 1999 and 2000, at Fetsund's Bridge (blue), Øyeren 2 (green) and Mørkfoss (red);  
Source: NVE (2011).

## 2.2 Delta geomorphology

Deltas are formed by the interaction between water river channels and a standing pond of water like an ocean, an estuary, a lake, a reservoir or another river and a flat area (Figure 4). This process is controlled by the hydraulic geometry of the river, a term introduced by Leopold and Maddock (1953). It refers to the ways in which changes in discharge are apportioned among changes in the component of discharge: width, mean depth and mean velocity (Dingman 1984). If the discharge is assumed to remain approximately constant, a major change in one component of discharge will lead to a decrease of the two other components. This means that since Glomma, Leira and Nittelva flow into the Øyeren Lake, they will be exposed to a sudden change in width, causing a decrease in the mean velocity of the flow. Sediments which until this point were confined within the river channels, will here flow into the lake and be deposited due to low water velocities. As bed load continues, the channel slope of the river decreases and causes two types of instabilities. First, water under gravity will tend to flow in the most direct course down the slope. Secondly, low channel slope causes a decrease in the shear stress of the bed, leading to smaller elevation differences between channel and floodplains. At the time of a flood event, these two instabilities may lead to breach in levees, creating distributary channels with more stable channel slope. After a certain time, deposition of sediments, erosion and creation of new distributary channels build the characteristics geographic pattern of a river delta, creating a multifaceted system of islands and lagoons with complex topography.

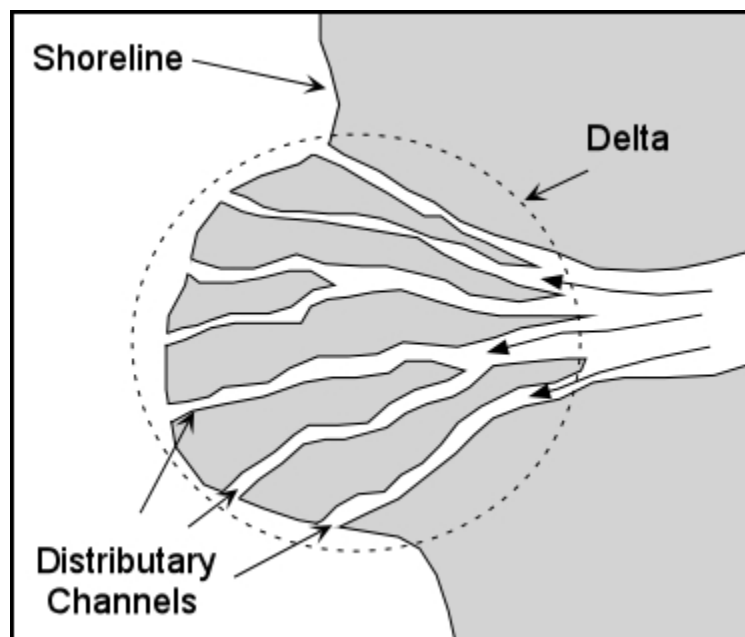


Figure 4. Sketch of a delta; Source : earthscience.org (2011).

The delta geomorphology is a system created by sediments delivered by Glomma, Leira and Nittelva. The delta's river channels are composed of medium sand grain and largest volume of sediments are supplied by the Glomma River. A mean yearly suspended load and bed load of 500 000 t.year<sup>-1</sup> and 75000-150000 t.year<sup>-1</sup> has been respectively observed in the period between 1995 and 1999. Leira and Nittelva contribute with a suspended load of respectively 90000 and 18000 t.year<sup>-1</sup> (Bogen and Bønsnes 2002). In their study, they also reported that successive regulation phases affected local sediment redistribution within the delta, decreasing over the years the downstream extent of the sedimentation zone. Therefore, sediments are mainly concentrated and deposited in the upper part of Øyeren delta, causing the extension of the delta plain and the number of lagoons, bays and backwater areas (Bogen and Bønsnes 2002). In addition investigations conducted by Eilertsen and Hansen (2008) reported a large range of bed forms with different scales in the delta. Modifications of the delta are mainly controlled by water level gradient and discharge and can have negative impacts on the vegetation and thus also affect the important wildlife activities in the delta.

## 2.3 Vegetation

The Øyeren delta has an exceptional biodiversity with more than 50 species of water plants, submerged more than 50% of the time (Rørslett 2002). Vegetation on the islands is mainly composed of trees, crop and grasses (Figure 5). Over the last 30 years, studies have shown a growing concern about the influence of water regulation on the limnology within the delta. In these papers, the effects of high suspended sediments concentration and water levels are assessed. Both tended to prevent the photosynthesis process of the fresh water plants, threatening plant growth and viability (Rørslett 2002, Bogen and Bønsnes 2002). Concerning the fish habitat, increase in suspended load has been concluded to be harmful. The delta is hosting every year migration of birds that are attracted by the lagoon and particular parts of the delta. Flood management that limit flood extent during flood events and minimize damage to wildlife will be a challenge.



*Figure 5. Vegetation and bank erosion process along the main river channel at Øyeren delta; Source: NVE (2011).*

### 3. Data and Instrumentation

In order to operate MIKE 11, MIKE 21 and MIKE FLOOD, an important set of input data is required. In flood extent predictions, the quality of the input will account for the overall quality of the model. Recent techniques allow the use of high resolution DEM, airborne and synthetic aperture radar (SAR) imagery to improve quality and validation of flood extent models (e.g. in Horritt and Bates 2002, Nicholas and Mitchell 2003, Horritt et al. 2007, Patro et al. 2009, Tuteja and Shaikh 2009). In addition, requirements of input parameters as water levels, hydrographs, Manning's  $n$  and calibration points are needed for the set up of the models. A full description of the various types of data and the instruments used to collect the bathymetry points will now be presented.

#### 3.1 Data

##### 3.1.1 Gauging stations

Today, three gauging stations operate at Øyeren:

- Rånåsfoss
- Mørkfoss
- Øyeren 2

Two gauging stations are no longer in operation:

- Fetsund's bridge
- Nordhagan

Mørkfoss and Øyeren are situated respectively 30 and 15 km downstream the delta. Due to the small channel slope between the lower part of the delta and Mørkfoss, water levels between Øyeren 2 and Mørkfoss only drops 3-4 cm, which makes both of them good candidates for the lower boundary of the model (Figure 3). Nordhagan was used in this study as calibration point, being the only gauging station situated within the Øyeren delta. In addition, the gauging station at Lillestrøm was not used due to the short record and a poor quality of the data. Therefore, the boundary conditions for Nittelva and Leira were simulated by NVE, by observing the inflow and the outflow of Lake Øyeren between the periods of 1982 to 2005. A summary of stations used in this study are listed below (Table 3).

*Table 3. Summary descriptions of gauging stations used in this study.*

Gauging station	Resolution	Period	Type	Unit	Quality
Rånåsfoss	Daily	1970-2009	Discharge	m <sup>3</sup> /s	Correct
Fetsund bridge	Daily	1989-2009	Water level	m	Correct
Øyeren, Mørkfoss	Daily	1881-2009	Water level	m	Good
Øyeren, Nordhagan	Daily	1995-2000	Water level	m	Missing years, irregular
Øyeren II	Daily	1998-2008	Water level	m	Correct

### 3.1.2 Collected data

As described earlier, the delta's topography is constantly under modification due to erosion, transport and deposition of sediments. Quality of the bathymetry and topography is the most important factors of the overall quality of the model. Therefore, more recent data collection was required for this study. Field data were collected prior to the start of the master thesis by NVE during a four-day fieldtrip in July 2010. The objective of this fieldwork was to obtain a detailed and up-to-date description of the bathymetry of the studied area. A good instrumentation choice, which can give information about flow behavior and flow description was looked after, to fully understand the exchange between the delta and Svellet.

An Acoustic Doppler Current Profilers (ADCP, see subsection 3.2.1) was attached to the front part of the boat (Figure 6). Above the acoustic device, a metal stick with a known height was placed with a GPS receptor. Absolute elevation (a.s.l.) and surface elevation were possible to determine by subtracting the metal stick elevation. Around 50 000 elevation points were collected during this fieldwork. In addition, few GPS points were measured on several islands within the delta. A DEM (Digital Elevation Model) was used for modeling the topography and the bathymetry of the delta. Interpolation and extrapolation were created with the help of tools in ArcGIS 9.3 software.





*Figure 6. Photos of the instrumentations used during the fieldwork conducted in July 2010. (a) GPS device; (b) The acoustic device was mounted at the front of the boat; (c) Bluetooth connection to the computer allowed real time measurements; (d) The speed of the boat was limited to avoid waves interaction; Source: NVE (2011).*

### **3.1.3 GIS data**

The different types of geographic information system (GIS) data used in this study are presented below (Table 4). Data were processed with the help of the software ArcGIS 9.3. ArcGIS is a powerful program that provides a variety of enhancements in cartography modeling and analysis,

3D visualization, and developer tools to enable high quality map production (ESRI<sup>3</sup> 2011). In this study, both the 3D analyst and spatial analyst tools have been used for extrapolating and interpolating different types of information as the topography, bathymetry and Manning's n map. More information concerning the different interpolation methods used in this paper will be presented later on.

*Table 4. List of GIS database prepared and used in this study.*

Data Type	Description	Usage
Contour	Contour layer at 10 m interval	DEM creation
Contour	Contour layer at 10 cm interval	DEM creation (on islands)
Manual points	Island points	DEM creation (on islands)
GPS points	Island points	DEM creation (on islands)
Elevation points	ADCP measurements	DEM creation (bathymetry)
Manual points	Lagoon points	DEM creation (bathymetry)
Polygons	Vegetation	DEM creation (resistance)
Channel	Major river channels	Visualization
Satellite photos	Photos of the area	Visualization
Geographical map	Map of the area	Visualization

## 3.2 Instrumentation

### 3.2.1 ADCP

The United States Geological Survey describes the operating characteristics of the ADCP as follow: Acoustic Doppler Current Profilers (ADCP) is a sonar that is used in various types of field research as in hydrology, meteorology and oceanography. It transmits sound into the water and receives reflected echoes from particles suspended in the water. The frequency shift between the transmitted sound and echoes is used to compute the velocities of the particles and the water in which they are suspended. ADCP's has unique features that allow them to be deployed on moving boats. It tracks the river bottom by measuring boat speed and direction and, is therefore able to compensate for the boat movement in computation of water velocities. The ADCP beam number and geometry are designed for the measurement of three-dimensional velocity profiles (USGS<sup>4</sup> 2007).

<sup>3</sup> <http://www.esri.com>

<sup>4</sup> <http://in.water.usgs.gov/hydroacoustics/ADCPuses.shtml>

ADCP measures a wide range of parameters such as: i) water current velocities, ii) water current discharge, iii) water depths and iv) the distribution of suspended sediments. The acoustic device used in this study is the Rio Grande <sup>5</sup>ADCP, produced by Teledyne RD Instruments <sup>6</sup>(Figure 7).



*Figure 7. The acoustic doppler current profilers, Rio Grande; Source: ADCP.com (2011).*

---

<sup>5</sup> [http://www.rdinstruments.com/datasheets/rio\\_grande\\_ds\\_lr.pdf](http://www.rdinstruments.com/datasheets/rio_grande_ds_lr.pdf)

<sup>6</sup> <http://www.ADCP.com>

## 4. Flood extent modeling

In the following a description of the theory back MIKE 11 (1D) and MIKE 21 (2D) are elaborated. Both models use the full equation of Saint Venant, in one and two-dimensional form. First, equations originally used to derivate Saint Venant's equation will be presented, and then a definition of the resistance of the flow will be given. Subsequently, a review of different techniques used in flood inundation modeling will be provided. Finally, relevant information concerning the MIKE FLOOD package will be supplied. Notations about units and parameters in different equations are given at p74.

### 4.1 Model theory

#### 4.1.1 Saint Venant's equations

Saint Venant equation is derived from conservation equations. As stated in Dingman (1984:39) "Conservation equations are fundamental statements of the fact that mass, energy and momentum cannot be created or destroyed in any process." The general conservation equation can therefore be written in the following way:

$$\frac{\Delta I}{\Delta t} - \frac{\Delta Q}{\Delta t} = \frac{\Delta S}{\Delta t} \quad (4.1)$$

The equation being equal to the average rate of inflow  $\frac{\Delta I}{\Delta t}$  during the period  $\Delta t$  minus the average rate of outflow  $\frac{\Delta Q}{\Delta t}$  during the same period  $\Delta t$  equals the rate of change in storage for that period.

The conservation equation (4.1) will be the starting point for conservation of mass, energy and momentum equations. A short presentation of the continuity equation and momentum equations are realized in this paper. For a full and detailed development of these equations, the reader is advised to refer to Dingmann (1984). Both continuity and conservation of momentum equations are based and derived upon the following four assumptions (Hammersmark 2003):

- The water is incompressible and homogeneous; therefore there is negligible variation in density.
- The bed slope is small, therefore the cosine of the slope angle can be assumed to equal 1.
- The water surface elevation wavelengths are large compared to the water depth, which ensures that the flow everywhere can be assumed to move in a direction parallel to the bottom.
- The flow is subcritical. Supercritical flow conditions are solved with a reduced momentum equation, which neglects the nonlinear terms.

### *Continuity equation*

After development, the continuity equation equals to:

$$q - \frac{\partial Q}{\partial x} = w \frac{\partial Y}{\partial t} \quad (4.2)$$

Thus we do have two equations with two independent variables  $x$  and  $t$  which represent respectively the distance and the time, two dependent variables,  $Q$  and  $h$  which are the discharge and the water level. A second equation with  $Q$  and  $h$  is needed in order to obtain solutions. Conservation of momentum equation is then developed to fulfill this requirement.

### *Momentum equation*

After development, the momentum equation equals to:

$$S_o - S_e = \frac{V}{g} \frac{\partial V}{\partial x} + \frac{\partial Y}{\partial x} + \frac{1}{g} \frac{\partial V}{\partial t} \quad (4.3)$$

Discharge can then be found with the use of Manning's equation:

$$Q = \frac{wY^{\frac{5}{3}}S_e^{\frac{1}{2}}}{n} \quad (4.4)$$

By replacing equation (4.4) into equation (4.3), we can find:

$$Q = \frac{wY^{\frac{5}{3}}}{n} \left( S_o - \frac{V}{g} \frac{\partial V}{\partial x} - \frac{\partial Y}{\partial x} - \frac{1}{g} \frac{\partial V}{\partial t} \right)^{\frac{1}{2}} \quad (4.5)$$

The two equations are then written in an algebraic form, as difference equations, for the use of numerical methods to solve equations, and thus obtain result (Dingman 1984).

The complete equations represent the full equations of Saint Venant, (4.2) and (4.5). Both models in this study are using the full complete dynamic equations. Nevertheless, the reader may be aware that possible simplifications of the equations of Saint Venant are possible and may be adequate in flood extent modeling, following water conditions and studies requirements (see Hunter et al. 2007). Two simplifications exist with the kinematic-wave models and the diffusion-analogy. The kinematic-wave is used in flow assumed to be uniform, velocity and depth are constant over the portion of the channel considered, therefore second, third and fourth terms in the bracket of equation (4.5) will be equal to 0. The diffusion-analogy approximation neglects the acceleration terms, third and fourth terms in the bracket of equation (4.5) will be not considered in this approximation of Saint Venant's equations.

### 4.1.2 Hydraulic roughness

In 1889, the Irish engineer Robert Manning presented a formula, which is now known as (Chow 1959):

$$V = \frac{1}{n} R^{\frac{2}{3}} S_e^{\frac{1}{2}} \quad (4.6)$$

This technique was developed to permit hydrologists and hydraulic engineers to estimate the velocity or the discharge when width, depth and slope were known (Dingman 1984). Manning's  $n$  represents the flow resistance, with the different types of factors contributing directly or indirectly to it. Difficulties lie into the determination of Manning's  $n$  roughness coefficient. In spite of the complexities associated with the concept of flow resistance, we can specify the factors that contribute to it within a reach of channel (Dingman 1984):

- Skin friction (grain size and shape of sediments)
- Form resistance (ripples, dunes and antidunes)
- Non-bed material obstruction (vegetation, man induced construction)
- Cross-section geometry
- Stage-discharge

It is possible to determine Manning's  $n$  by looking at these different factors, on photographs. But the chosen value of  $n$  will only be determined at a given cross section and at a given time. It is known however that roughness coefficient is often assumed by engineers to be constant through the reach studied (Chow 1959).

Constant advance in technology, especially in computational resources allows us now to calibrate and validate Manning's  $n$  value by adjusting his value, to match simulated with observed water levels. This procedure was before only possible concerning the resistance of the flow in the water channel, resistance on floodplains being still guessed from different influencing factors. But now satellite images give the possibility to calibrate and validate the resistance on floodplains, by comparing predicted inundated areas against observed ones.

In this study Manning's  $n$  will be used for the one-dimensional part and Manning's  $M$  for the two-dimensional part of the model. For a problem of easiness, only Manning's  $n$  will be referred to in this paper, relation between Manning's  $n$  and  $M$  being:

$$M = \frac{1}{n} \quad (4.7)$$

## 4.2 Review of floodplain modeling methods

It has been widely accepted between hydrologists that the most effective way to reduce future flood damages is to restrict development in areas that are subject to flooding (Dingman 1984). The process of identifying and mapping possible areas put at risk can be identified in three steps. In a first step, return periods are determined. Inflow and outflow hydrographs are then created for selected return periods. In a second step, water levels are determined through the use of numerical methods and numerical codes, and finally the computed elevations are used to create flood maps.

Derivation of flood maps can be realized with different types of approaches, ranging from extremely simple (1D, quasi-2D model) to complex two and three-dimensional modeling codes (Werner and Lambert 2007). Until recently, most applications considering flood extent modeling, used simple methods as the approximation or full treatment of Saint Venant Equations (e.g. with MIKE 11, HEC-RAS), the equations of continuity and momentum being solved with the help of numerical solution techniques (Tayefi et al. 2007). Flood maps are then simply derived from the projection of water levels on digital elevation models (DEMs). Even if these methods present some advantages as the computational efficiency and the ease of parameterization (Horritt and Bates 2001), and not necessarily perform less than the two-dimensional modeling methods (see Bates and De Roo 2000, Horritt and Bates 2002), it will only give a partial and limited representation of the complex processes between the channel and the floodplains (Menendez 2001, Petersen et al. 2002, Rungø and Olesen 2003, Tayefi et al. 2007).

Limitations of the one-dimensional unsteady hydraulic model need to be overcome. Use of two-dimensional modeling codes is likely to provide the best approach to flood extent modeling (e.g. with MIKE 21, TELEMAC-2D). These codes have the ability to represent complex floodplains topography, dynamic wetting and drying of the floodplain, and prediction of the exchange of momentum between channel and floodplains (Horrit et al. 2007). However, common problems regarding two-dimensional approach are data requirements and significant computational time. Due to these inconveniences, a new method was developed: coupled one and two-dimensional unsteady hydraulic model (e.g. with MIKE FLOOD). The possible use of cross sections within the channel and high-resolution digital elevation model to describe complex floodplains topography, has made this method an increasingly practical flood analysis tool (Tuteja and Shaikh 2009, Patro et al. 2009).

However, natural flows are known to be three-dimensional, use of 3D methods may appear obvious. Zinke et al. (2010) successfully used the SSIIM three-dimensional unsteady hydraulic model (Olsen 1994) to simulate the discharge distribution within the Øyeren delta. Nevertheless, simplification of the reality by the use of 2D methods may be adequate to describe flow processes, especially in study with incomplete data collection for model construction and

validation (Bates and De Roo 2000, Hunter et al. 2005a, Werner et al. 2005, see in Hunter et al. 2007). Ideally, the simplest method giving the best satisfactory results will be preferred. Criterion for model evaluation is how well the model will reproduce the flood extent when calibrated and validated (Horritt and Bates 2002).



## 4.3 Modeling methodology

### 4.3.1 MIKE 11

MIKE 11 is a hydrological model created by the Danish Hydraulic Institute (DHI) in 1987. The model consists of a network of cross sections that are linked by a one-dimensional channel (Figure 8). The model calculates the downstream gradient between the river's cross sections. The one-dimensional model is based on the cross-sectional average Saint-Venant equations (see 4.1.1). As mentioned earlier, MIKE 11 uses the full one dimensional Saint Venant equation. Results are obtained from a finite difference formulation of the equations, using a numerical code, which is based on alternating discharge and water level points (Abbott and Ionescu 1967, see also DHI 2011a).

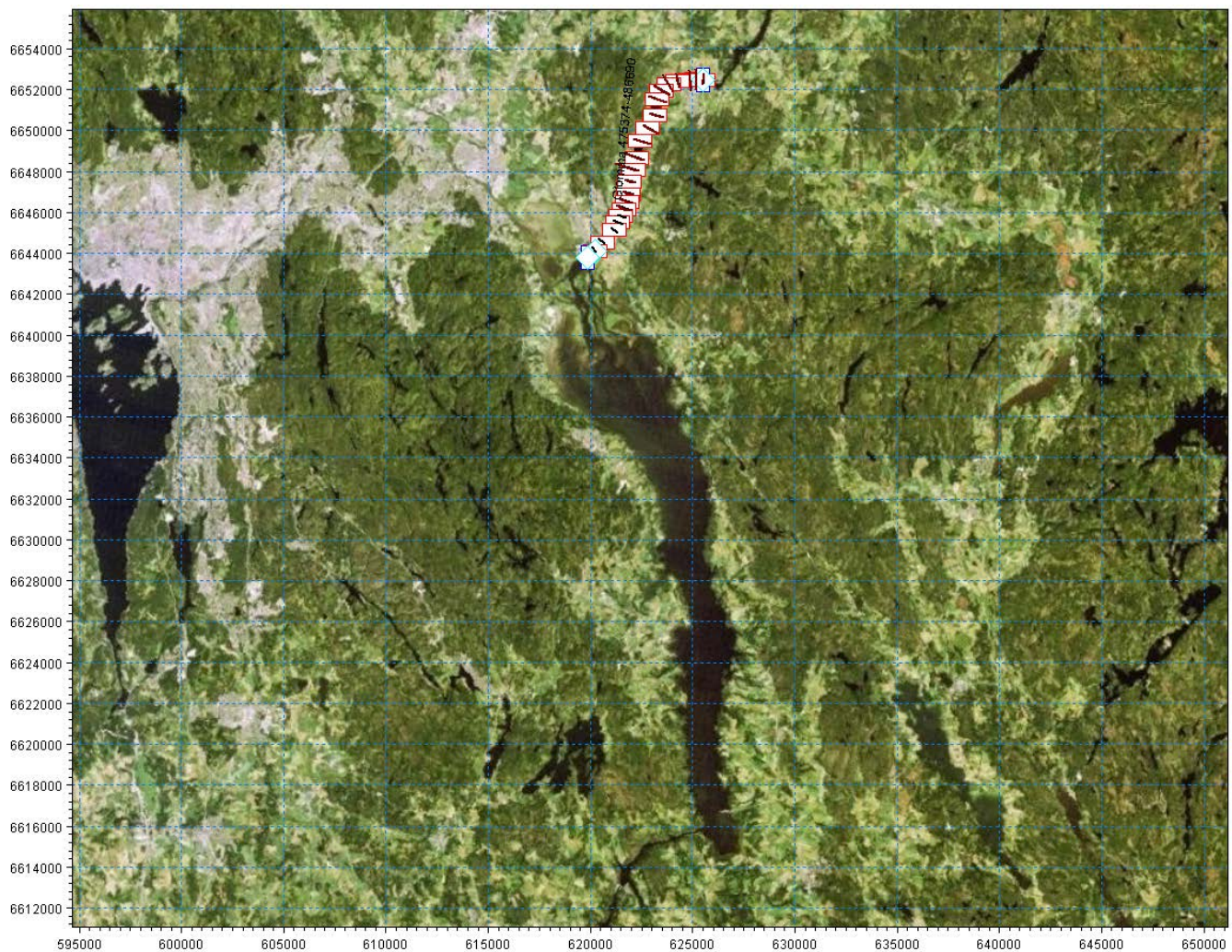


*Figure 8. MIKE 11 set-up from Bingsfoss to Fetsund's bridge, cross sections are marked with white rectangles and red lines; Source: Statkart.no (2011) (background photo)*

### 4.3.2 MIKE 21

The two dimensional model is based on the depth averaged Saint-Venant equations, describing the evolution of the water level and two velocity components (DHI 2011b). The two velocity components permit a detailed description of the flow velocity on complex floodplains. The two-dimensional model simulates the water depth and the velocities on a two-dimensional grid (Figure 9). The two-dimensional grid can be a normal rectangular grid or a mesh. A mesh is a grid composed of triangular or/and rectangular elements, where spatial resolution can be modified in different areas following the requirements and the nature of the study.

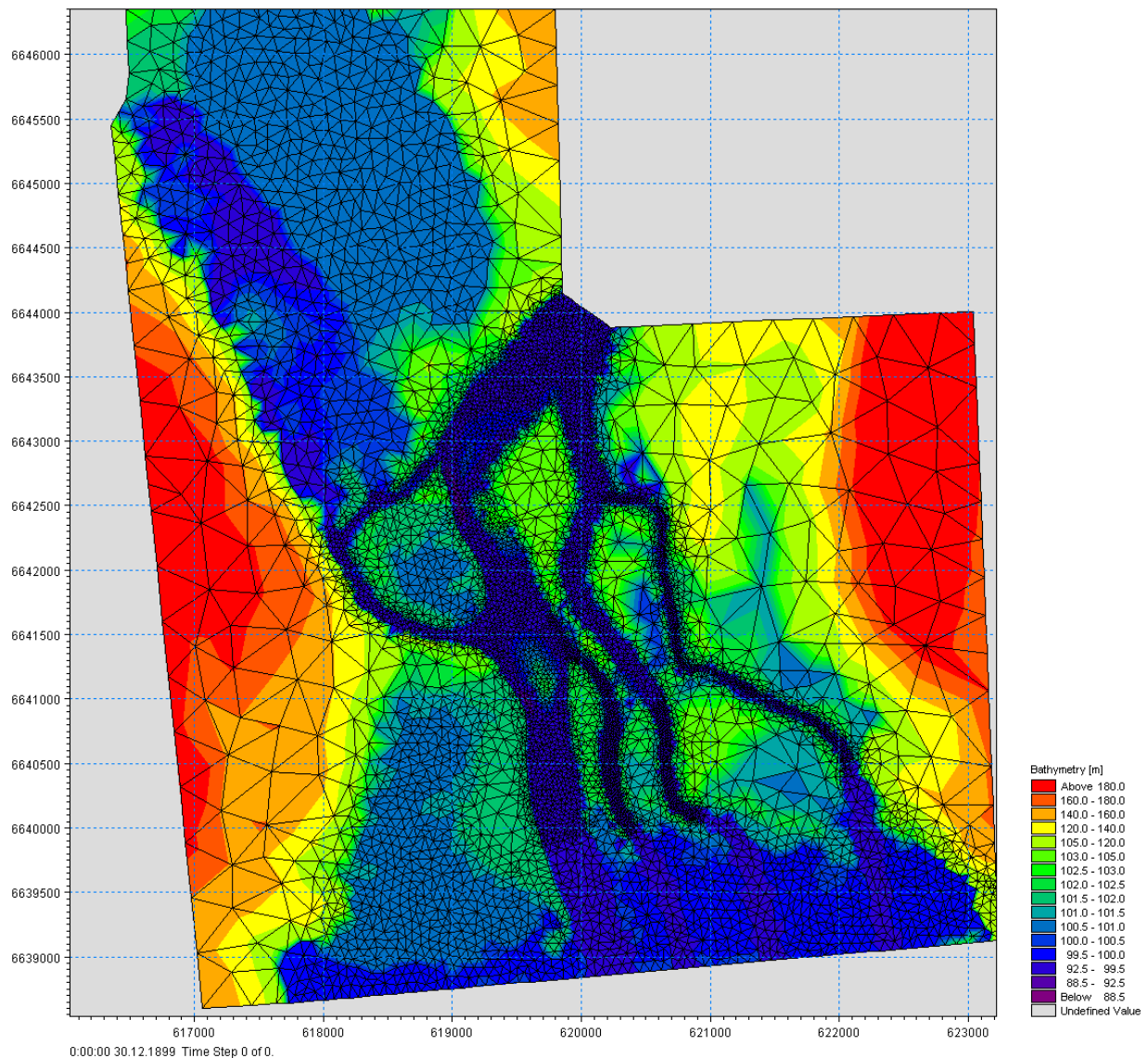


Figure 9. MIKE 21 set-up of the delta, the mesh is composed of elements corresponding to the topography of the area.



After the mesh has been created, the bathymetry is interpolated on these elements. The mesh will therefore represent the terrain at a defined spatial resolution. The numerical solution is obtained on every element of the mesh from a finite difference form of the equations using an ADI two-step algorithm (Abbott and Rasmussen 1977). This algorithm describes well the propagation of flood waves across initially dried or very shallow areas, making its use adequate in flood extent prediction (Petersen et al. 2002).

### 4.3.3 MIKE FLOOD

One and two-dimensional models are dynamically linked in a package called MIKE FLOOD developed by the Danish Hydraulic Institute (Rungø and Olesen 2003). Since the study area is composed of complex floodplains and water channels, and being in possession of new bathymetry measurements in the delta, the use of a 1D-2D coupled technique was ideal in our case.

MIKE 11 and MIKE 21 are coupled with the help of links. It exists various type of links that can be used in various situations. Standard link and lateral links are the most appropriate for our study. Description of both links will be next presented, but only one of them will be used in this study. For further description of additional type of links, the reader is advised to refer to DHI (2011c).

#### *Standard link*

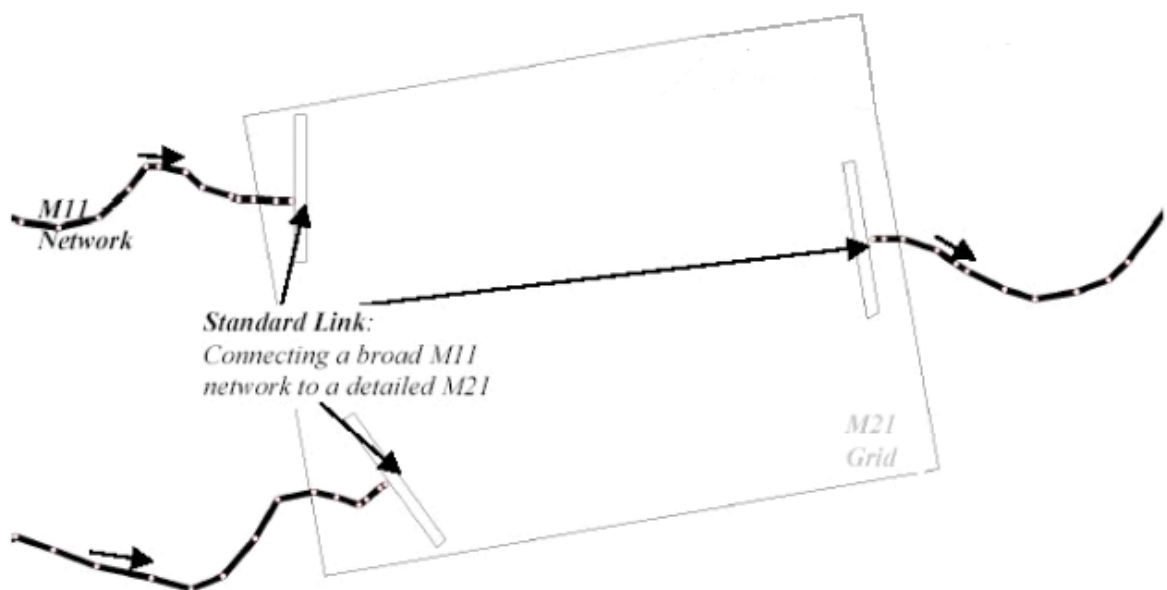
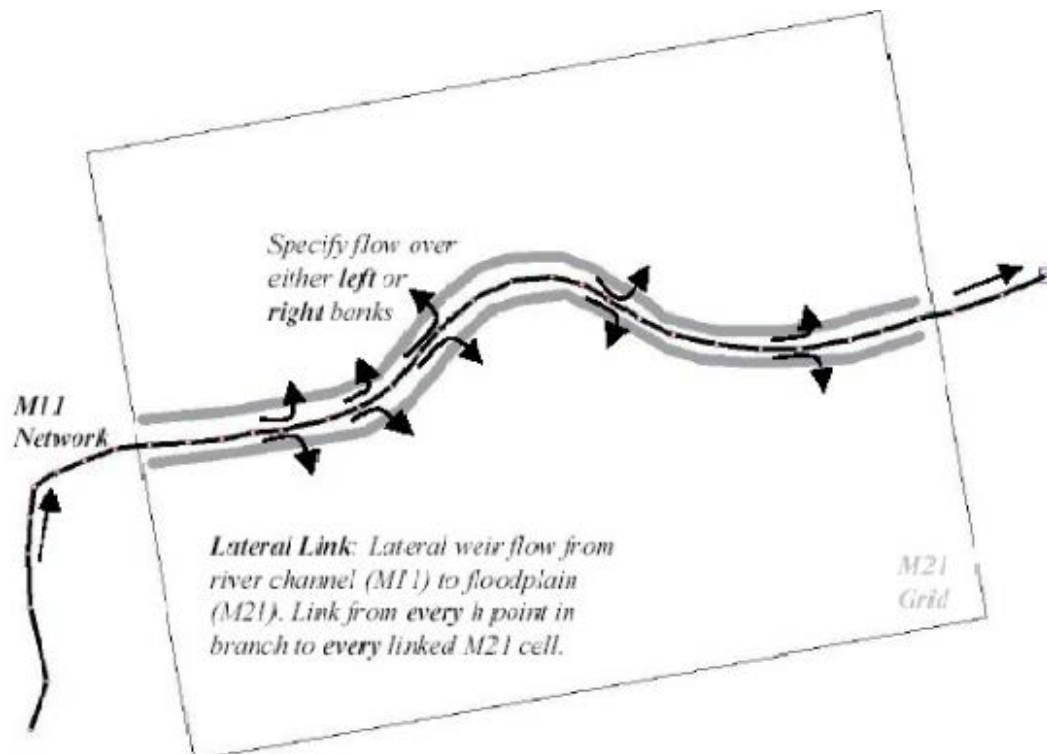


Figure 10. Sketch representing the application of a standard link; Source: DHI (2011c).

The standard link is used throughout this study. It corresponds to the standard linkage in MIKE FLOOD (Figure 10.). The standard link is ideal to use, in study where rivers interact with areas with more complex hydraulic processes as a delta or an estuary, where the description of the flow will be simplified with a one-dimensional model. In this type of study, the modeling of the river will be supplied by a simple and efficient MIKE 11 model. As for the delta, modeling of complex processes will be provided by MIKE 21. The standard link connects the one-dimensional model MIKE 11 (see 4.3.1), with a detailed two dimensional grid, MIKE 21 (see 4.3.2).

### *Lateral links*



*Figure 11. Sketch representing the application of lateral links; Source: DHI (2011c).*

Lateral links are ideal to use, in floodplains study (Figure 11). As mentioned earlier, it has been reported that MIKE 11 may simplify complex turbulent exchange and hydraulic processes between the channel and the floodplains (Menendez 2001, Petersen 2002, Rungø and Olesen 2003, Tayefi et al. 2007). In order to solve that problem, the use of a two-dimensional grid to model flow on floodplains can be used. The water channel will be therefore modeled by MIKE 11. During flood, bank full discharge will be reached, causing water to spill over floodplains where two-dimensional modeling will take over.

The lateral links vary from the standard link in the following ways (DHI 2011c):

- Flow through the link is dependent upon a structure equation and water levels in MIKE 11 and MIKE 21 (see below).
- Flow through the link is distributed in between MIKE 11's water depth points and MIKE 21 cells.
- The lateral links do not guarantee momentum conservation

As cited above, a structure is required to calculate the flow between MIKE 11 and MIKE 21. This structure is typically a weir that represents over topping of a river bank.

Structure equation, Weir formula 1 (DHI 2011c):

$$Q = wCh_1^k \left[ 1 - \left( \frac{h_2}{h_1} \right) \right]^{k-0.385} \quad (4.8)$$

### *Standard link versus Lateral links*

The standard link was considered to be the type of link the most appropriate in this study. The use of the lateral links would have required further developments of the MIKE 11 one channel representation of the delta, created by NVE in 2010. In addition, due to the representation of the channels by the one-dimensional part, processing of the acoustics measurements into cross sections would have been required. The use of the standard link was therefore the most advantageous approach, requiring the least changes in the MIKE 11 set up and describing the best the multifaceted system of the delta.

The Glomma River will be therefore modeled by the one-dimensional part of the model and will give inputs (discharge and water level) on to the two-dimensional grid that represents the delta. The standard link will distribute the input on the 2D grid as a function of depth; i.e higher discharges will be distributed in mesh elements of the 2D-grid with deeper water depth (DHI 2011c).

### *Stability*

The Courant number is a factor quantifying the stability of the model. It gives information on how fast a fluid is travelling through the computational domain relative to the velocity of the fluid (see Tuteja et al. 2007). The Courant's number (4.9) needs to fulfill the requirement of being lower than 1 (DHI 2011b). Higher values may lead to a crash of the model.

Courant's number formula is (DHI 2011b):

$$C_R = \frac{(v + \sqrt{gy}) * \Delta t}{\Delta x} \quad (4.9)$$

The model's stability depends on several factors such as the time step and the resolution of the mesh. A coarser resolution will permit the use of a higher time step, whereas it will give a less accurate description of the area. A detailed mesh with a high number of elements and nodes will increase the computational time (CPU time), and thus will require a smaller time step, if Courant's number lower than 1 is to be satisfied. Consequently, modeling of high-resolution mesh or large scale area will require days or weeks of CPU time (e.g. in Tuteja and Shaikh 2009).

A compromise needs to be determined between the stability, the time step, and the resolution of the mesh. In addition, abrupt changes in the bathymetry will lead to instabilities and therefore crash of the simulation (DHI 2011b). A smoothing of the bathymetry will be therefore advised. A more detailed description about the influence of the resolution of the mesh on the model will be treated in the model responses of the model (see subsection 6.3).

## 5. Methodology

A summary of the main steps followed in this paper is shown in Figure 12. Creation of the model inputs under form of grids as the bathymetry, topography and resistance were conducted. Then calibration and verification of the model were proceed, weight being put on the assessment of the model responses to interpolation methods, mesh resolution, roughness and other model parameters. Optimized model parameters were deduced from the verification and the observation of model responses, giving an optimum set-up of MIKE FLOOD. This set-up was finally used to observe the response of the delta to eight various water levels and discharges scenarios. Only the methodology will be described in this section, results being presented in section 6.

### 5.1 Input parameters

#### 5.1.1 Topography

Nowadays, interpolation of river channel bathymetry is a major factor in computational fluid dynamics (CFD). The need for a representation of the bathymetry in a good and correct way is a challenge. Due to the cost induced by manpower and instrumentation needed for data collection, it will always be impossible to measure the bathymetry at every point within a geographic area. Interpolation of values from known observations is therefore a solution. Although various interpolation methods have been used for different studies, the comparison of methods for spatial interpolation of river channel bathymetry is not well documented (Merwade et al. 2006). Therefore, a certain time is used in this study to determine the best spatial interpolation methods. Due to the high importance of the DEM, different interpolation methods are used in this study, namely Inverse distance weight (IDW), Spline, Natural Neighbor and TopoGrid (described in Merwade et al. 2006). The bathymetry of the different channels is interpolated from the 50000 points collected from acoustic measurements.

The different interpolation methods will be tested as the procedure described in Merwade et al. 2006. Twenty percents of the ADCP measurements are previously removed of the total sample of 50000 points. Only eighty percents of the ADCP measurements is used to create the interpolated surface, and the performance of the interpolation method is evaluated by comparing the interpolated values against the observed values in the test dataset.

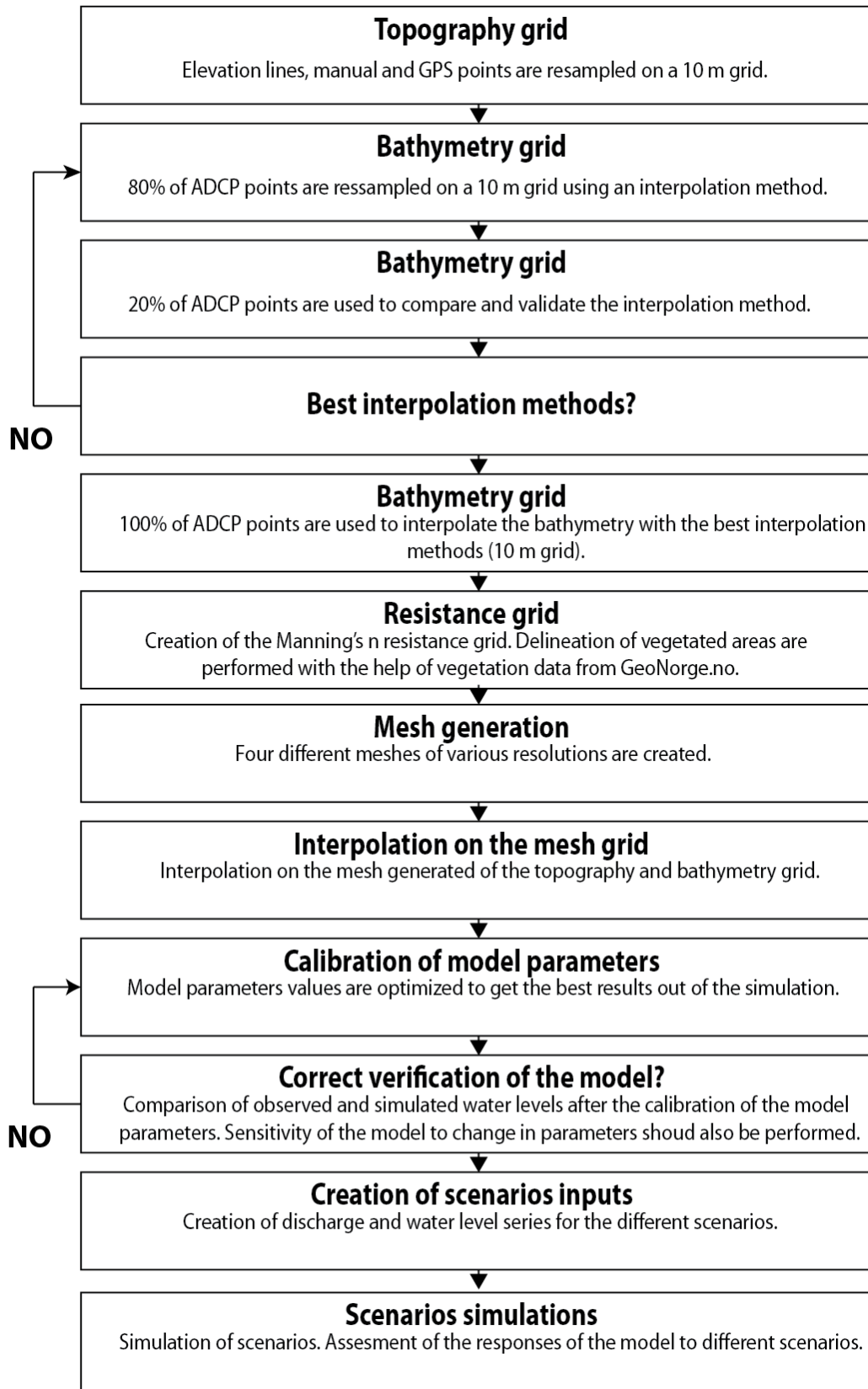


Figure 12. Chart presenting the methodology followed during this study.



Influence of interpolation methods was only assessed for the bathymetry of the river. A digital elevation model (DEM) of the area outside of the delta was created from elevation lines of 10 m. The topography within the delta and on the different islands was created from elevation lines of 10 cm, GPS points measured in 2010 and manual points extrapolated from GPS points measured on islands. The topography of the model was interpolated using the TopoGrid tool of ArcGIS. The Topo to Raster tool (or TopoGrid) is an interpolation method specifically designed for the creation of hydrological correct digital elevation model (ESRI<sup>7</sup> 2011). TopoGrid is a spline technique for which the roughness has been modified to allow the fitted DEM to follow abrupt changes in terrain, such as streams and ridges (Wahba 1990). Only this interpolation tool was used in this study due to the ease of the method and the adequacy of it. Extrapolation and interpolation of the topography and the bathymetry were realized in two separates interpolations, so the limited bathymetry points were not affected by the abundant dry elevation points.

### 5.1.2 Resistance

The original resistance map for the two dimensional model has been created from different types of vegetation observed by satellite and presents in the topography files provided by GEOnorge<sup>8</sup>. Original n values used in this study were determined by the use of Manning's n table (Chow 1959). Due to the lack of satellite pictures, calibration was only realized for the water channel. Manning's n values were assumed to be correct and left untouched for the vegetation on floodplains and the islands (Table 5).

*Table 5 Manning's n values estimated at the start of the study with the help of Manning's table (Chow 1959).*

Type	Manning's n
No Crop	0.030
Crop	0.035
River channel	0.038
Tree	0.050

After the first simulation of the model, calibration of the resistance has been carried out. Value for the water channel was then calibrated to match the best observation made in the nature. The one-dimensional and two-dimensional part of the model were used in this study, therefore both models were calibrated. A detailed description of Manning's calibration was given in the calibration methodology in this section.

<sup>7</sup> <http://help.arcgis.com/> - How Topo to Raster works

<sup>8</sup> <http://www.geonorge.no>

### 5.1.3 Mesh resolution

Assessment about the impact of mesh resolution in flood extent modeling was looked at in different studies, showing the need to carefully determine the mesh resolution (Hardy et al. 1999, Horritt and Bates 2001a, Horritt et al. 2006). Resolution of the mesh will play an important role, deciding in which part of the model more or less description is required. The aim is to find a balance between the number of nodes, elements and computational time. The best result is expected to be with the highest resolution but will require an important computational time that will not be advantageous. The most adequate mesh is therefore the one describing the most correctly hydraulics processes and which is composed of the less number of nodes.

The effect of mesh resolution on the predictions of the two-dimensional unsteady hydraulic model is assessed in this study. As recommend in Hardy et al. (1999), four different mesh grids of different spatial resolutions will be constructed, to evaluate the impact of mesh resolution. The mesh difficulties were increased proportionally as the number of mesh rose (Table 6). Mesh grids are constituted of triangular and/or rectangular elements and represent different areas with smaller or coarser elements. Uses of rectangular elements are advised in channels, fluxes of water being transmitted from elements to elements more easily along then across the stream. The four different mesh grids used to assess the influence of the mesh resolution will be next presented:

Mesh 1: Overall medium average of elements, smaller triangular elements in the main channel. Only the main channel was distinguished from the rest of the model area (Figure 13).

Mesh 2: Default mesh resolution, with fine average of rectangular elements in the distributary channels of the delta, and with medium average triangular elements in the main channel and on floodplains. In addition the area outside of the delta is described with coarse resolution (Figure 14).

Mesh 3: Mesh 2 + finer mesh resolution in the main channel and in the lower part of the delta. The main channel and distributary channels are only composed of triangular elements (Figure 15).

Mesh 4: Mesh 3 except that some parts of the grid have rectangular elements, and a coarse representation of the lowest part of the delta is made. Floodplains have finer average elements size (Figure 16).

Due to computationally demanding calibration, observation of mesh resolution impact is realized only for one resistance value. Ideally, transfer of parameters values should not occur (Hardy et al. 1999). Calibration and model responses of other parameters than mesh resolution were observed with the use of mesh 2, which is the default mesh.

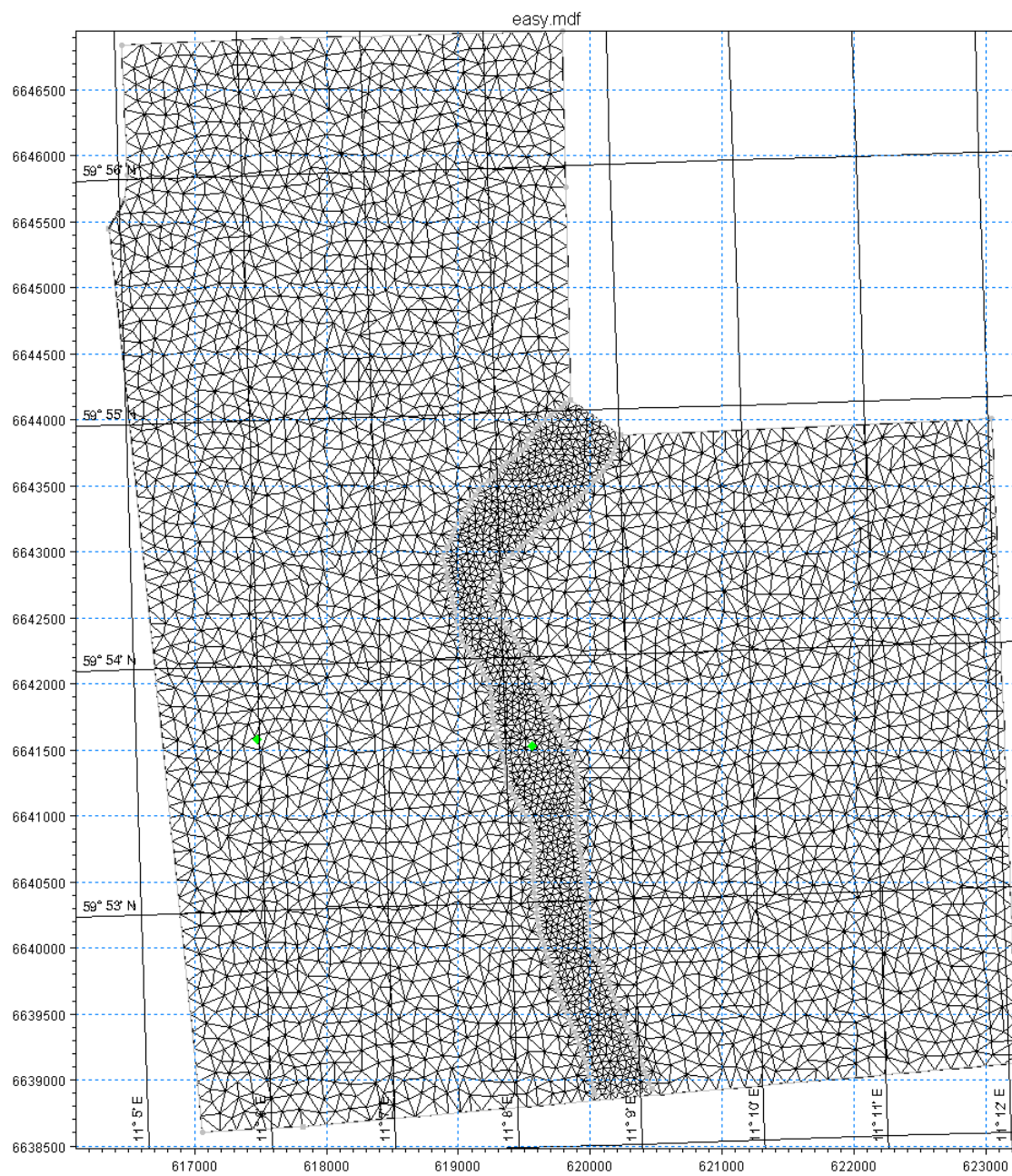


Figure 13. The lowest mesh resolution, MESH 1.

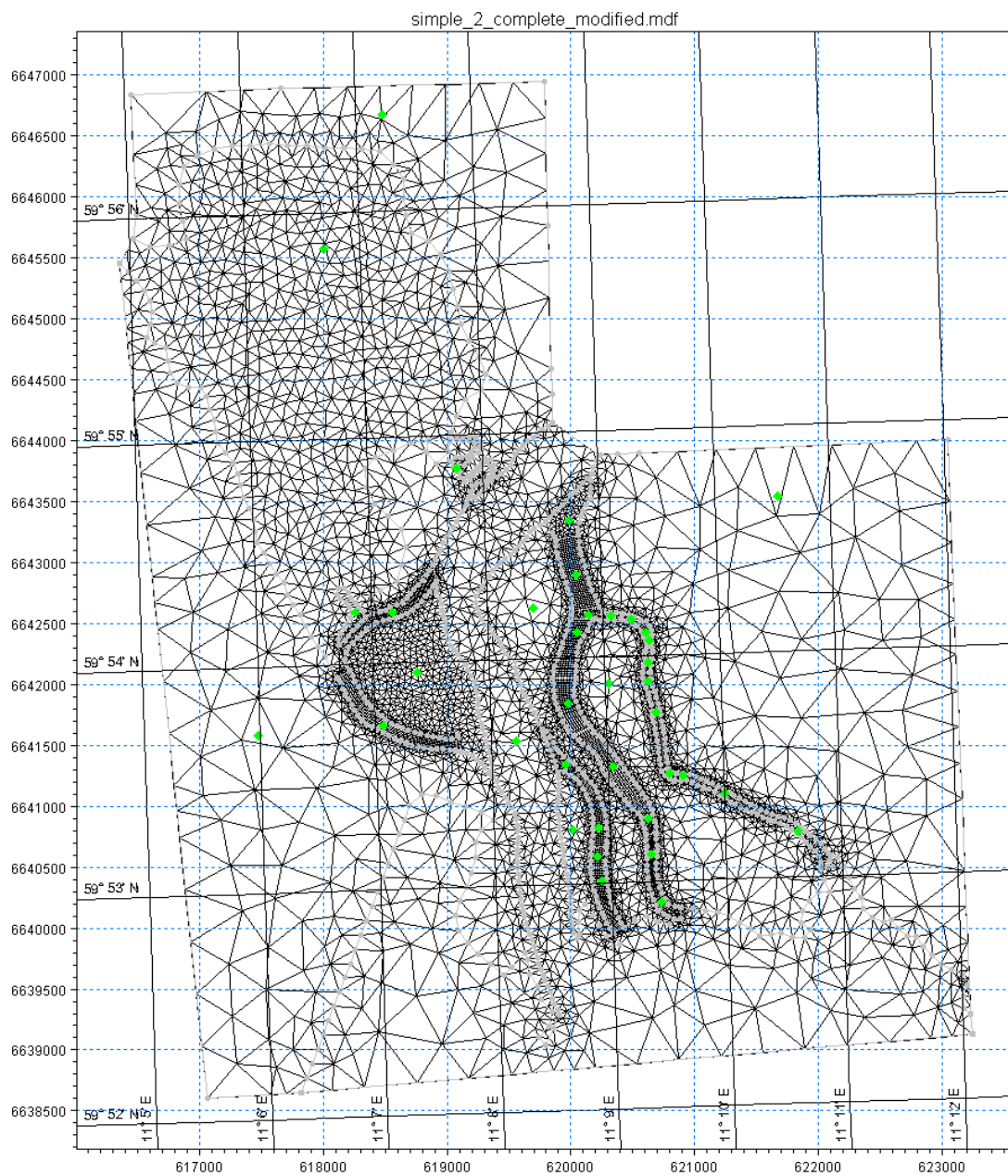


Figure 14. The default mesh resolution, MESH 2.

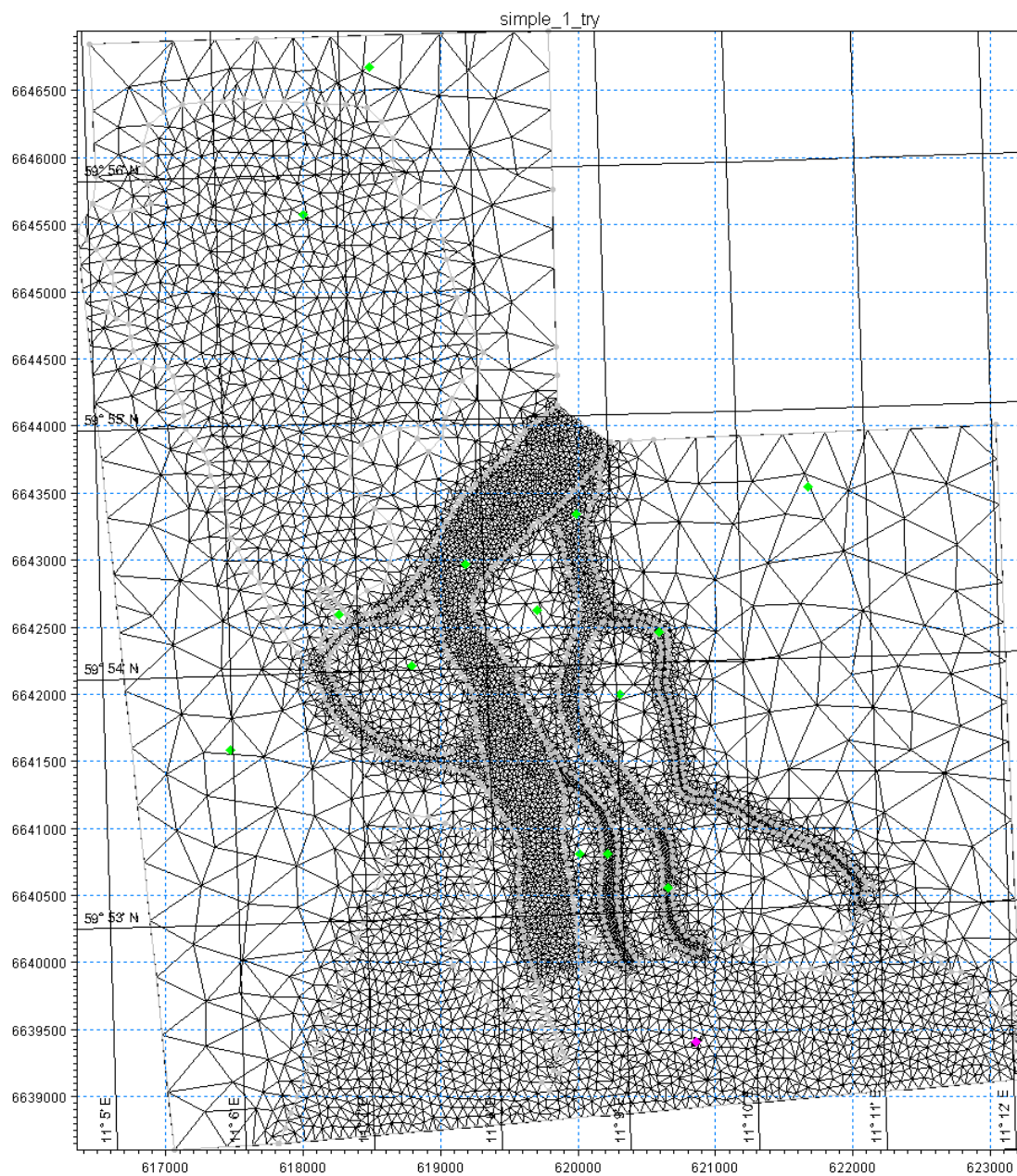
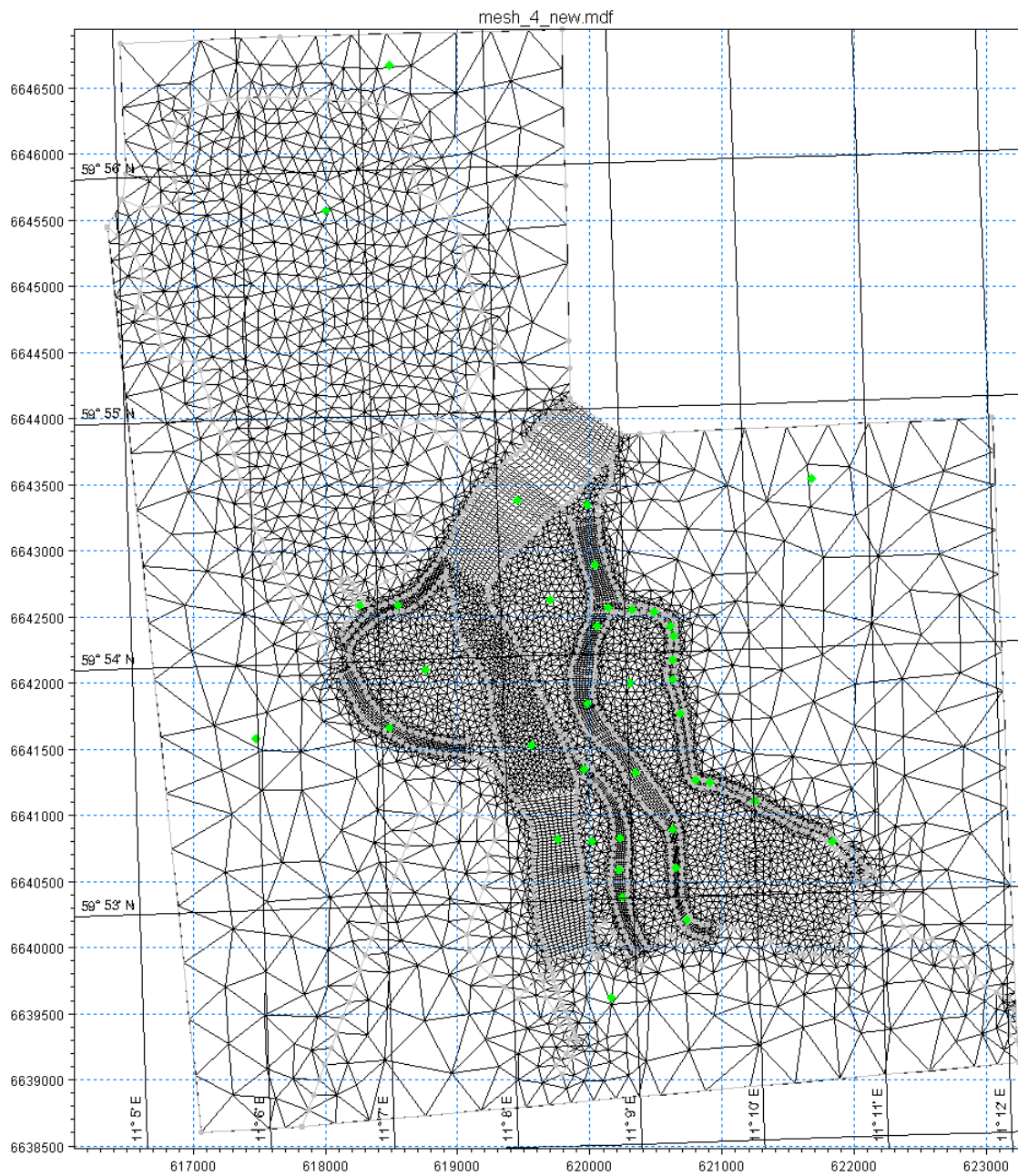


Figure 15. The highest mesh resolution with triangular elements, MESH 3.





*Figure 16. The highest mesh resolution with triangular and rectangular elements, MESH 4.*

Table 6. Description of various mesh resolution.

	Mesh			
	1	2	3	4
Number of nodes	8395	13114	14180	16251
Number of elements	4324	8581	7493	10734
Max. Area [m <sup>2</sup> ]	9997	99800	99995	102477
Min. Area [m <sup>2</sup> ]	692	29	31	27

### 5.1.4 Boundary conditions

The boundary conditions represent the different inputs of parameters in the model. Boundary conditions are usually defined by hydrographs upstream and water levels at the downstream boundaries of the model. The model setup is composed of a 1D and 2D model. Therefore additional boundary conditions are required. During the calibration and verification of the model, discharge series at Bingsfoss and water level series at Fetsund's bridge were used as boundary conditions in MIKE 11 (M11) model. In MIKE 21 (M21) model, inflow from the Glomma River is provided by M11 through a standard link and simulated summed discharge from Nittelva and Leira. Downstream boundary at the lower part of the delta is assumed to be equal to water levels at Mørkfoss.

### 5.1.5 Eddy viscosity

Eddy viscosity represents the loss of energy due to the creation of eddies in the water. In applications with significant flooding and drying of the MIKE 21 grid cells, the equation of Smagorinsky is the most suitable eddy viscosity formulation (DHI 2011b). For further description, the reader is advised to refer to Smagorinsky (1963).

## 5.2 Calibration methodology

Every hydraulic model needs a calibration and a validation to perform and represent well the complexity of natural processes. The reader should be aware that models are always a simplified representation of the reality, and thus will always need to be calibrated and validated regarding to observed data. The development of a complex and well described floodplains area is possible, but due to the considerable CPU time the law of Parsimony will be applied in this study: *“Principle that one should not multiply entities unnecessarily, or make further assumptions than are needed, and in general that one should pursue the simplest hypothesis.”*. During the calibration of the model, the easiest description of the floodplains which performs

and represents the best the reality will be preferred at more complex representations of the delta that requires longer computational time.

Once the one and two-dimensional models are set up and coupled together with the standard link, calibration and verification can be performed. Optimum parameters are found by keeping all the model parameters to their default values except one that will be adjusted. Thus model parameters will be calibrated one after one. Due to the limitation of data, only one dismantled gauging station, Nordhagan is used in this study for calibrating the model. As said earlier, calibration is realized only according to water levels. Even though no calibration of the flood extent was conducted, it will be still possible to observe the main patterns in water levels and inundations within the delta.

The calibration of the model regarding to the resistance has been carried out following this method. The delta was split up in two zones. One zone downstream the calibration point (Nordhagan) and one zone upstream it. The water flow being subcritical, calibration was carried out from downstream to upstream. The hydraulic roughness values were modified to fit as best as possible water levels observed at Nordhagan. Calibration was realized for a relative short period of 10 days (15/06/1999 to 25/06/1999). Ideally, several gauging stations within the delta would have been necessary for a correct calibration of the resistance.

### 5.3 Statistical tools

The quality of the verification of the model, calibration and validation of the interpolation methods, and the responses of the model to change in parameters will be quantified with the help of two statistical tools: the root mean square error (RMSE) and the Nash and Sutcliffe efficiency coefficient (Nash and Sutcliffe 1970). Both statistical tools are shortly described next and will be used to describe the results in **Section 6**.

The RMSE is an estimator of the differences between values predicted by a model and values observed. It is defined in the following way:

$$RMSE = \sqrt{\frac{1}{N} \sum_{i=1}^N (Z_i - E_i)^2} \quad (5.1)$$

Where N is the number of data points in the dataset with observed values  $Z_i$  ( $i= 1,2,\dots,N$ ) and  $E_i$  are the corresponding values estimated by an interpolation method.



The Nash and Sutcliffe model efficiency coefficient is used to assess the predictive power of hydrological models (Nash and Sutcliffe 1970). The development of the equations leading to the final expression of  $R^2$  is provided below:

$$F^2 = \sum (h' - h)^2 \quad (5.2)$$

Where  $F^2$  is the index of disagreement and  $h$  and  $h'$  are the observed and computed water levels at corresponding times.  $F^2$  represents the residual variance.

The initial variance  $F_0^2$  is defined by:

$$F_0^2 = \sum (h - \bar{h})^2 \quad (5.3)$$

The efficiency of the model is defined by  $R^2$ :

$$R^2 = \frac{F_0^2 - F^2}{F_0^2} \quad (5.4)$$

## 5.4 Model setup

### 5.4.1 Computer properties

All the simulations in this paper were performed with a computer with the following properties:

Intel Dual Core with 3.33 GHz processor speed and 3.87GB of RAM.

### 5.4.2 MIKE FLOOD

#### *MIKE 11 (quasi 2D)*

The area covered by the MIKE 11 setup corresponds to a reach length of 11316 meters, the upstream boundary is at Bingsfoss and the downstream boundary at Fetsund's bridge. A total of 21 geo-referenced cross sections were used with an average reach length of 500 m between one another. In addition of these cross sections, water level's and discharge's calculation points were added into the model with an average distance of 400 m between one another. Manning's  $n$  was set to a default value 0.025, with an increase resistance on floodplains with a multiplier factor of 2.3 (0.057). These values performed good results during calibration/validation test realized on 1999 and 2000 data by NVE, in between Bingsfoss and Mørkfoss. A rating curve developed for Glomma's catchment was used in MIKE 11 to determine the median flood and 200-year flood

discharges and water levels at both Bingsfoss and Fetsund's bridge. The time step used in the model is 30s. Scenario simulations time tend to vary between 1 to 2 minutes.

## **MIKE 21**

The area covered by the MIKE 21 grid is in the order of 7500 m in width and 8500 m in length. Mesh 3 was preferred to other mesh after comparison. The elements sizes range from 31 to 99995 m<sup>2</sup>, with a fine description of the delta's channels and floodplains. The significant size of elements in areas of small interest allows us to use a time step of 30s with still keeping the model stabilize with a Courant's number lower than 1. The Manning's n was set to 0.018 in water channels after calibration and model's responses assessment. The value of the Smagorinsky's parameter was set to 0.34. The Coriolis force was not taken into account in this study due to the relative low area covered by the delta. However the Coriolis force may have an impact on hydraulic processes, especially in area located in high latitude, but we will neglect its effect. Median flood and 200-year flood discharges and water levels were used as model inputs. Drying, flooding and wetting depths remained unchanged, with 0.005, 0.05 and 0.1 respectively. Scenario simulations time tend to vary between 85 to 95 hours.

## **5.5 Creation of scenarios inputs**

### **5.5.1 Scenarios description**

Creation of hydrographs, corresponding to different return periods, specific flood event, and simulation of them will give engineers a good and advanced overview of hydraulic processes, making flood management studies more credible and believable. In an attempt to observe the different possible responses of the delta, eight various scenarios were observed (Table 7). The model runs were made assuming steady conditions, with constant discharges and water level at the boundaries of the model.

Median flood and 200-year flood discharge and water levels were specified at the three boundaries conditions of the model (see subsection 5.1.4). Boundaries were defined at Bingsfoss, "Nittelva and Leira" and at the lower part of the Øyeren delta. Inputs data were determined by NVE from different types of techniques. Discharge and water levels at Bingsfoss, Fetsund and at the downstream boundary of the model were created from the use of a new rating curve developed at NVE. The rating curve (Q-h) was developed for Mørkfoss, and used in MIKE 11 to get results. Results were compared to previous rating curve developed by GLB (Glommens and Lågens Water Management Association) and gave results of the same order. Discharge values at Nittelva+Leira were made by summing flood calculations for Leira and Nittelva (Pettersen 2002, Soot 2007). A summary of values used during scenario simulations is given below (Table 8).

Table 7. List of various scenarios used in MIKE FLOOD model.

<b>Different scenarios</b>			
	Bingsfoss	Nittelva+Leira	Lower Øyeren delta
Scenario 1	$Q_M$	$Q_M$	$H_M$
Scenario 2	$Q_M$	$Q_M$	$H_{200}$
Scenario 3	$Q_M$	$Q_{200}$	$H_M$
Scenario 4	$Q_M$	$Q_{200}$	$H_{200}$
Scenario 5	$Q_{200}$	$Q_M$	$H_M$
Scenario 6	$Q_{200}$	$Q_M$	$H_{200}$
Scenario 7	$Q_{200}$	$Q_{200}$	$H_M$
Scenario 8	$Q_{200}$	$Q_{200}$	$H_{200}$

Table 8. Discharge and water level values corresponding to  $Q_M$ ,  $Q_H$ ,  $H_M$  and  $H_{200}$  at the three boundaries of MIKE FLOOD model.

	Bingsfoss	Nittelva+Leira	Lower Øyeren delta
$Q_M$ [m <sup>3</sup> /s]	2180.00	177.50	-
$Q_{200}$ [m <sup>3</sup> /s]	4320.00	485.00	-
$H_M$ [m]	-	-	102.26
$H_{200}$ [m]	-	-	105.43

With:

$Q_M$ : Median return period discharge.

$Q_{200}$ : 200-year return period discharge.

$H_M$ : Median return period water level.

$H_{200}$ : 200-year return period water level.

## 6. Results

The results are discussed in the order listed in chapter 5. In subsection 6.1, results from the different techniques used to interpolate the bathymetry will be given. In subsection 6.2, verification of the model is presented by comparing observed and simulated water levels. Then results of the response of the model to different parameters are presented in subsection 6.3. In subsection 6.4, results from the delta's responses to eight different scenarios are presented. Finally, a summary of uncertainties observed throughout this study is made in subsection 6.5.

### 6.1 Interpolation methods

Comparisons of various methods to interpolate the bathymetry of the delta are now assessed. Table 9 shows the optimum values for model parameters of each interpolation method. In addition the root mean square error is observed by comparing interpolated with measured heights. The following four interpolation methods are studied in this section: Inverse Distance Weighted (IDW), Natural Neighbor, Topo to Raster and Spline with barriers. Optimum parameters were only obtained by performing a sensitivity analysis using RMSE for the IDW interpolation method. The Natural neighbor, Topo to raster and Spline with barriers do not require calibration due to user specified parameters (Merwade et al. 2006).

*Table 9. Optimum values for parameters and statistical analysis of different interpolation methods (N= number of closed points selected to interpolation, p= exponential power, S= smoothing parameter).*

Method	Optimum values for parameters	RMSE Statistics
		Average [m]
IDW	N = 20, p=2	0.32
Natural Neighbor	-	0.36
Topo to Raster	-	0.42
Spline with Barriers	S = 1	0.33

Methods performed equally well with RMSE ranging from 32 (IDW) to 42 cm (Topo to Raster). Spline with barriers gave an RMS error of 33 cm. In addition this interpolation method provides a smooth bathymetry that may be ideal to avoid instabilities created by abrupt change in bathymetry. Nevertheless comparisons of elevation points with simulated one were usually done in area well covered by ADCP measurements. An observation of interpolation methods on two zones: one with high sampling density and one with poor sampling density, will be conducted in subsection 6.5.

Interpolation of the total sample of acoustic measurements was performed with the Spline with barriers interpolation method. To assess the validity of the topography, a comparison with earlier topography data of the area was carried out. The test terrain was derived from 2007, using data provided by Terratec<sup>9</sup>, NGU<sup>10</sup>, NVE and GEOnorge. Figure 17 shows the elevation difference between the maps created for this study and the test topography. Elevations from Spline method tend to show interpolated values higher in the main channel and lower for Svellet. However, interpolated bathymetry in distributary channels shows a similar representation. Comparison indicates a correct agreement of topography, with 70% of the two bathymetry maps within an -1 / +1m interval.

## 6.2 Verification

Optimized model parameters found during the calibration of the model were verified for a period other than the period used for the calibration. Due to missing years in the Nordhagan water levels series, the validation period selected was the longest period without interruption in water levels, which is in 1999 (25/06/1999 to 15/08/1999). Observed and simulated water series will give us an overview over the quality of the model for reproducing water levels within the delta.

A visualization of the verification results are shown in Figure 18. The x axis shows the variable of the verification period in days. The y axis shows the variable of water levels in meter above the sea level. Modeled and observed water levels at Nordhagan were compared with identical techniques (RMSE and  $R^2$ ).

Match of simulated and observed water levels are close with the same averaged values (Table 10). The absolute difference is ranging from 0 to 10 cm, with a root mean square error equals to 3 cm. The Nash coefficient has a high model efficiency coefficient value with 0.98. Figure 18 depicts a better agreement for water levels higher than 101.7 m a.s.l. For values lower than 101.7 m, differences between values are increased with values ranging from 4 to 10 cm.

*Table 10. Average observed and simulated water level at Nordhagan gauging station, during the verification of the model.*

Observed [m]	Simulated [m]	MaA. Difference [m]	MiA. Difference [m]	RMSE [m]	$R^2$
101.76	101.76	0.1	0	0.03	0.98

*MaA. Difference = Maximum Absolute Difference*

*MiA. Difference = Minimum Absolute Difference*

<sup>9</sup> <http://www.terratec.no>

<sup>10</sup> <http://www.ngu.no>

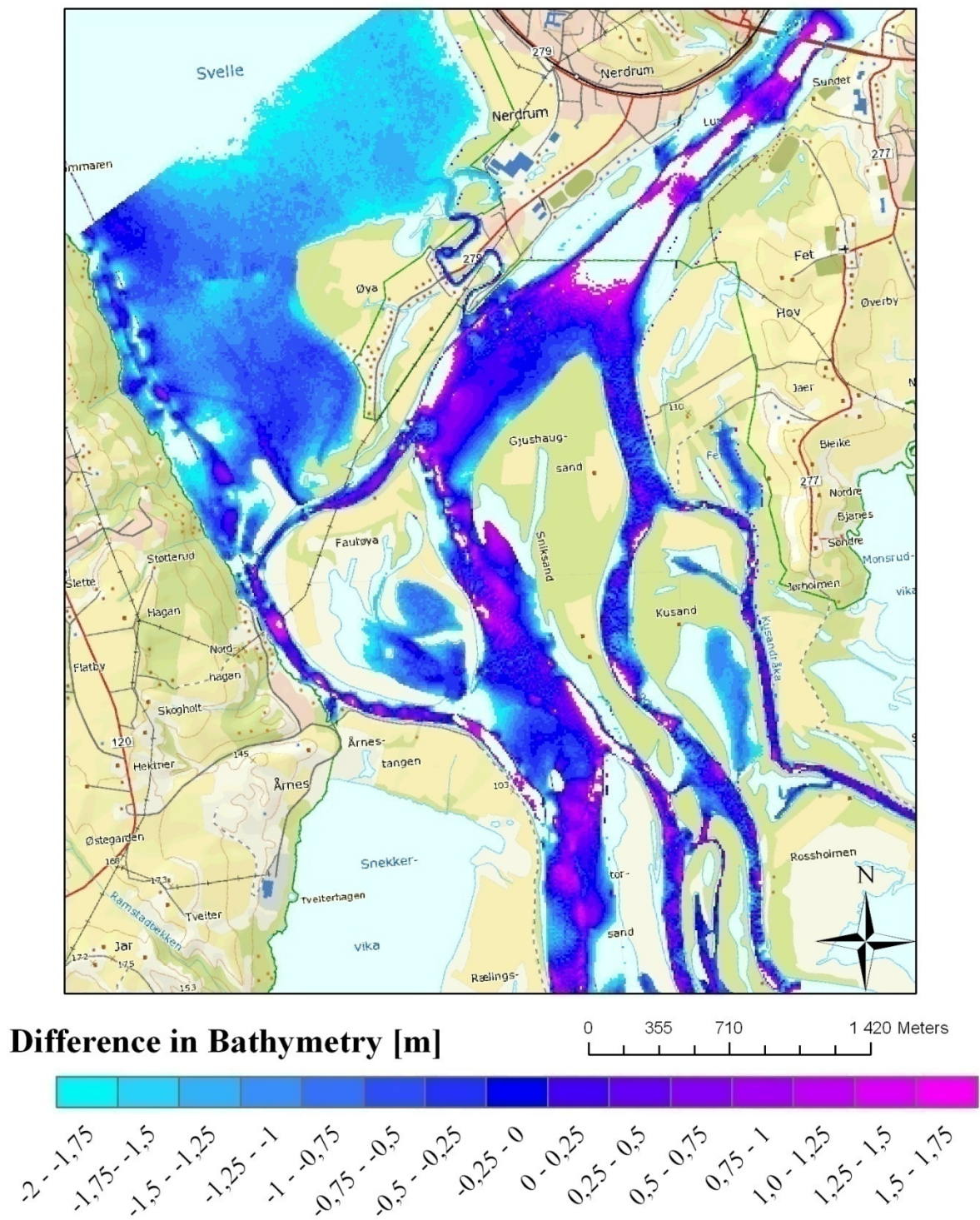


Figure 17. Difference in meters of the bathymetry created in this study minus the test bathymetry, Øyeren delta; Source: Statkart.no (2011) (background map)

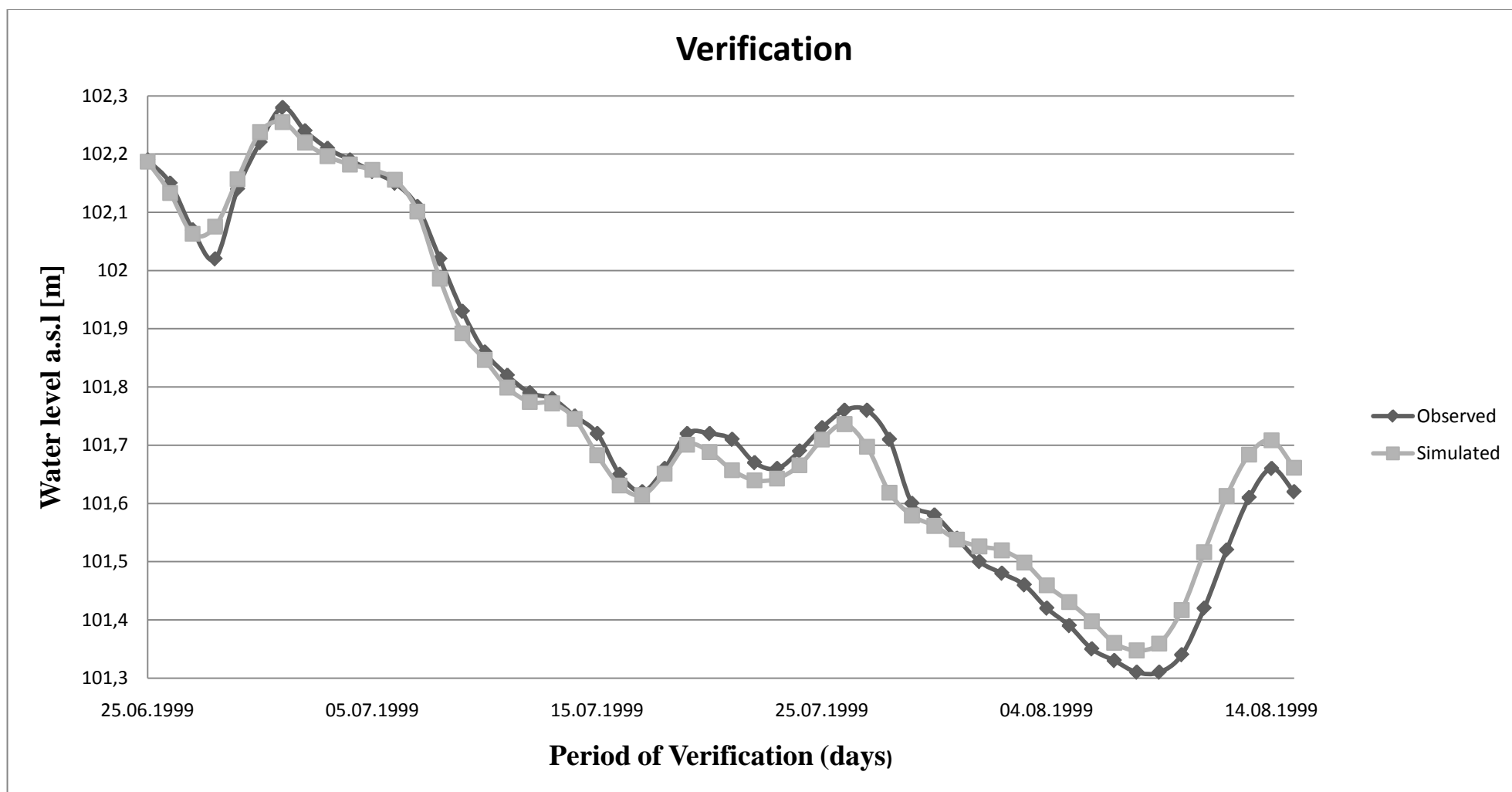


Figure 18. Calibrated data for the MIKE FLOOD model compared with runoff data from Nordhagan; Source: NVE (2011).

## 6.3 Model responses

Model responses were checked simultaneously as the calibration. The aim was to estimate optimum parameters for the model. Each parameter was subjected to a change in values while other parameters were unchanged. Observed and simulated water levels at Nordhagan were then compared. The efficiency of the model was assessed by looking at residuals with the root mean square error and the  $R^2$  Nash and Sutcliffe efficiency parameter. The model sensitivity of four different types of inputs parameters was investigated:

- Channel resistance (Manning's  $n$ )
- Eddy viscosity ( $S$ )
- Distance of discharge's and water level's calculation points in MIKE 11 setup ( $dX$ )
- Mesh resolution

Results from the model responses are presented in Table 11. Observation of the root mean square error for different values of Manning's  $n$  indicate lower errors for Manning's  $n$  equal to 0.016, 0.017 and 0.018 (Figure 19). Patterns show considerable errors for low (0.011) and high  $n$  value (0.025), with errors being equal to 3.7 and 6.6 cm respectively. Errors tend to show that calibration of the  $n$  value is a necessary to avoid bias in results. It is also necessary to understand the impact of mesh resolution in the flood extent modeling, observation of various mesh grids of different complexities is realized. If one look at the results in Figure 20, it is possible to directly observe the considerable error (50 cm) resulting from the use of a coarse mesh (Mesh1). The three other mesh are composed of approximately the same number of nodes and elements (see Table 6). They performed equally well, with a slightly better result for Mesh 2 (2 cm error) and 3 (1 cm error), due to the finer resolution in the main channel of the delta.

On the contrary of the roughness parameter and the mesh resolution, value of  $dX$  and eddy viscosity parameters had little influence on the model responses. Only two  $dX$  values were looked at, due to the similarities of the results for 25 and 400 m (Figure 22). Changes in Smagorinsky coefficient parameter were traduced by a small difference (0.5 cm) in RMS errors (Figure 21). A look at the Nash-Sutcliffe efficiency parameter, gives us an overview over the best optimized parameters, with the model being optimized for the values below:

- $n = 0.018$
- $S = 0.34$
- $dX = 400$  m
- Mesh 3



Table 11. Model responses, with observation of the average observed and simulated water levels, the root mean square error and the Nash-Sutcliffe efficiency coefficient. Bolded values correspond to optimized values.

Location	Nordhagan			
	Avg. Observed WL	Avg. Simulated WL	RMSE	R <sup>2</sup>
Calibration parameters				
<b>Manning's n</b>				
n = 0.011	102.22	102.18	0.04	0.09
n = 0.017	102.22	102.22	0.02	0.56
<b>n = 0.018</b>	102.22	102.22	0.02	0.81
n = 0.019	102.22	102.23	0.02	0.75
n = 0.025	102.22	102.28	0.07	0
<b>Eddy Viscosity (Smagorinsky function)</b>				
S = 0.15	102.22	102.2	0.02	0.64
S = 0.28	102.22	102.23	0.02	0.56
<b>S = 0.34</b>	102.22	102.22	0.02	0.81
S = 0.4	102.22	102.23	0.02	0.65
<b>Distance between calculation's points</b>				
dX = 25	102.22	102.22	0.02	0.81
<b>dX = 400</b>	102.22	102.22	0.02	0.81
<b>Mesh resolution</b>				
Mesh 1	102.22	102.70	0.48	0
Mesh 2	102.22	102.22	0.02	0.81
<b>Mesh 3</b>	102.22	102.22	0.01	0.85
Mesh 4	102.22	102.20	0.02	0.73

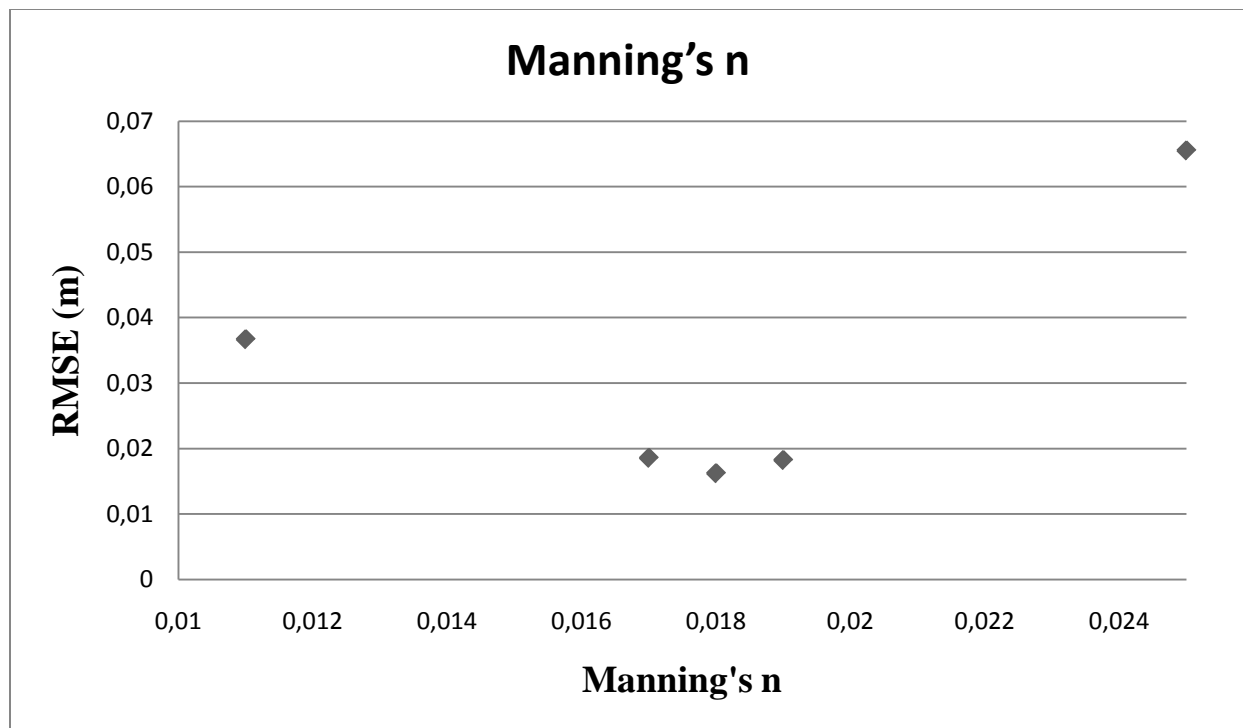


Figure 19. Model's responses to change in Manning's  $n$  values are quantified with the help of the RMSE statistical tool.

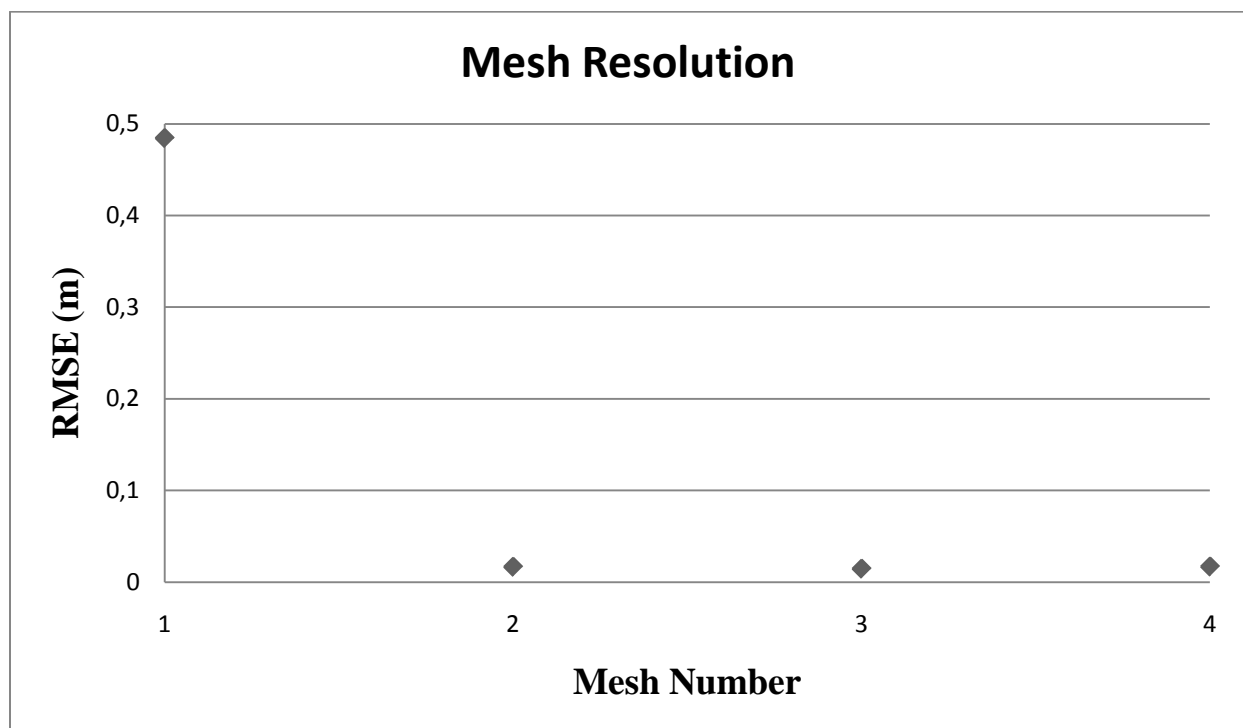


Figure 20. Model's responses to change in mesh resolution are quantified with the help of the RMSE statistical tool.

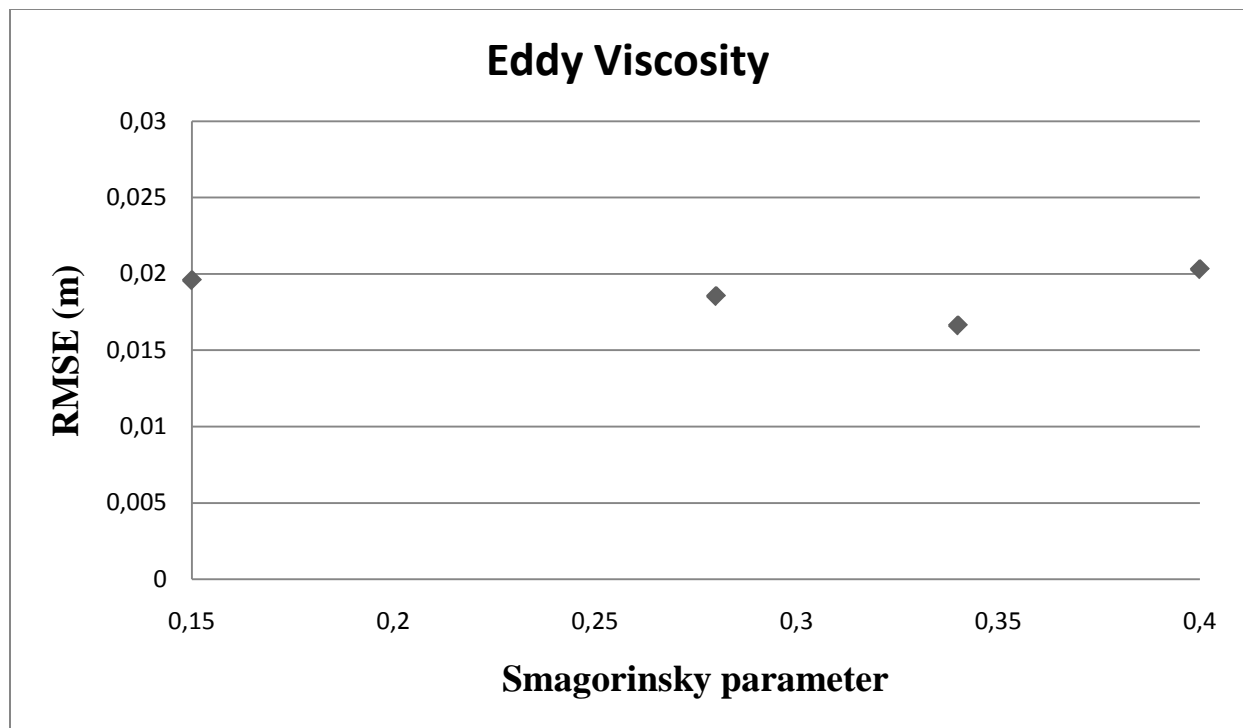


Figure 21. Model's responses to change in Smagorinsky parameter values are quantified with the help of the RMSE statistical tool.

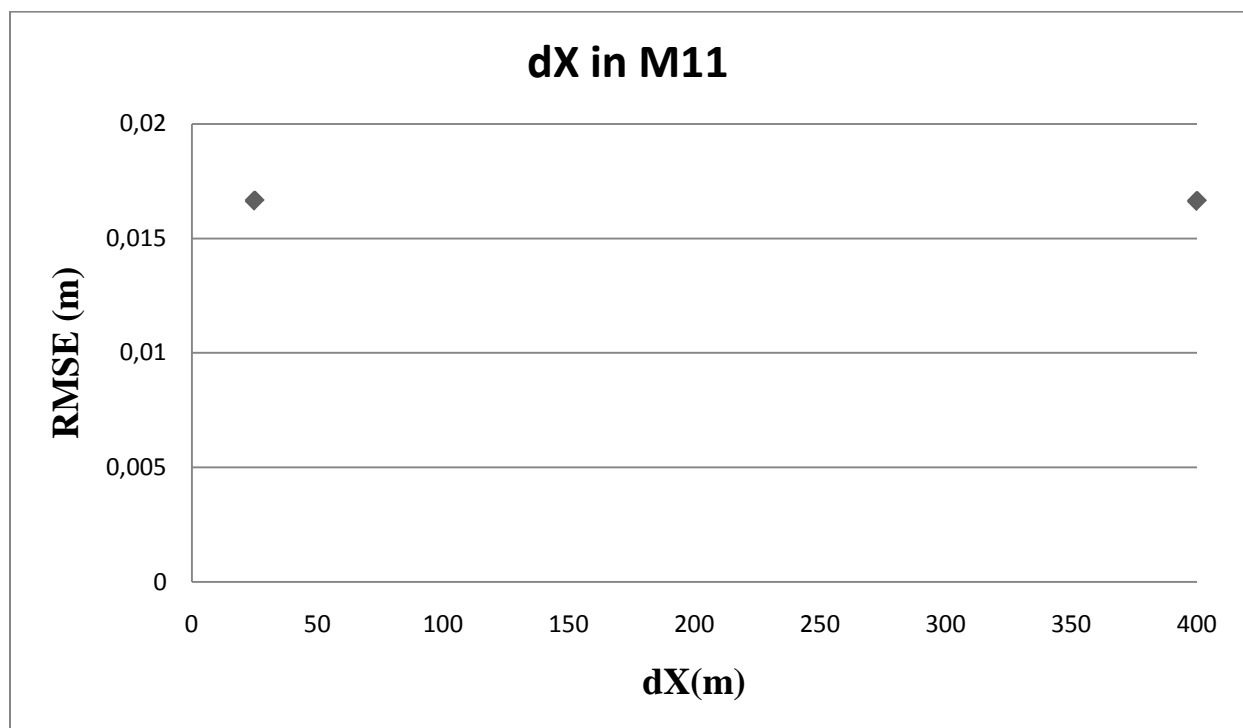


Figure 22. Model's responses to change in dX values are quantified with the help of the RMSE statistical tool.

## 6.4 Scenario simulations

Simulation of different scenarios will make it possible to compare the water level differences between Lillestrøm and Fetsund for each scenario and for the six observation points (Figure 23). In addition, the current speed for the different scenarios will be examined, giving us a good idea over possible erosion in the delta. Results will first be presented independently, and then summarized together. The water levels at the six observation points for the eight scenarios are presented in Figure 24 and Figure 25.

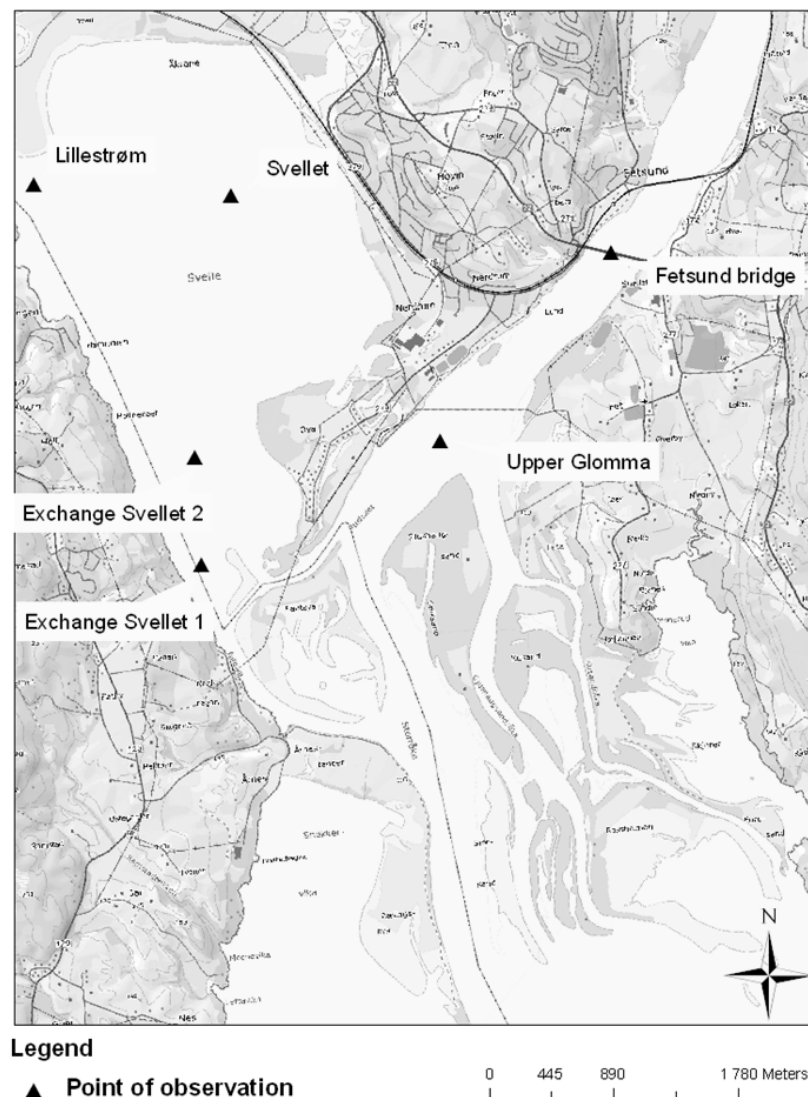


Figure 23. Observation points in the Øyeren area where simulated water levels were looked at; Source: Statkart.no (2011) (background map).

### ***Scenario 1 ( $Q_M, Q_M, H_M$ )***

Results from scenario 1 (Figure 26) indicate no or small interaction between Svellet and the delta. Velocities are up to 1 m/s in the distributary channels, and reach 1.4 m/s in the deepest water depths in the main channel. Most of islands are completely flooded, with only few areas that are still not under water. There is 11 cm difference between Fetsund (102.65 m) and Lillestrøm (102.54 m).

### ***Scenario 2 ( $Q_M, Q_M, H_{200}$ )***

Simulation results from scenario 2 (Figure 27) show also small interaction between Svellet and the delta, with velocities between 0 and 0.1 m/s. Low velocities are also dominant in the delta, with maximum velocities up to 0.6 m/s in the upper part of Øyeren delta. Velocities in the distributary channels are around 0.2 m/s. The delta is fully flooded in this scenario. Deviation between Fetsund (105.73 m) and Lillestrøm (105.72 m) is only 1 cm.

### ***Scenario 3 ( $Q_M, Q_{200}, H_M$ )***

Scenario 3 results (Figure 28) are close from Scenario 1, except that 200-year discharge from Leira+Nittelva creates velocities up to 0.3 m/s between Lillestrøm and the delta. Due to the interaction of Svellet and the delta, velocities are slightly higher in the main channel. Most of the islands are completely flooded, with only few areas still not under water. In this scenario, there is 5 cm change between Fetsund (102.71 m) and Lillestrøm (102.66 m).

### ***Scenario 4 ( $Q_M, Q_{200}, H_{200}$ )***

Scenario 4 provides results (Figure 29) similar to scenario 2, in addition of the interaction between Svellet and the delta, with velocities up to 0.3 m/s. As observed in Scenario 3, the interaction causes velocities to be slightly higher in the main channel of the delta, being of the order of 0.5 m/s in average. The delta is fully flooded in this scenario. There is 2 cm difference between Fetsund (105.74 m) and Lillestrøm (105.72 m).

### ***Scenario 5 ( $Q_{200}, Q_M, H_M$ )***

No or small interaction is observed between Lillestrøm and the delta in Scenario 5 (Figure 30). Velocities are overall high with values up to 1.4 m/s in the main channel. Most of the islands are completely flooded, with only few areas still not under water. A considerable difference between Fetsund (103.33 m) and Lillestrøm (103.00 m) can be observed with 33 cm difference.

### ***Scenario 6 ( $Q_{200}, Q_M, H_{200}$ )***

All the area in the delta is flooded in Scenario 6 (Figure 31). No major interaction can be observed between Svellet and the delta. Nevertheless it is possible to observe velocities up to 0.8 m/s in the main channel. The difference in this scenario is 6 cm, with water levels at Fetsund and Lillestrøm equal to 105.82 and 105.76 respectively.

### Scenario 7 ( $Q_{200}$ , $Q_{200}$ , $H_M$ )

In this scenario, it is possible to observe the highest velocities of all scenarios, with velocities up to 1.4 m/s in every distributary channels of the delta (Figure 32). These velocities are combined with a water level around 103.10 m, corresponding to a nearly complete flooding of the delta. Difference observed between Fetsund (103.38 m) and Lillestrøm (103.14 m) is 24 cm.

### Scenario 8 ( $Q_{200}$ , $Q_{200}$ , $H_{200}$ )

The last scenario corresponds to the worst configuration in the reality, combining a 200-year return period discharge from Bingsfoss, Leira+Nittelva and 200-year water level at the downstream part of the delta (Figure 33). It results in total flooding of the delta, with medium velocities, similar to Scenario 6. Besides, interaction of Svellet and the delta cause slightly higher velocities in the main channel of the delta. The divergence between Fetsund (105.82 m) and Lillestrøm (105.77 m) is of 5 cm.

### Scenarios summary

A summary of the observations made through the simulations is given in Table 12. Information about the average velocity and water levels at Fetsund and Lillestrøm are presented. Averaged velocity will be separated in three types of velocities:

- Low (averaged velocity lower than 0.4 m/s)
- Moderate (averaged velocity between 0.5 and 1 m/s)
- High (averaged velocity higher than 1 m/s)

For Scenario with 200-year water level at the downstream boundary: 2, 4, 6 and 8, a complete flooding of the delta occurs. In these cases, observed averaged velocity tend to be low/moderate. Whereas for scenario with median water level: 1, 3, 5 and 7, have approximately 90% of the delta flooded coupled with high/moderate velocities. Biggest differences in water levels were observed for scenario 5 and 7 (24 and 33 cm respectively). For low and moderate velocities, differences ranged from 1 to 11 cm.

*Table 12. Summary of results from scenario simulations with: the type of velocities and the difference of water levels at Fetsund and Lillestrøm.*

	Velocity [m/s]	Fetsund WL [m]	Lillestrøm WL[m]	Difference [m]
Scenario 1	Moderate	102.65	102.54	0.11
Scenario 2	Low	105.73	105.72	0.01
Scenario 3	Moderate	102.71	102.66	0.05
Scenario 4	Low	105.74	105.72	0.02
Scenario 5	High	103.33	103.00	0.33
Scenario 6	Moderate	105.82	105.76	0.06
Scenario 7	High	103.38	103.14	0.24
Scenario 8	Moderate	105.82	105.77	0.05

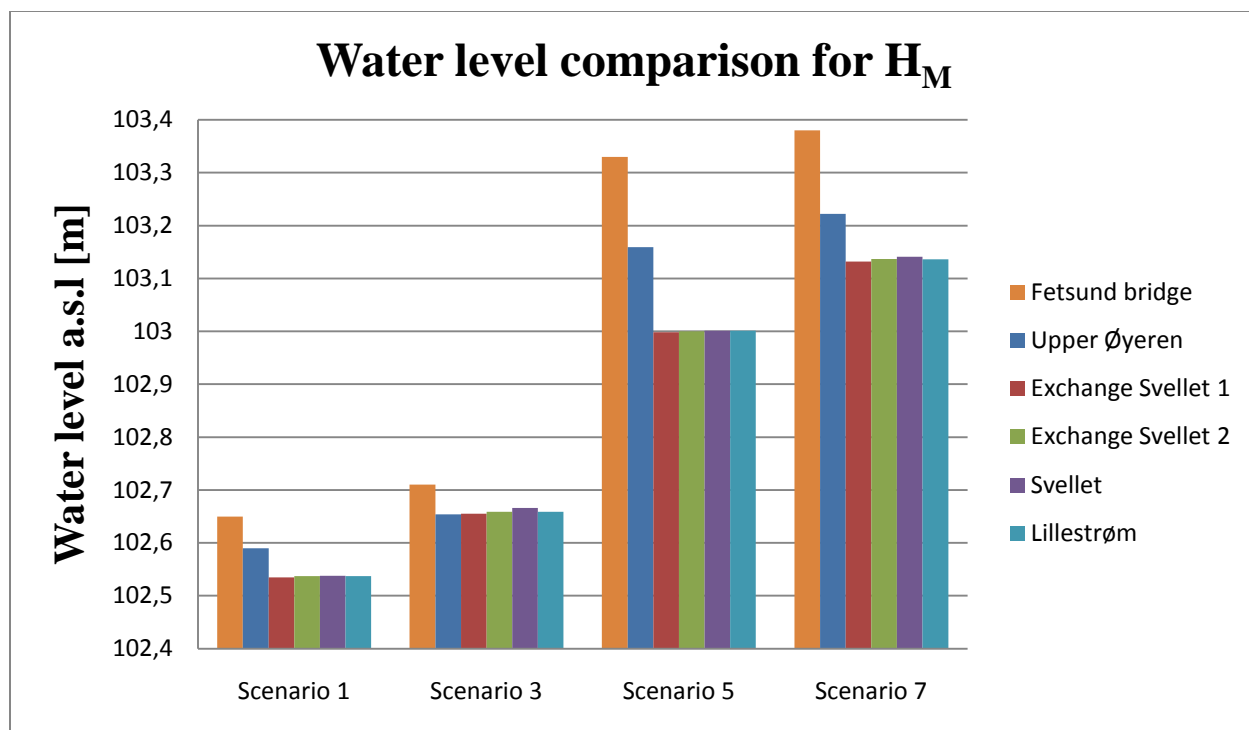


Figure 24. Water level comparison at the observation points in the model area (Scenario 1,3,5 and 7).

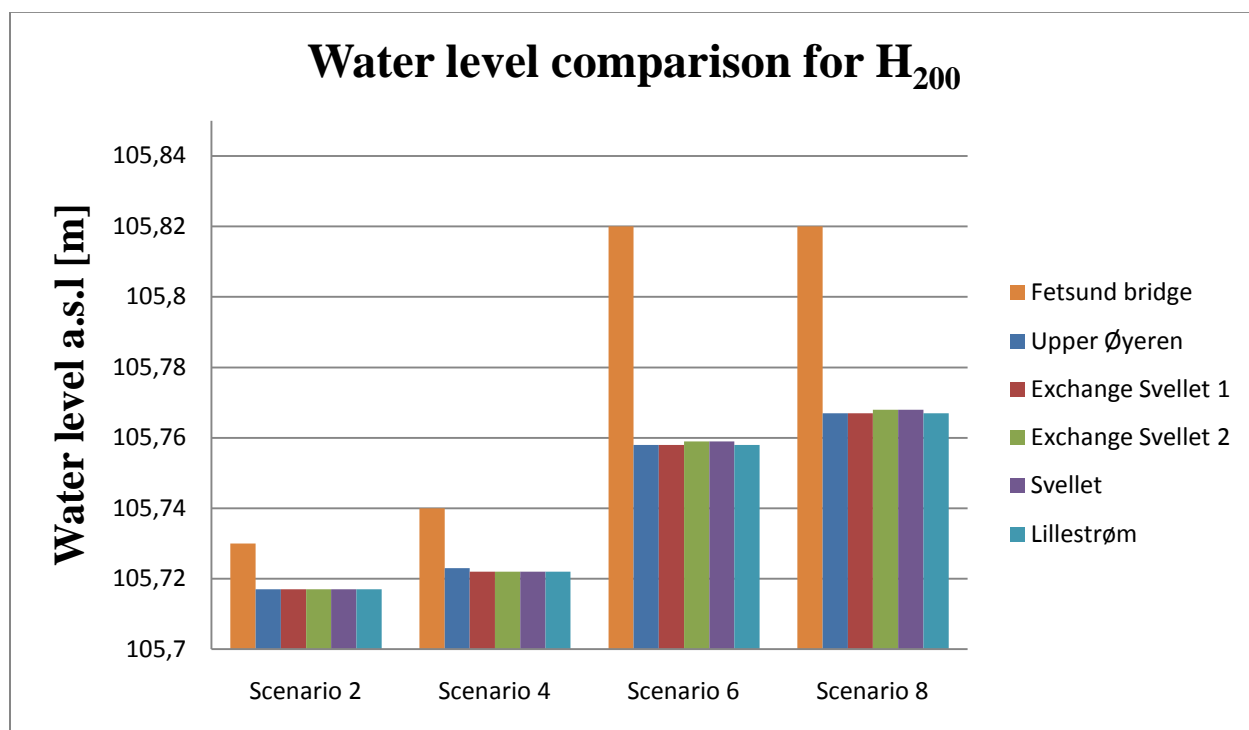


Figure 25. Water level comparison at the observation points in the model area (Scenario 2,4,6 and 8).

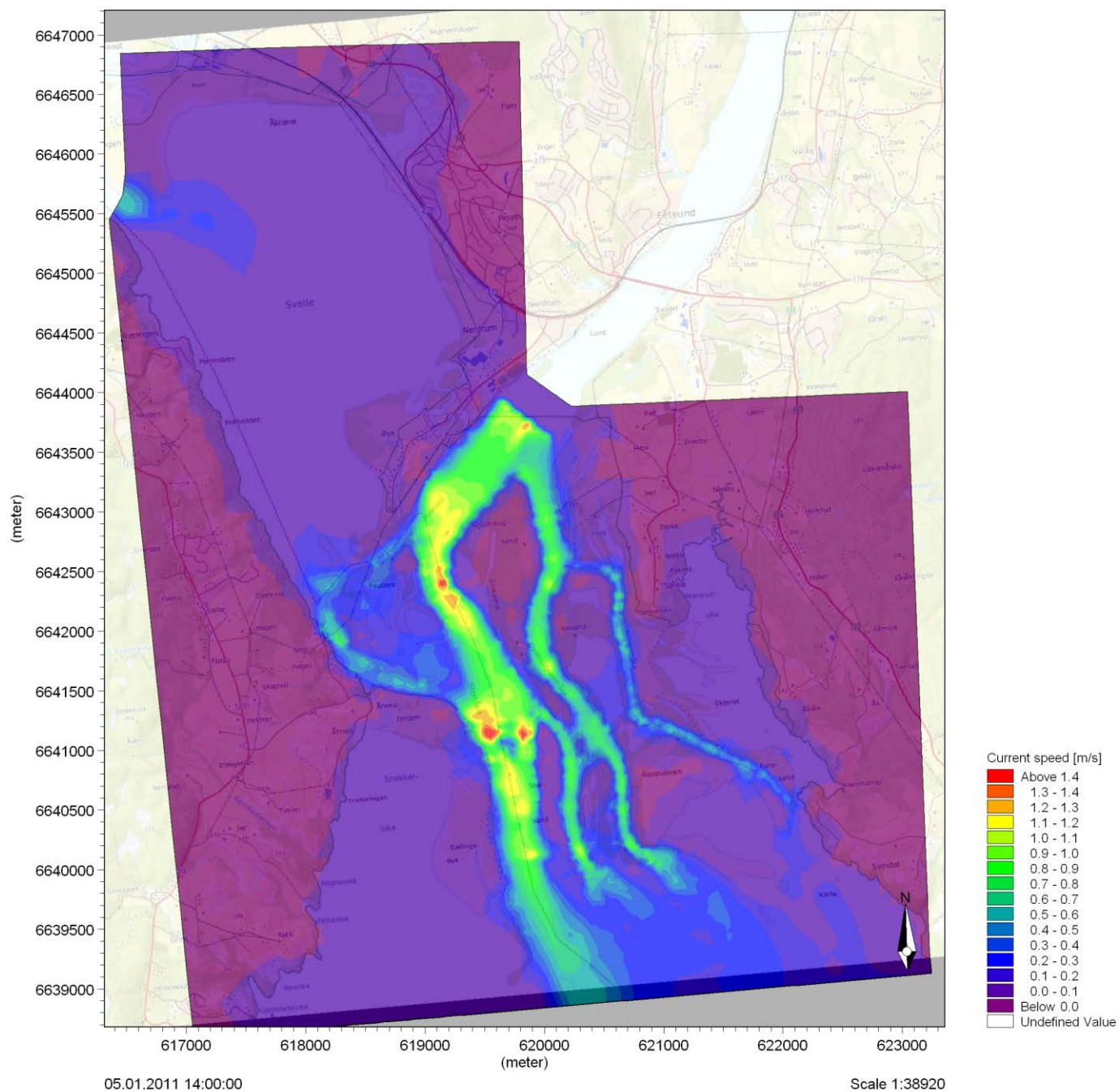


Figure 26. Simulated current speed (m/s) at Øyeren delta for scenario 1;  
Source: Statkart.no (2011) (background map).



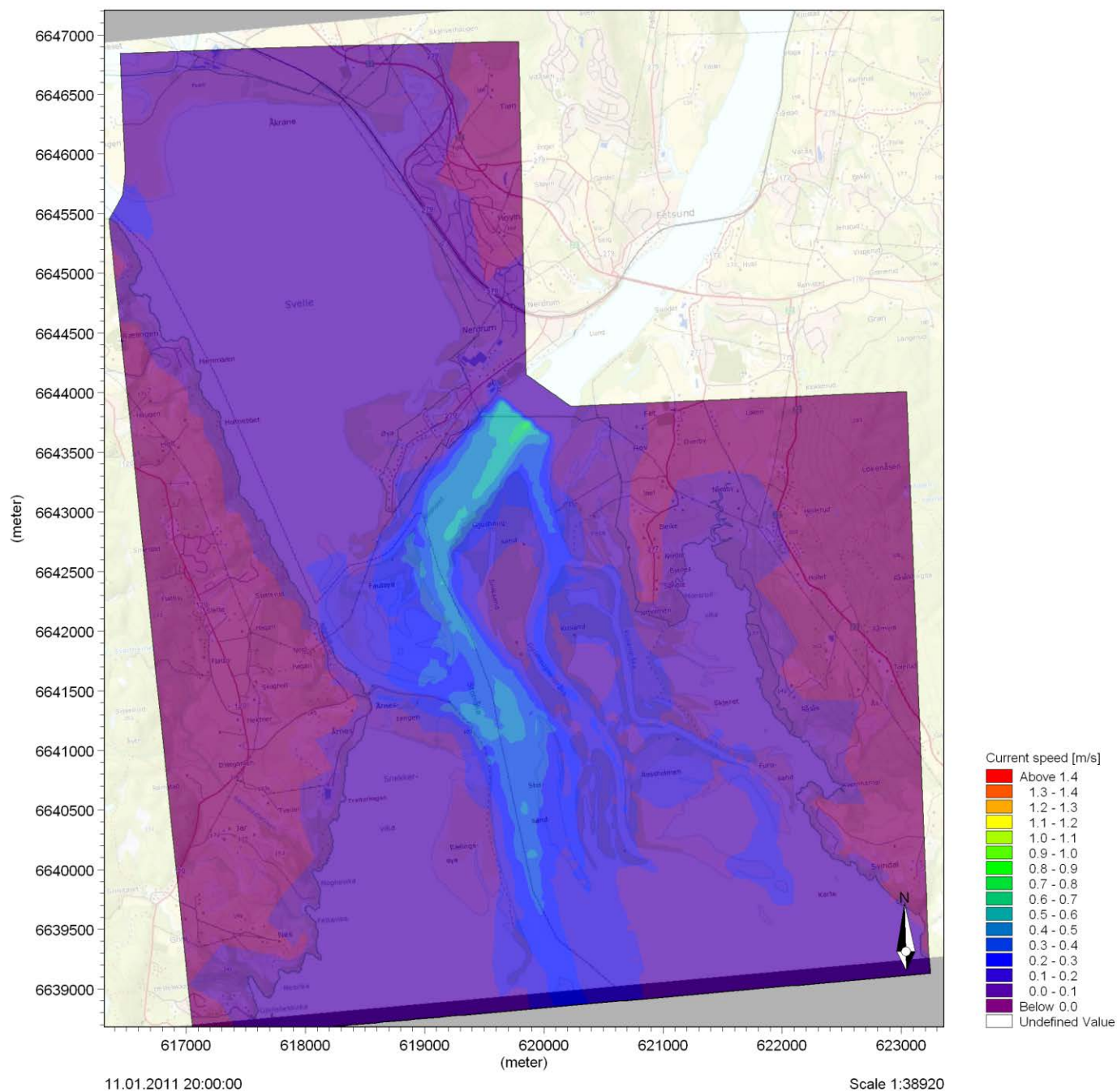


Figure 27. Simulated current speed (m/s) at Øyeren delta for scenario 2;  
Source: Statkart.no (2011) (background map).

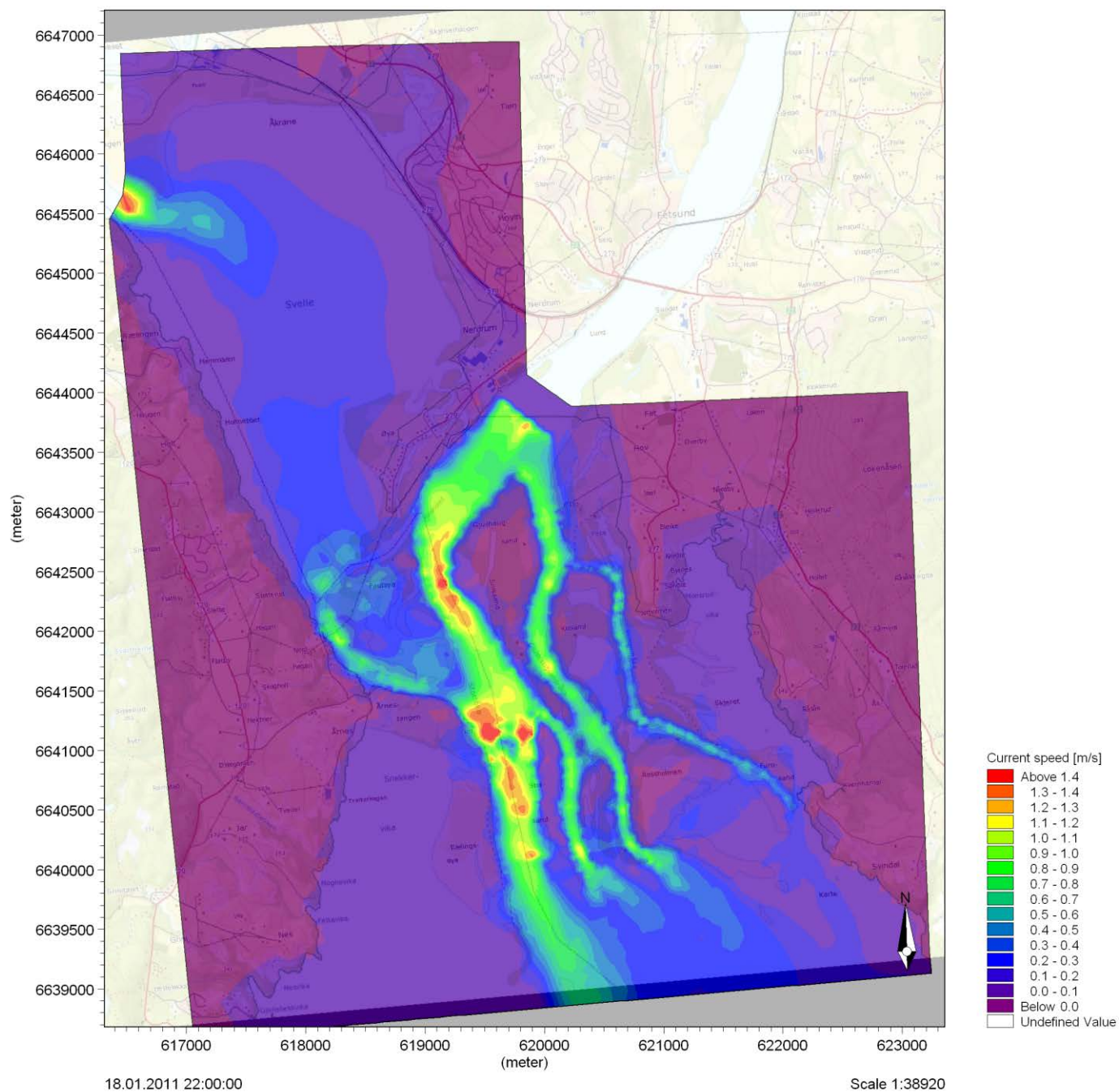


Figure 28. Simulated current speed (m/s) at Øyeren delta for scenario 3;  
Source: Statkart.no (2011) (background map).



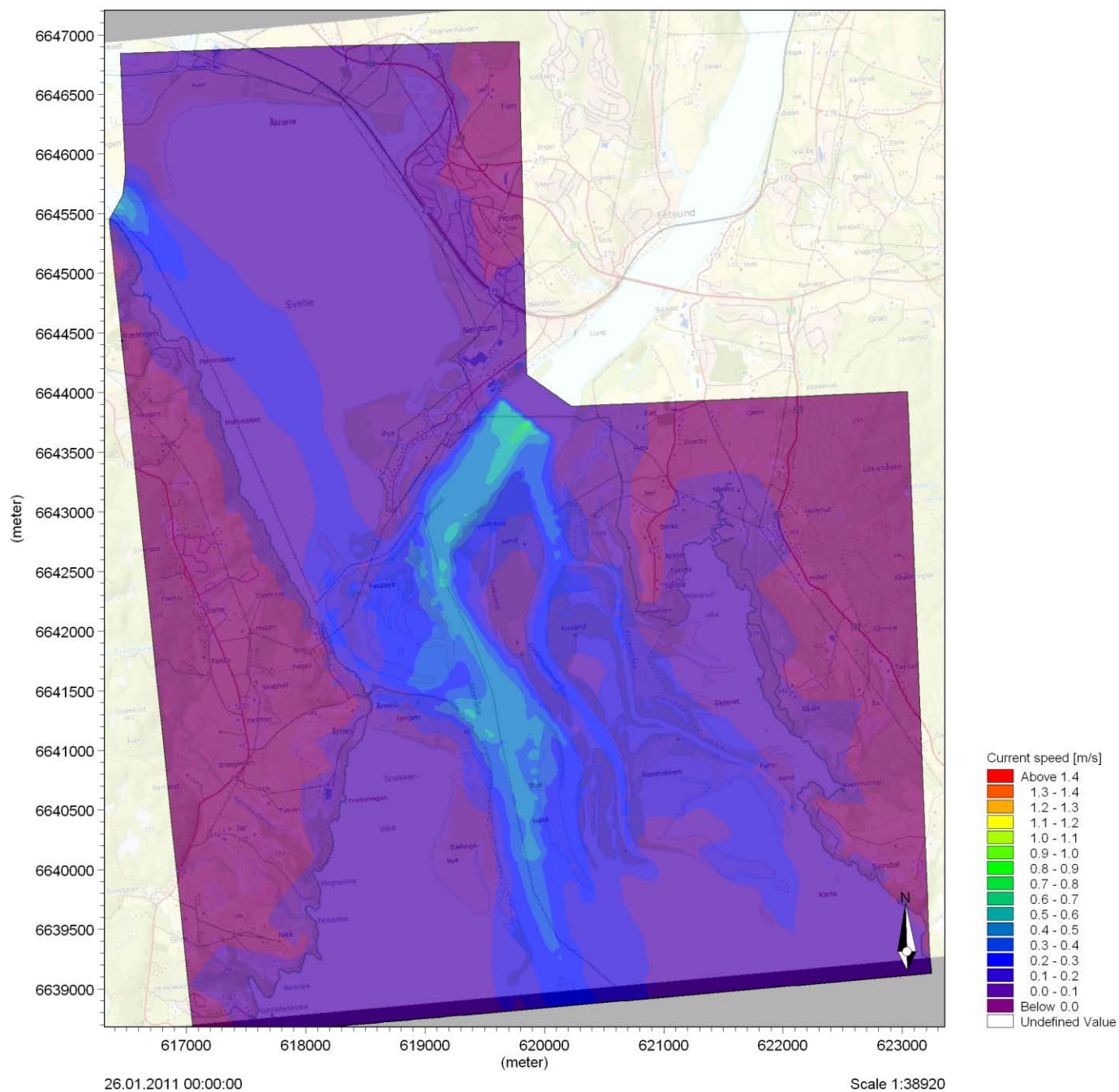


Figure 29. Simulated current speed (m/s) at Øyeren delta for scenario 4;  
Source: Statkart.no (2011) (background map).

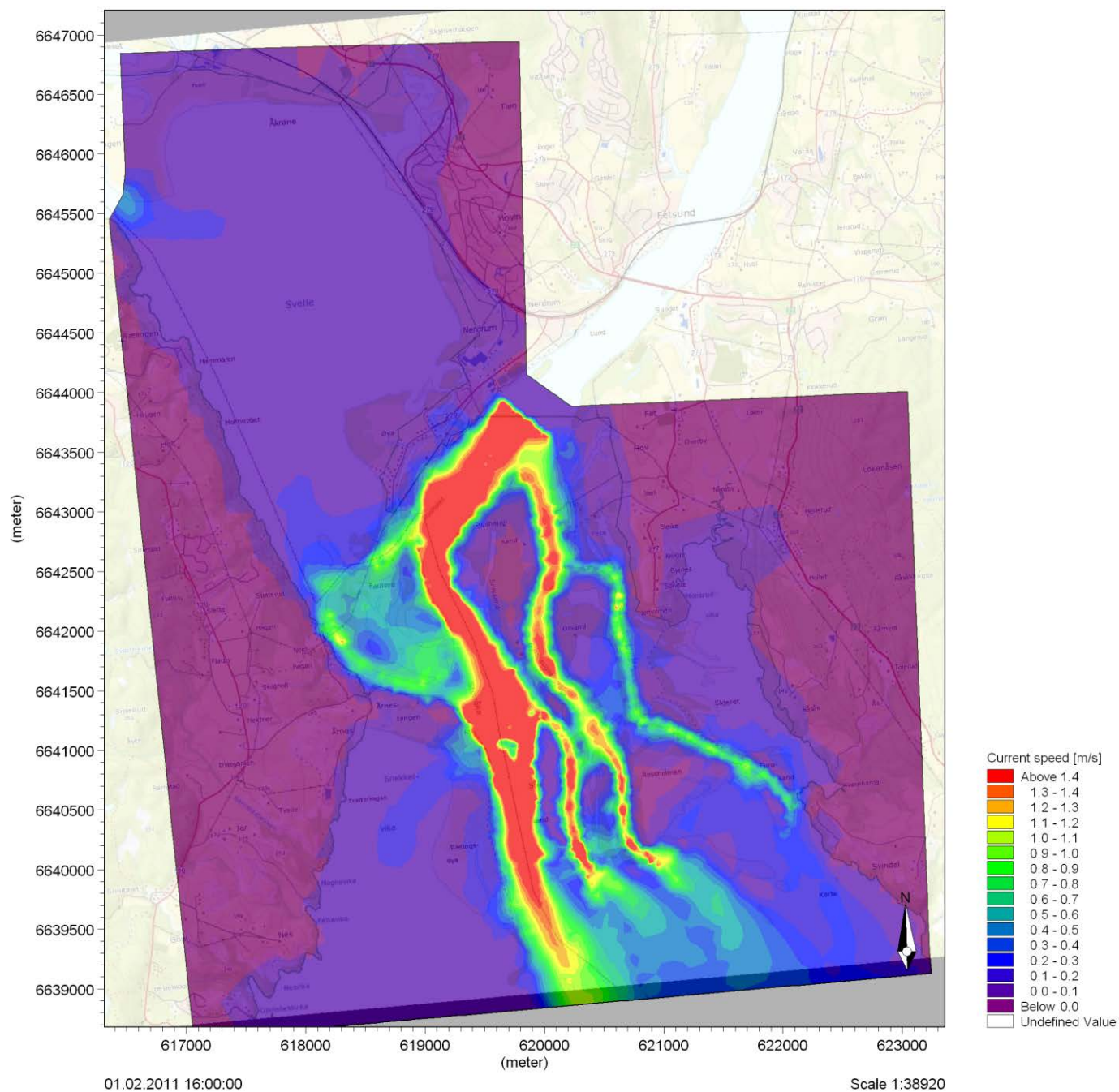


Figure 30. Simulated current speed (m/s) at Øyeren delta for scenario 5;  
Source: Statkart.no (2011) (background map).



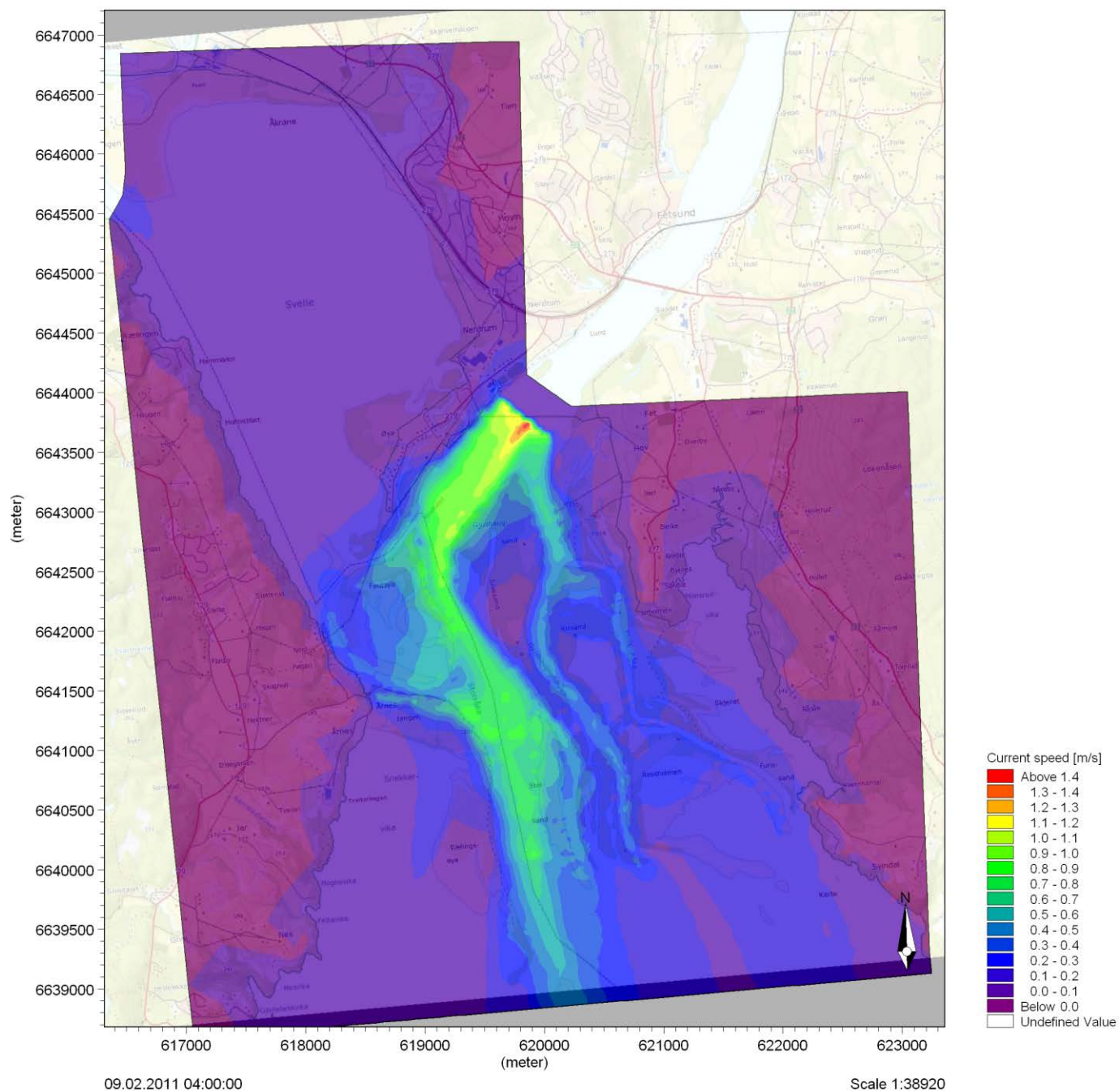


Figure 31. Simulated current speed (m/s) at Øyeren delta for scenario 6;  
Source: Statkart.no (2011) (background map).

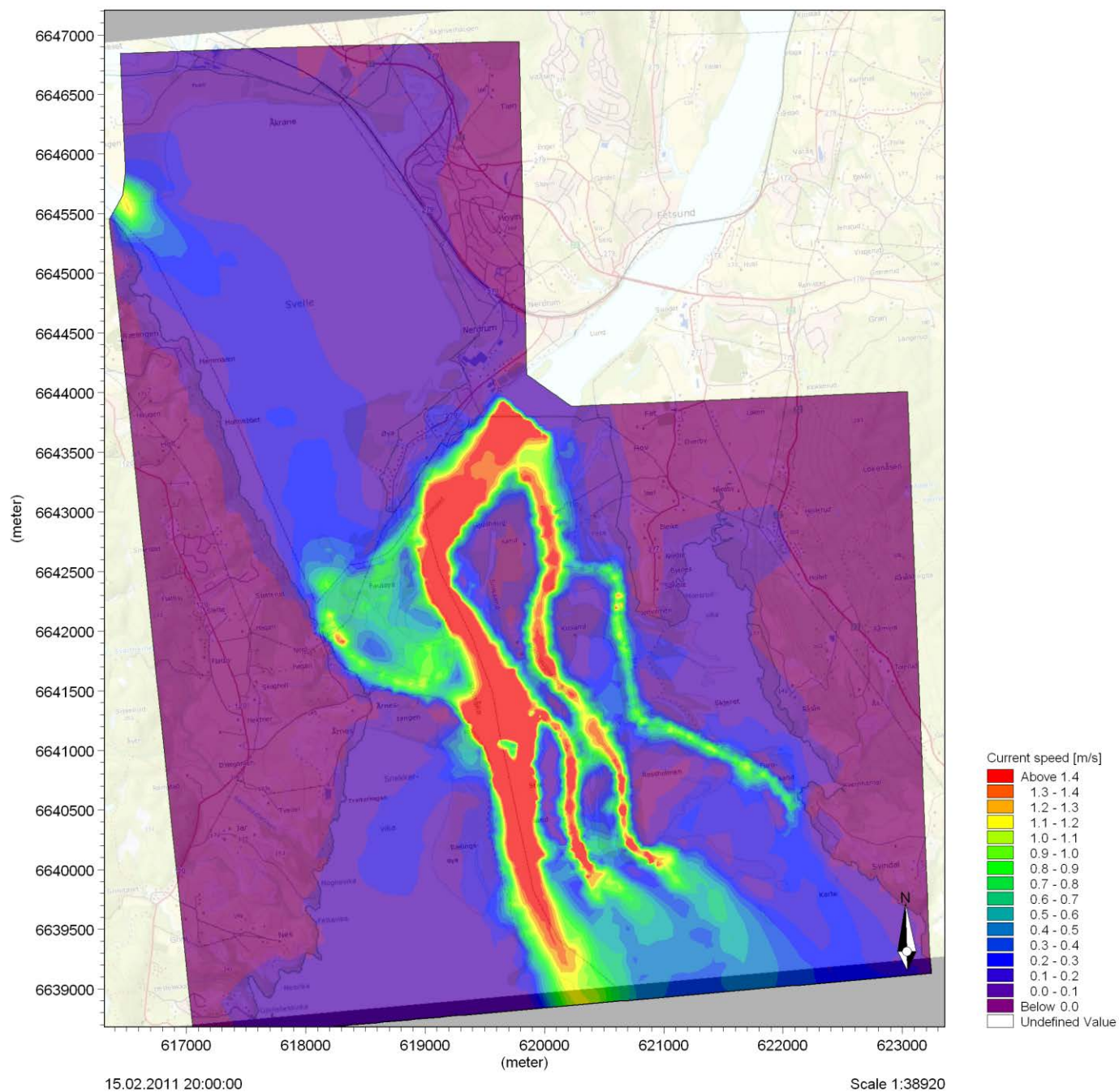


Figure 32. Simulated current speed (m/s) at Øyeren delta for scenario 7;  
Source: Statkart.no (2011) (background map).



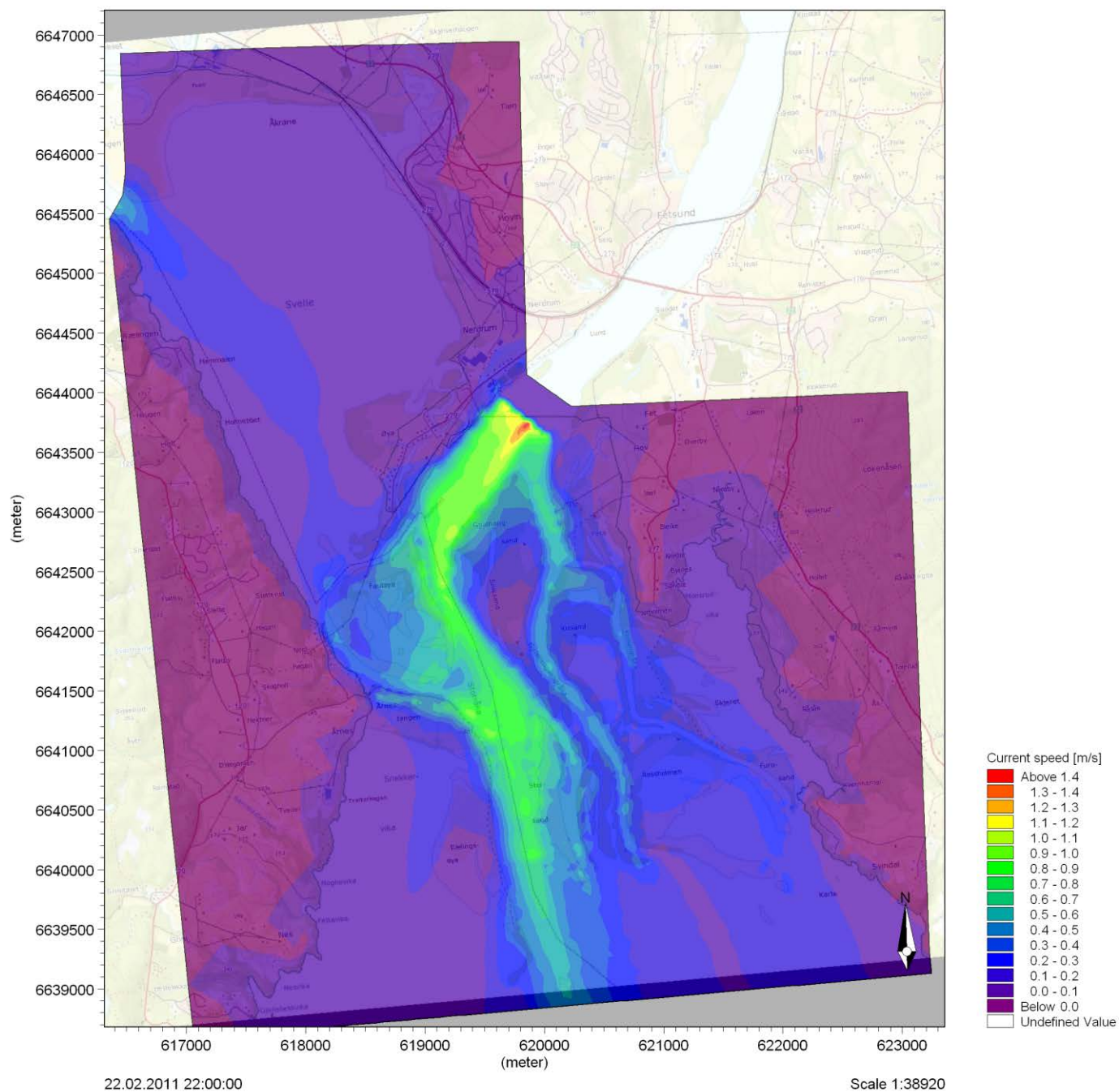


Figure 33. Simulated current speed (m/s) at Øyeren delta for scenario 8;  
Source: Statkart.no (2011) (background map).

## 6.5 Uncertainties

First, estimation of major uncertainties in flood management is shortly presented. Then the results of uncertainties due to sampling density, interpolation methods, precision of ADCP measurements and mesh resolution are provided.

### 6.5.1 Uncertainties in flood management

Estimation of the uncertainty is a major and vital challenge in flood management. There are several potential difficulties in hydrology studies that may lead to uncertainties. Some of them are presented below (Samuels et al. 2001):

#### Issues in uncertainty

- The number of modeling methods and the variation of their results
- The confidence of choice of Manning's  $n$
- Seasonal variability affecting vegetation
- Lack of adequate calibration data-errors in data
- Variations of parameters along a river reach

#### Gaps in knowledge

- Effect of vegetation - hedges - banks - bushes on flow levels and extent of flooding
- Interaction between the main channel and the floodplain

#### Barriers to uptake knowledge

- Lack of understanding and consensus of the best approach arising from lack of confidence in knowledge
- Tradition, risk from using the unfamiliar and inertia
- The time to do project work coupled to the cost of the project (i.e budget constraints)

### 6.5.2 Uncertainty results

The amount of uncertainty caused by the limited amount of data and the interpolation methods was assessed. To do this, two different areas were compared with the interpolation methods named in subsection 5.1.1; one with high sampling density and one with poor sampling density (Figure 34). Figure 35 indicates that the area with higher sampling density gives little variation in how different interpolation methods performed. However, Figure 36, showing the area with low sampling density, indicates high variation in how the bathymetry was interpolated. Here it was observed water depths differences up to the meter scale.



As mentioned earlier in model responses, the type of resolution mesh will also contribute deeply to the uncertainty of the output. Figure 37 displays a mesh describing the topography of the delta. It can be seen from this figure, how the delineation of the shoreline and mesh resolution can possibly influence model responses.

In addition, uncertainties in the model can be also caused by other different factors such as:

- ADCP's precision.
- The topography on the islands of the delta.
- The bathymetry in shallow water areas.
- Calibration regarding only one gauging station.

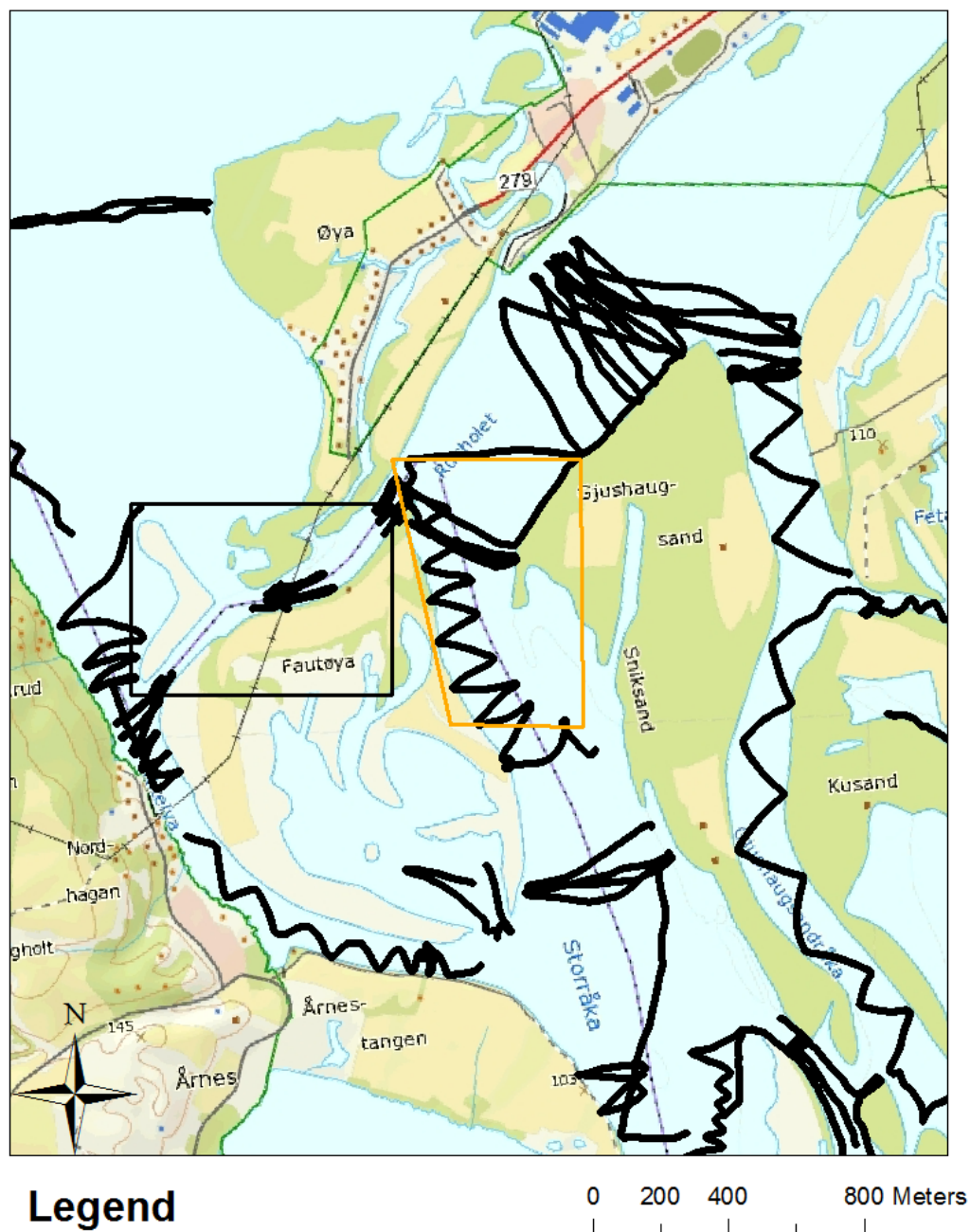


Figure 34. Location of the two different interpolated areas, areas with good and poor density sampling are enlarged respectively in Figure 35 and Figure 36;  
Source: Statkart.no (2011) (background map).

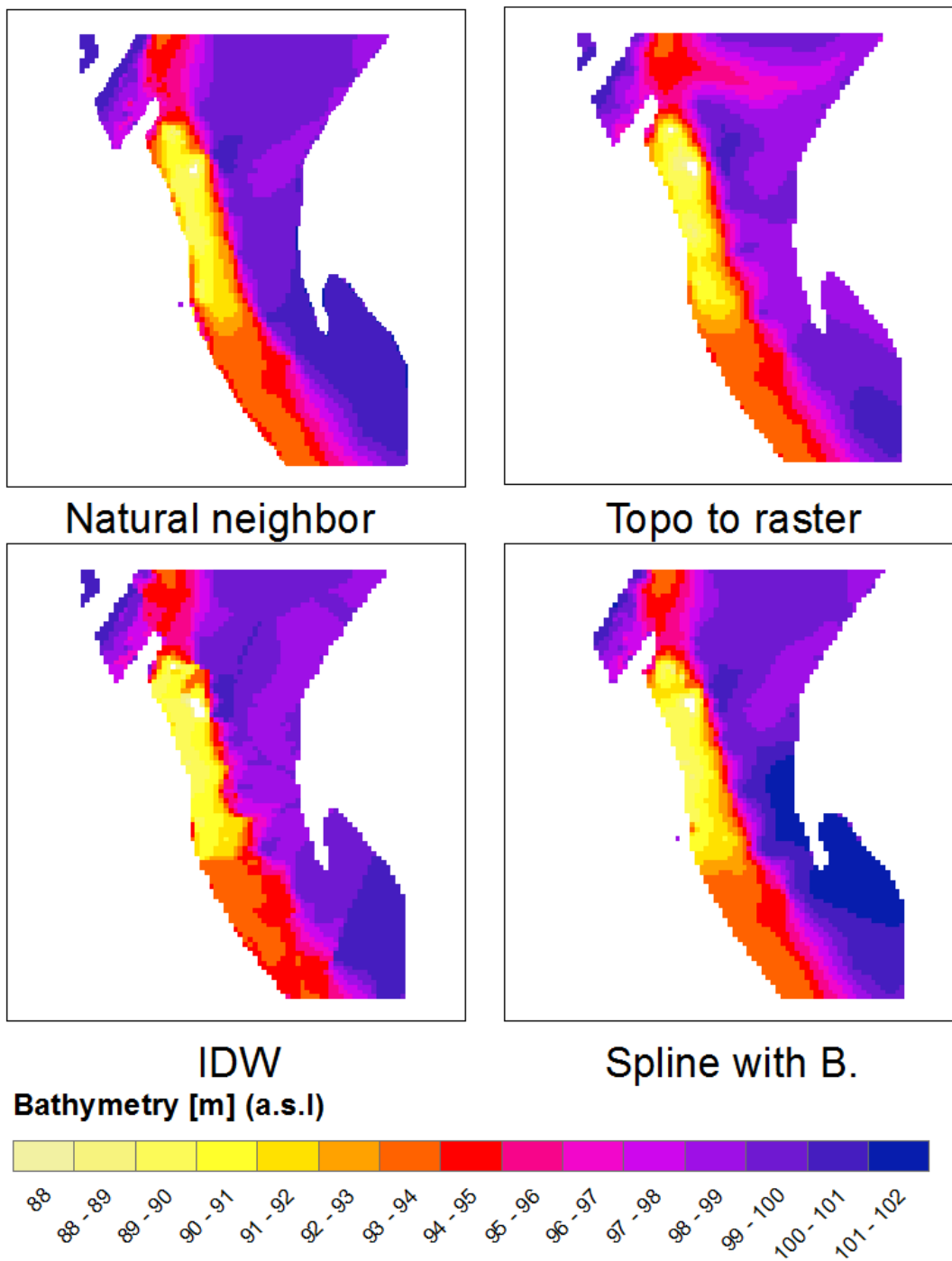
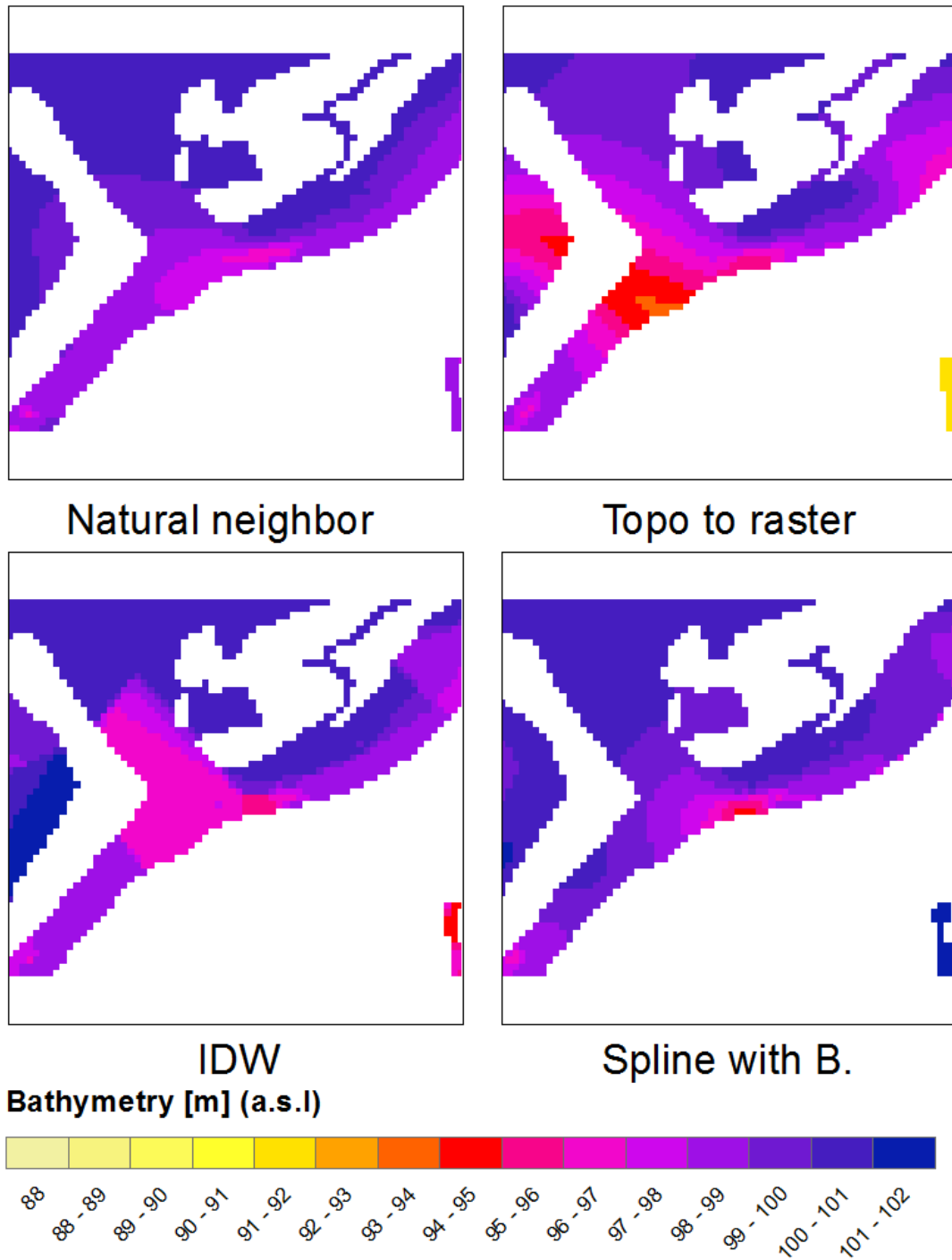
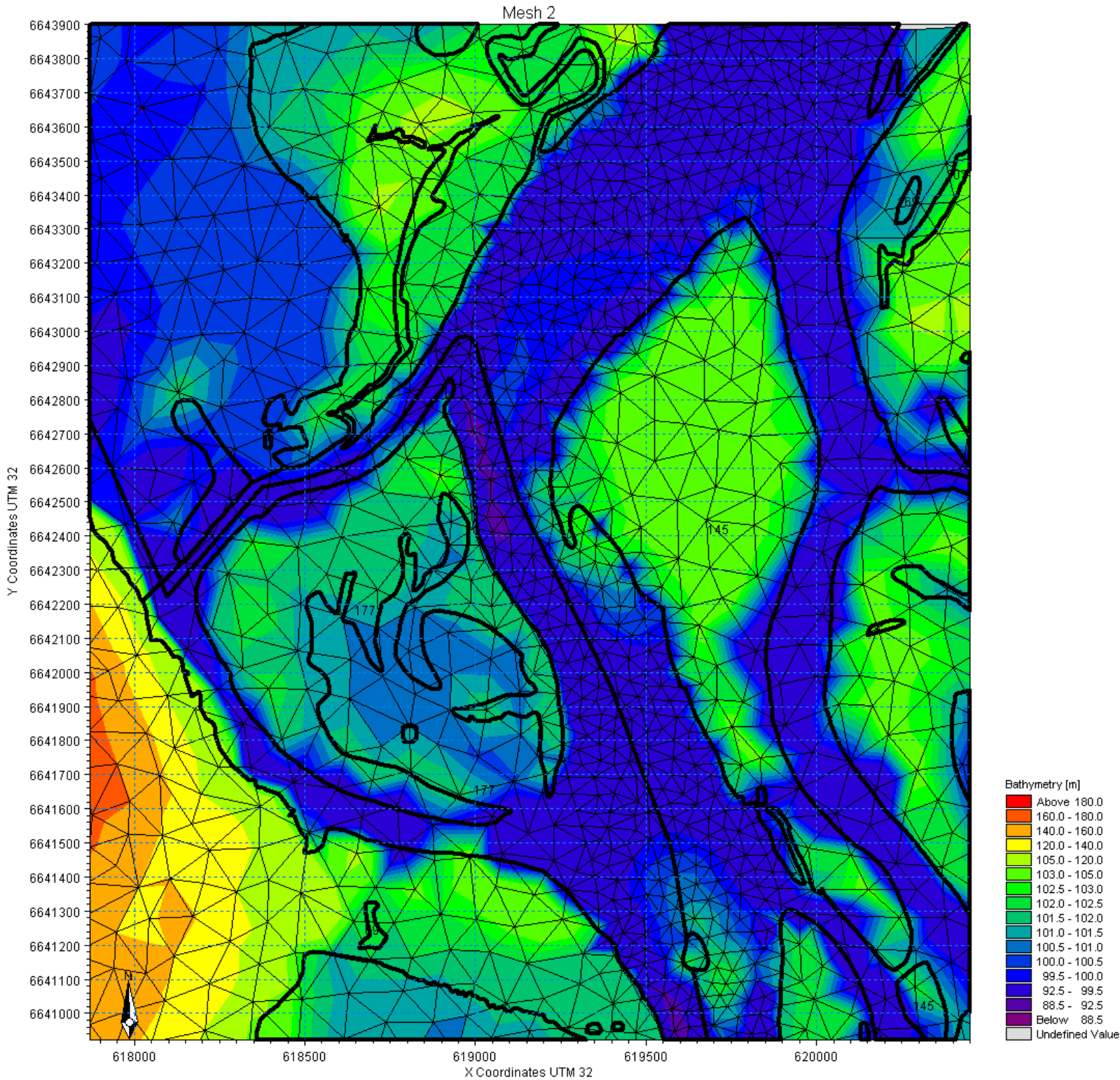


Figure 35. Interpolation of the bathymetry with Natural Neighbor, Topo to Raster, IDW, and Spline with barriers interpolation methods in an area with good sampling density.



*Figure 36. Interpolation of the bathymetry with Natural neighbor, Topo to Raster, IDW, and Spline with barriers interpolation methods in an area with poor density sampling.*



*Figure 37. Representation of the delta with a coarse mesh composed of elements describing the topography of the delta.*

## 7. Discussion

This section comments on methods and results of this thesis, starting with a discussion of choices made concerning interpolation methods and giving possible suggestions for better interpolation of limited bathymetry data. It continues with the presentation of results from the calibration, verification and model responses of MIKE FLOOD. The most and least sensitive parameters to tune during the calibration will be examined, with suggestions on approaches to create a mesh of an adequate and good resolution. In the subsection 7.4, discussion of the responses of the delta, subjected to 200-year discharges and water level will be given. In addition, the assessment of the validity of the assumption that water levels at Fetsund and Lillestrøm are equal will be completed.

### 7.1 Interpolation methods

The effects of sampling density and interpolation methods for scattered sample data were evaluated in this master thesis. The accuracy of the interpolated heights on the Digital Elevation Model (DEM) was assessed by the calibration and validation of interpolation methods with the help of bathymetry measurements. Four various types of techniques, namely IDW, Natural Neighbor, Spline with barrier and TopoGrid were applied. The best performing interpolation was the Inverse Distance Weighted technique. IDW gave the best results after parameterization, calibration and validation of the technique. Neglecting these steps can lead to higher errors. It has been observed that in area with good sampling density, interpolation methods performed equally well with RMSE ranging from 32 to 42 cm.

However, when looking at a poorly described areal, interpolation methods perform in various ways, having different interpretations of how the bathymetry should be interpolated. Water depths differences were up to the meter scale. As analyzed by Chaplot et al. (2006), greater sampling density tends to show lower impact of the interpolation, simply due to the decrease of space between sample points. Whereas for lower values of sampling density, observations indicate that the accuracy of the height estimation is more dependent on the choice of the interpolation techniques. There is a strong need for new interpolation methods that limit the uncertainties due to lower sampling density.

As mentioned in Merwade et al. (2006), topographic variability is greater transverse to the flow direction than along the flow direction. Use of interpolation methods that account for the anisotropic nature of a river channel bed, should be thus advised (e.g. with EIDW method, Merwade et al. 2006). Even though, it should perform better than other methods that are not considering the anisotropic nature of the river, a procedure for calibration and validation of other interpolation methods is advised, as different methods could possibly perform better depending on the terrain morphology and sampling density (Aguilar et al. 2005).

Spline with barrier method was chosen to interpolate heights in this study, due to the use of smoothing of the bathymetry. Smooth bathymetry limits possible uncertainties due to irregular representation of the river bed channel. Even though data was limited in this study, extrapolation of the 50000 ADCP points gave satisfying results. When tested with the bathymetry map used in the study conducted by Zinke et al. (2010), 70% of the points were in an interval  $[-1; 1]$  m (Figure 17). Although a good agreement, the readers need to be aware that the quality of the test bathymetry map is uncertain due to collection of data from different sources (see subsection 5.1.1). In addition areas with lower sampling density will tend to have a much higher uncertainties, leading to possible major errors. It has been understood throughout this section, that choosing an appropriate interpolation methods is a critical step, particularly in study with limited data collection.

## 7.2 Verification

MIKE FLOOD was calibrated using water level data at Nordhagan for the period of 15<sup>th</sup> June to 25<sup>th</sup> of June, 1999. During the process Manning's  $n$  were adjusted to match simulated and observed water levels. The verification was realized for the period of 25<sup>th</sup> of June to 15<sup>th</sup> of August, 1999. Calibrated and simulated values showed an overall good agreement with a Nash and Sutcliffe model efficiency coefficient equal to 0.98. A better agreement was observed for water levels higher than 101.7 m a.s.l. Whereas, deviations between 3 to 10 cm were observed for lower water levels. This pattern could be explained by a calibration of the model for water levels higher than 102 m a.s.l. Higher gaps between the observed and simulated water levels are accounted for the constant influence of water level and discharge on Manning's  $n$ .

Although MIKE FLOOD simulated successfully water levels at Nordhagan, the quality of the model was difficult to assess. If the model is a good predictor of water levels, then it should be a good predictor of the flood extent. However, as reported by Horritt and Bates (2001), when only using hydrometric data for model calibration, errors in model performances may not be apparent, hence the necessity to calibrate and validate the model regarding to the flood extent.

## 7.3 Model responses

Sensitivity analysis was performed over a short time scale by comparing the responses of the model to different parameters during a period of 10 days, corresponding to the calibration period. It is however known that a sensitivity analysis can be a time consuming process, especially with the use of new numerical models. Due to the limitations in terms of run of simulations, results were later assumed to be more correctly referred as model responses. Nevertheless, it did not prevent a conclusion to be drawn about model sensitivity regarding Manning's  $n$ , mesh resolution, eddy viscosity and  $dX$ .

### 7.3.1 Mesh resolution

In this study, MIKE FLOOD showed a great sensitivity to mesh resolution, with root mean square error of 50 cm for the coarser mesh (Mesh 1). The results presented here confirm some of the observations usually made for mesh resolution. Use of a coarse mesh includes risk to oversimplify areas, cut-off narrow channels and small scale features. Moreover, delineation between the water channel and the shoreline caused uncertainties for channels geometry (see Figure 37). Due to limited data, examination of the spatial resolution on floodplains was not possible. Consequently, differences between mesh 2, 3 and 4, were only controlled by the size of elements in the channels and the form of the elements (triangular or rectangular). Mesh 3 gave the best result, with fine triangular elements in the channel. The use of slightly finer elements in the channel and rectangular elements in water channels did not improve results as seen with Mesh 4.

An increase of model performance with increasing spatial resolution can be underlined in this study. Further augmentation in spatial resolution would have been possible in the mesh studied, but was considered to be computationally unreasonable. Development of an adequate mesh, and appropriate resolution should be done regarding several factors: i) the nature of the study (i.e floodplain modeling, flow distribution, sediments transport) ii) that areas of high importance should be represented with a high resolution and iii) that a mesh with a feasible required computational time should be created.

### 7.3.2 Hydraulic roughness

Evaluation of the uncertainty of the roughness was also provided in the observation of the model responses. Manning's  $n$  value was originally set to 0.038. After calibration and validation of the roughness parameter, the value was found to be optimized at 0.018. The value found by optimization can be defined as relatively low, when considering the large scale bed forms observed by Eilertsen and Hansen (2008). It is known that models simplify processes in nature, even with the use of more complex numerical models as MIKE FLOOD. Manning's  $n$  will as result often have discrepancies between calibrated model values and roughness which would have been estimated based on the nature of the channel and observation of influencing factors (Pappenberg et al. 2004, Werner and Lambert 2007). Table 11 shows a limited influence of the roughness parameter, when compared to mesh resolution. Ideally, a complete sensitivity analysis would have been required to fully observe the impact of the calibration of Manning's  $n$  in the water channel. It is however known and reported that a detailed description and calibration of the roughness parameters, both in water channel and floodplains is required to represent well processes in the nature (Horritt and Bates 2002, Horritt et al. 2007).



### 7.3.3 Eddy viscosity and dX

Additional parameter responses, were also considered such as eddy viscosity, which is modelled by the Smagorinsky formulation, and the distance in between discharge's and water level's calculation points in MIKE 11 set up (dX). Both parameters showed a small control on the model responses. Nevertheless, both parameters may influence the results in cases where: i) important loss of energy due to eddies occur and ii) the source of MIKE 21 grid is provided by a long MIKE 11 reach.

Observation of model responses and different interpolation techniques demonstrate that simulation of water levels and flood extent is strongly controlled by three main factors : i) the topography, ii) the mesh resolution and iii) the roughness parameter. A good representation of these factors is necessary to greatly improve the performance of the model.

## 7.4 Scenario simulations

The calibrated and validated MIKE FLOOD model was used to simulate the flood inundation, water levels and water velocities caused by floods of different magnitudes in the region of Øyeren delta. Investigations of the response of the delta to different scenarios are discussed in these subsections. Results were used to analyze the response of the delta to different scenarios, and then a conclusion over the assumption made behind flood zone maps at Lillestrøm was accomplished.

### 7.4.1 Flood extent

During median water stage at the downstream boundary of the model, the flood extent was observed to be approximately corresponding to 90% of inundated areas in the delta. For 200-year return period water level, simulations showed a complete inundation of the area. A comparison of scenarios with flood zone map from NVE was made. These flood zone maps show only the area inundated due to a 10-year or a 200-year return period flood. In both cases, total inundations of the delta are predicted by the flood zone maps. Even if direct comparisons are difficult, MIKE FLOOD indicates a credible representation of the flood extent. The model may therefore predict inundated areas well, but further validation of the flood extent with respect to satellite pictures is required to correctly assess the model performance.

### 7.4.2 Water level

The water level pattern indicated that the magnitude of the water surface gradients actually controlled the water level differences between Fetsund and Lillestrøm. Considerable water gradients are caused by an abrupt increase or decrease of water levels upstream, while water

levels downstream are low or high respectively. The hypothesis made by NVE in 2005 that water levels are comparable, is highly violated, water levels difference being as much as 33 centimetres in scenario 5. During high water surface gradients, large discharges at Leira+Nittelva caused a decrease in the water level differences, higher discharges attenuating slightly the deviation (24 centimeters, scenario 7). For other scenarios, water level gradients were lower, causing differences in water levels to range from 1 to 11 cm. It was observed that gradients tend to be smaller when the water level of Øyeren Lake was originally high (e.g. with scenario 2, 4, 6 and 8).

Interaction between Svellet and the delta occurred for simulations where large discharges were provided by Leira and Nittelva. It was possible to observe that the water surface of Svellet rose 1 to 2 centimeters higher than the water stage at Lillestrøm. This difference demonstrates that the water surface of the earlier shallow pond rose and interacted with the rest of the delta.

Model runs indicate three main patterns concerning the water level:

- The difference in the water levels at Fetsund and Lillestrøm is controlled by the magnitude of the water level gradient.
- Water levels at Lillestrøm are mainly controlled by Øyeren Lake, or more precisely by Solbergfoss.
- Large discharges at Leira and Nittelva cause the interaction of Svellet with the delta (water level 1-2 cm higher at Svellet than at Lillestrøm).

### 7.4.3 Velocity

Scenario simulations gave an overview over the pattern of water velocities within the delta. Highest velocities occurred for scenarios with highest difference in water levels (Scenario 5 and 7). High velocities were generated from high water level gradients, causing averaged velocities over 1.4 m/s in the delta. Low velocities were observed for scenarios with high water level and low gradients (Scenario 2 and 4). Whereas, Moderate velocities were observed for scenarios with return-period discharges and water levels of the same order, corresponding to moderate water gradients (Scenario 1, 3, 6 and 8). In addition, interaction with Svellet caused higher current speed in the western part of the delta. Velocities were here increased in average by 1 to 2 m/s.

Comparison of velocities, simulated and observed, made in Øyeren delta, is a good indicator of the quality of the model to reproduce velocities in the delta. It was found a good agreement with the highest velocities at the deepest points of the delta. Scenario 1 showed a good agreement with areas exposed to a higher erosion in the delta.

To summarize, the simulations indicate two main patterns concerning velocities in the delta:

- Velocities are also controlled by the amplitude of the water gradient.
- Interaction between Svellet and the delta influence exclusively the western part of the delta.

## 7.5 Summary of the scenario simulations

In this study, several simulated scenarios were observed to determine the main patterns concerning the flood extent, the water stage and the velocities. As reported by Bogen and Bønsnes (2002), the worst case scenario was also here observed to be a rapid increase or decrease in the variation of the water surface gradient. Under these circumstances, high surface gradients were accompanied with high velocities, hence also increasing the risk of the degradation of the delta by erosion. In addition, the assumption made behind the creation of flood zone maps at Lillestrøm tended to be conservative with 33 cm overestimation of the water levels at Lillestrøm.

A special focus of this study was to assess the validity of the assumption by the development of a more advanced hydrodynamic model. As mentioned earlier, the one-dimensional set up extending from Bingsfoss to Mørkfoss simplifies the complex system of islands, lagoons and distributary channels. In this simplified approach, water levels for the area of Svellet and Lillestrøm were only represented by one water level at a cross section within the delta. The use of a more advanced numerical method shows considerable differences in water levels in the model area, proving the validity of this method. Moreover, MIKE FLOOD shows to be a reliable and credible modeling tool to reproduce the main patterns already observed and reported in the delta. Model runs showed that the reservoir operational practices for Bingsfoss, Rånåsfoss and Solbergfoss should avoid high water surface gradients in the delta, to limit the damage due to erosion. However, conclusions about appropriate flood management measures were not the scope of this study.

## 8. Conclusion

The present study aimed to develop a 1D-2D coupled hydrodynamic model for the Øyeren delta. The model chosen and the data gathered, provided an appropriate test of a coupled one and two-dimensional floodplain flow modeling for the area. A methodology for the set up of the model was followed throughout this study, based on a systematic calibration and validation of several interpolation methods, and observation of model responses for different mesh resolutions and model parameters.

The assessment of the model responses regarding known sources of uncertainties has given a good overview over requirements to the data to increase quality and accuracy of flood extent models. Selection of appropriate techniques and procedures concerning the interpolation methods has shown to be a critical step, especially in studies with a limited amount of data. Verification of the model for a period of approximately two months has demonstrated a good representation of observed water levels at Nordhagan. In addition, assessment of MIKE FLOOD responses has tended to point less sensitivity to Manning's  $n$  values and more sensitivity to mesh resolution.

Known limitations did not prevent useful evaluation of flood responses of the delta. MIKE FLOOD was successfully used to compute water levels and velocities, the output being in accordance with the measurements observed in the delta (Bogen and Bønsnes 2002, Bogen et al. 2002). The use of a more advanced numerical tool to simulate hydraulic processes in the delta has been valuable. The hypothesis realized during the construction of the flood maps at Lillestrøm indicates that it is too conservative during high water surface gradients, showing a maximum water level difference of 33 cm, when compared with Fetsund.

Even though the model performs well, the satellite photos should in the future be required to validate the performance of the model regarding to the flood extent. In addition, simulation of observed events under unsteady condition and a better description of the terrain morphology should be considered. However, the study is sufficiently encouraging to continue further development of coupled one and two-dimensional floodplain flow modeling. If developed further and extended to other areas in Norway, this model could greatly assist decision in flood management.

## 9. Notation

$C$ : Weir coefficient (1.838) [ $\text{m}^{1/2}/\text{s}$ ]

$C_R$ : Courant's number [-]

$dX$ : Distance between discharge's and water level's calculation points in MIKE 11 set up [ $\text{m}$ ]

$g$ : Gravitational constant [ $\text{m}^2/\text{s}$ ]

$h_1$ : Depth of water above weir level upstream [ $\text{m}$ ]

$h_2$ : Depth of water above weir level downstream [ $\text{m}$ ]

$k$ : Exponential coefficient (1.5) [-]

$M$ : Manning's  $M$  [ $\text{s}/\text{m}^{1/3}$ ]

$n$ : Manning's  $n$  [ $\text{s}/\text{m}^{1/3}$ ]

$Q$ : Discharge [ $\text{m}^3/\text{s}$ ]

$q$ : Lateral inflow [ $\text{Q}/\text{m}$ ]

$R$ : Hydraulic radius [ $\text{m}$ ]

$S$ : Value of Smagorinsky parameter [-]

$S_o$ : Channel slope [-]

$S_e$ : Energy slope [-]

$v$ : Velocity [ $\text{m}/\text{s}$ ]

$w$ : Water surface width [ $\text{m}$ ]

$Y$ : Mean depth [ $\text{m}$ ]

$y$ : Water depth [ $\text{m}$ ]

$\Delta t$ : Time step [ $\text{s}$ ]

$\Delta x$ : Grid spacing [ $\text{m}$ ]

$\frac{\partial Q}{\partial x}$ : Downstream rate of change of discharge [ $\text{Q}/\text{m}$ ]

$\frac{\partial Y}{\partial t}$ : Time rate change of depth [ $\text{m}/\text{s}$ ]

## 10. References

- Abbott, M. B., Ionescu, F. (1967). "On the Numerical Computation of Nearly Horizontal Flows." *Journal of Hydraulic Research* 5(2): 97-117.
- Abbott, M. B., Rasmussen, C. H. (1977). On the Numerical Modelling of Rapid Contractions and Expansions in Models that are Two-dimensional in Plan. Proc. 17 th Congress IAHR. Baden-Baden, Germany.
- Aguilar, F. J., Aguera, F., Aguilar, M. A., Carvajal, F. (2005). "Effects of Terrain Morphology, Sampling Density, and Interpolation Methods on Grid DEM Accuracy." *Photogrammetric engineering and remote sensing* 71(7): 805-816.
- Bates, P. D., De Roo, A. P. J. (2000). "A simple raster-based model for flood inundation simulation." *Journal of Hydrology* 236: 54-77.
- Bates, P. D., Lane, S. N., Ferguson R. I. (2005). *Computational Fluid Dynamics: Applications in Environmental Hydraulics*. Chichester, England: John Wiley & Sons, Ltd.
- Bogen, J., Bønsnes, T. (2002). "The impact of reservoir regulation on the processes of erosion and sedimentation of the delta in Lake Øyeren, Norway." *IAHS* 276.
- Bogen, J., Bønsnes, T., Elster, M. (2002). *Miljøfaglige undersøkelser i Øyeren 1994-2000. Erosjon, sedimentasjon og deltautvikling. Norges vassdrags- og energidirektorat (NVE)*. Oslo.
- Chaplot, V., Darboux, F., Bourennane, H., Leguedois, S., Silvera, N., Phachomphon, K. (2006). "Accuracy of interpolation techniques for the derivation of digital elevation models in relation to landform types and data density." *Geomorphology* 77: 126-141.
- Chow, V. T. (1959). *Open-Channel Hydraulics*. New York: McGraw-Hill.
- Connell, R. J., Painter, D. J., Beffa, C. (2001). "Two-Dimensional Floodplain Flow. Model Validation." *Journal of Hydrologic Engineering* September 2001: 406-414.
- DHI(2011a). "MIKE11 reference manual"  
[http://www.hydroeurope.org/jahia/webdav/site/hydroeurope/shared/Teams-2011/team1/Manuals/Mike\\_11\\_ref.pdf](http://www.hydroeurope.org/jahia/webdav/site/hydroeurope/shared/Teams-2011/team1/Manuals/Mike_11_ref.pdf). Accessed the 27/05/2011.
- DHI (2011b). "MIKE 21 Flow model."  
[http://www.hydroasia.org/jahia/webdav/site/hydroasia/shared/Document\\_public/Project/Manuals/WRS/MIKE21\\_HD.pdf](http://www.hydroasia.org/jahia/webdav/site/hydroasia/shared/Document_public/Project/Manuals/WRS/MIKE21_HD.pdf). Accessed the 27/05/2011.

DHI (2011c). "MIKE FLOOD user manual."

[http://www.hydroasia.org/jahia/webdav/site/hydroasia/shared/Document\\_public/Project/Manuals/WRS/MIKE\\_FLOOD\\_UserManual.pdf](http://www.hydroasia.org/jahia/webdav/site/hydroasia/shared/Document_public/Project/Manuals/WRS/MIKE_FLOOD_UserManual.pdf). Accessed the 27/05/2011.

Dingman, S. L. (1984). Fluvial Hydrology. New York: W. H. Freeman.

Earth.Science.Australia (2011). "Streams and Drainage."

<http://earthsci.org/education/teacher/basicgeol/stream/stream.html>. Accessed the 27/05/2011.

Eilertsen, R. S., Hansen, L. (2008). "Morphology of river bed scours on a delta plain revealed by interferometric sonar." *Geomorphology* 94: 58-68.

ESRI (2011). "ArcGIS." <http://www.esri.com/>. Accessed the 27/05/2011.

ESRI (2011). "How Topo To Raster work."

[http://help.arcgis.com/en/arcgisdesktop/10.0/help/index.html#/How\\_Topo\\_to\\_Raster\\_works/](http://help.arcgis.com/en/arcgisdesktop/10.0/help/index.html#/How_Topo_to_Raster_works/). Accessed the 27/05/2011.

GeoNorge (2011). "Norge Digital " <http://www.geonorge.no/geonetwork/srv/no/main.home>. Accessed the 28/05/2011.

Gjerde, H. (2006). "Naturfotograf Harald Gjerde " <http://www.naturfotograf.info/>. Accessed the 27/05/2011.

Hammersmark, C. T. (2003). Hydrodynamic Modeling and GIS Analysis of the Habitat Potential and Flood Control Benefits of the Restoration of a Leveed Delta Island. *Hydrology*. Davis, University of California. Master Thesis: 1-102.

Hardy, R. J., Bates, P. D., Anderson, M. G. (1999). "The importance of spatial resolution in hydraulic models for floodplain environments." *Journal of Hydrology* 216: 124-136.

Horritt, M. S., Bates P. D. (2001a). "Effects of spatial resolution on a raster based model of flood flow." *Journal of Hydrology* 253: 239-249.

Horritt, M. S., Bates P. D. (2001b). "Predicting floodplain inundation: raster-based modelling versus the finite-element approach." *Hydrological Processes* 15: 825-842.

Horritt, M. S., Bates P. D. (2002). "Evaluation of 1D and 2D numerical models for predicting river flood inundation." *Journal of Hydrology* 268: 87-99.

Horritt, M. S., Bates P. D., Mattinson, M. J. (2006). "Effects of mesh resolution and topographic representation in 2D finite volume models of shallow water fluvial flow." *Journal of Hydrology* 329: 306-314.

- Horritt, M. S., Di Baldassarre, G., Bates, P. D., Brath, A. (2007). "Comparing the performance of a 2-D finite element and a 2-D finite volume model of floodplain inundation using airborne SAR imagery." *Hydrological Processes* 21: 2745-2759.
- Hunter, N. M., Bates, P. D., Horritt, M. S., De Roo, A. P. J., Werner, M. G. F. (2005a). "Utility of different data types for calibrating flood inundation models within a GLUE framework." *Hydrology and Earth System Sciences* 9(4): 412-430.
- Hunter, N. M., Bates, P. D., Horritt, M. S., Wilson, M. D. (2007). "Simple spatially-distributed models for predicting flood inundation : A review." *Geomorphology* 90: 208-225.
- Leopold, L. B., Maddock, T. Jr. (1953). "The Hydraulic Geometry of Stream Channels and Some Physiographic Implications." U.S. Geological Survey Professional Paper 252: 1-64.
- Menendez, A. N. (2001). Modelling Flow through Physical Connections across Floodplains with Environmental Restrictions. International Symposium on Environmental Hydraulics.
- Merwade, V. M., Maidment, D. R., Goff, J. A. (2006). "Anisotropic considerations while interpolating river channel bathymetry." *Journal of Hydrology* 331: 731-741.
- MET.no (2011). "eklima.no - Mean monthly temperature at Lillestrøm." <http://www.eklima.no>. Accessed the 28/05/2011.
- Nash, J. E., Sutcliffe, J. V. (1970). "River flow forecasting through conceptual models, part I - A discussion of principles." *Journal of Hydrology* 10(3): 282-290.
- Nicholas, A. P., Mitchell, C. A. (2003). "Numerical simulation of overbank processes in topographically complex floodplain environments." *Hydrological Processes* 17: 727-746.
- NGU (2011). "Norwegian Geology for Society." <http://www.ngu.no>. 27/05/2011.
- NVE (2011). "Norges vassdrags- og energidirektorat." <http://www.nve.no>. 27/05/2011.
- Olsen, N. R. B. (1994). SSIIM - A three-dimensional numerical model for simulation of water and sediment flow. HYDROSOFT-94. Porto Carras, Greece.
- Pappenberger, F., Beven, K., Horritt, M., Blazkova, S. (2004). "Uncertainty in the calibration of effective roughness parameters in HEC-RAS using inundation and downstream level observations." *Journal of Hydrology* 302: 46-69.
- Patro, S., Chatterjee, C., Mohanty, S., Singh, R., Raghuwanshi, N. S. (2009). "Flood Inundation Modeling using MIKE FLOOD and Remote Sensing Data." *Indian Soc. Remote Sens.* 37: 107-118.
- Petersen, O., Rasmussen, E. B., Enggrob, H., Rungø, M. (2002). "Modelling of Flood Events Using Dynamically Linked 1-D and 2-D Models." DHI Water & Environment.



- Petterson, L. E. (2005). Flomberegning for Leira (002.CAZ). Oslo, Norges vassdrags- og energidirektorat (NVE).
- Pridal, D. B., Remus, J. I., Boys, P. M. (2007). Two-Dimensional Modeling Applications for Use with Missouri River Restoration. World Environmental and Water Resources Congress, ASCE.
- Rungø, M., Olesen, K. W. (2003). "Combined 1- and 2- Dimensional Flood Modelling." DHI Water & Environment.
- Rørslett, B. (2002). Miljøfaglige undersøkelser i Øyeren 1994-2000. Oslo, NIVA - Norsk institutt for vannforskning.
- Samuels, P. G., Bramley, M. E., Evans, E. P. (2002). "Reducing Uncertainty in Conveyance Estimation."
- Soot, A. (2007). Flomberegning for Nitelva. Oslo, Norges vassdrags- og energidirektorat (NVE).
- Statkart.no (2011). "Background maps." <http://www.statkart.no/>. Accessed the 27/05/2011.
- Tayefi, V., Lane, S. N., Hardy, R. J., Yu, D. (2007). "A comparison of one- and two-dimensional approaches to modelling flood inundation over complex upland floodplains." John Wiley & Sons, Ltd 21(Hydrological Process): 3190-3202.
- Teledyne, R. D. I. (2006). "Workhorse Rio Grande ADCP." [http://www.rdinstruments.com/datasheets/rio\\_grande\\_ds\\_lr.pdf](http://www.rdinstruments.com/datasheets/rio_grande_ds_lr.pdf). Accessed the 27/05/2011.
- Teledyne, R. D. I. (2011). "ADCP " <http://www.ADCP.com/>. Accessed the 27/05/2011.
- Terratec (2011). "Terratec." <http://www.terratec.no>. Accessed the 27/05/2011.
- Tuteja, N. K., Shaikh, M. (2009). Hydraulic Modelling of the spatio-temporal flood inundation patterns of the Koondrook Perricoota Forest Wetlands - The Living Murray. 18th World IMACS / MODSIM Congress. Cairns, Australia.
- USGS (2007). "Synopsis of ADCP's and Their Use by the USGS Indiana District Office " <http://in.water.usgs.gov/hydroacoustics/ADCPuses.shtml>. Accessed the 28/05/2011.
- Wahba, G. (1990). Spline models for observational data. Philadelphia: SIAM.
- Werner, M. G. F. (2004). Spatial flood extent modeling - A performance based comparison, Delft University, Netherlands. Ph. D.
- Werner, M. G. F., Hunter, N., Bates, P. D. (2005). " Identifiability of distributed floodplain roughness values in flood extent estimation." Journal of Hydrology 314: 139-157.

Werner, M. G. F., Lambert, M.F. (2007). "Comparison of modelling approaches used in practical flood extent modelling." *Journal of Hydraulic Research* 45(2): 202-215.

Yang, X., Grönlund A., Tanzilli, S. (2002). "Predicting flood inundation and risk using geographic information system and hydrodynamic model." *The association of Chinese Professionals in Geographic Information Systems*.

Zinke, P., Olsen, N. R. B., Bogen, J. (2010). *Numerical Modeling of Water and Sediment Flow in a Delta with Natural Vegetation*. Norwegian University of Science and Technology, Department of Hydraulic and Environmental Engineering. Trondheim, NTNU. Ph.D.

# 11. Appendix

## 11.1 Project

To:	Nils Prieur			Drammensveien 211
From:	Péter Borsányi	NVE	HV	P.O. Box 5091 Majorstua
Responsible:				N-0301 OSLO
Date:	09.09.2010			NORWAY
Our ref.:	NVE			Telephone:+47 22 95 95 95
File no.:				Telefax:+47 22 95 90 00
Copy:	Lena Tallaksen UiO, inst for geofag			E-mail: nve@nve.no

**Student:** Nils Charles PRIEUR

**Supervisors:** Lena Tallaksen, Peter Borsanyi

**Project:** The study will contribute to the FoU research project “302H52 – Utvikling kompetanse og målemetodikk for flerdimensjonal hydraulisk modellering og flomsonekart revidering” run by NVE.

**Title:** Development of a 1D-2D coupled hydrodynamic model for upper Øyeren (Øyeren delta)

### Background

Lake Øyeren is a reservoir managed for hydropower use and for flood regulation. In addition, the so called “delta” is a nature protected area with important wildlife present. Øyeren is part of the Glomma river system in Eastern Norway which is the largest river in the country with a history of some demolishing floods.

The town of Lillestrøm lies on the northern shore of the lake and is exposed to flooding. The municipality has been busy constructing a number of dikes and protection measures which prevent the low-lying parts of the town from being flooded. The common (static) flood level maps were used in this work to identify the areas at risk and to design the elements of the flood protection measures.

It is however known, that the limited amount of data on flood measurements and topography resulted in a somewhat simplified modeling work behind the flood level maps. In the last years, increase of computational resources permits to observe hydrologic features in details. With the

evolution and emergence of fast and inexpensive personal computers, using 2D, 3D hydraulic models and coupled techniques is now a possibility.

It is therefore important to improve these results by using additional data and more complex methods to simulate water levels during floods in the delta area and especially around Lillestrøm.

## **Objectives**

The aim of this thesis is the development of a 1D-2D coupled hydrodynamic model for Øyeren Delta in order to improve quality of flood inundation map and elucidate the performance and potential limits of it.

Special focus should be:

- Calibration of the hydraulic model from limited available data, validation and quality analysis of results.
- Estimation and mapping of flooding areas for different type of scenarios and return periods (e.g. simultaneous extreme events for Glomma, Leira and Nittelva).
- Evaluate the uncertainty in the estimation by a model sensitivity analysis.

## **Data and Methods**

This thesis will be realised with the collaboration of NVE (Norges Vassdrags- og Energidirektorat) and UiO (University of Oslo).

The main focus will be the Øyeren delta which is the largest freshwater delta in Northern Europe (Zinke et al. 2010). Øyeren delta is situated at the meeting point of three rivers: Glomma, Leira and Nittelva.

Data have been collected prior to the start of the master thesis by NVE. This includes the use of ADCP (Acoustic Doppler Current Profiler) for measuring velocities, discharge and water levels in Øyeren delta. This field data collected during summer 2010 permit an up-to-date description of the bathymetry of the studied area. A DEM will be used for modeling the topography of the delta. As part of the master study a field visit will be organized during fall 2010, but the work does not include the collection of own data.

Water level and discharge are observed at different places around the delta and the rivers. Long streamflow and water level records are available from active gauging stations, earlier gauging stations and regulated sites. In addition, shorter historical records are available.

In this study the hydrodynamic characteristics of the delta are determined by calibrating the hydraulic module of the MIKE FLOOD modeling system to a minor flood event.

MIKE FLOOD is a hydraulic module of the Mike software family which has been developed by the Danish Hydraulic Institute. Mike by DHI is a powerful tool permitting study of water resources as rivers, groundwater, flood and sediments transports.

## **Questions**

The master's thesis should give an answer on the following questions:

- What are the discharge components, regulation levels, their variation and possible combinations in Lake Øyeren in various floods?
- Is it possible to describe the topography (including bathymetry) of the delta using the existing data?
- What grid structure, size and layout should be used and is reasonable for a 2D hydrodynamic model (MIKE 21) covering the delta area considering available computer capacity.
- How to create a MIKE FLOOD model incorporating the delta area in 2D and Glomma in 1D?
- Is it possible to run any combination of flow/regulation scenarios for this model? What are the limitations?

## **Structure**

The final work should fulfill the requirements of a professional scientific work. Therefore it is important to have a clear structure where the chapters can be easily distinguished from each other by their content. At least the following parts should be distinguished in the work:

- contents, list of figures, list of tables
- abstract
- introduction
- background
- methods and models
- results, analysis and discussion
- conclusions
- references

## **Delivery**

In addition to the paper/print version it is necessary to deliver the work in PDF and the files used by the model (input, output and result files) on a CD or memory stick. It can be assumed the target groups of readers are professionals with some knowledge of numerical modeling in the field of hydrology and hydraulics. The work should be written in English. This text should also be included in the work as it will be used as starting point for evaluation.

## 11.2 ADCP measurements

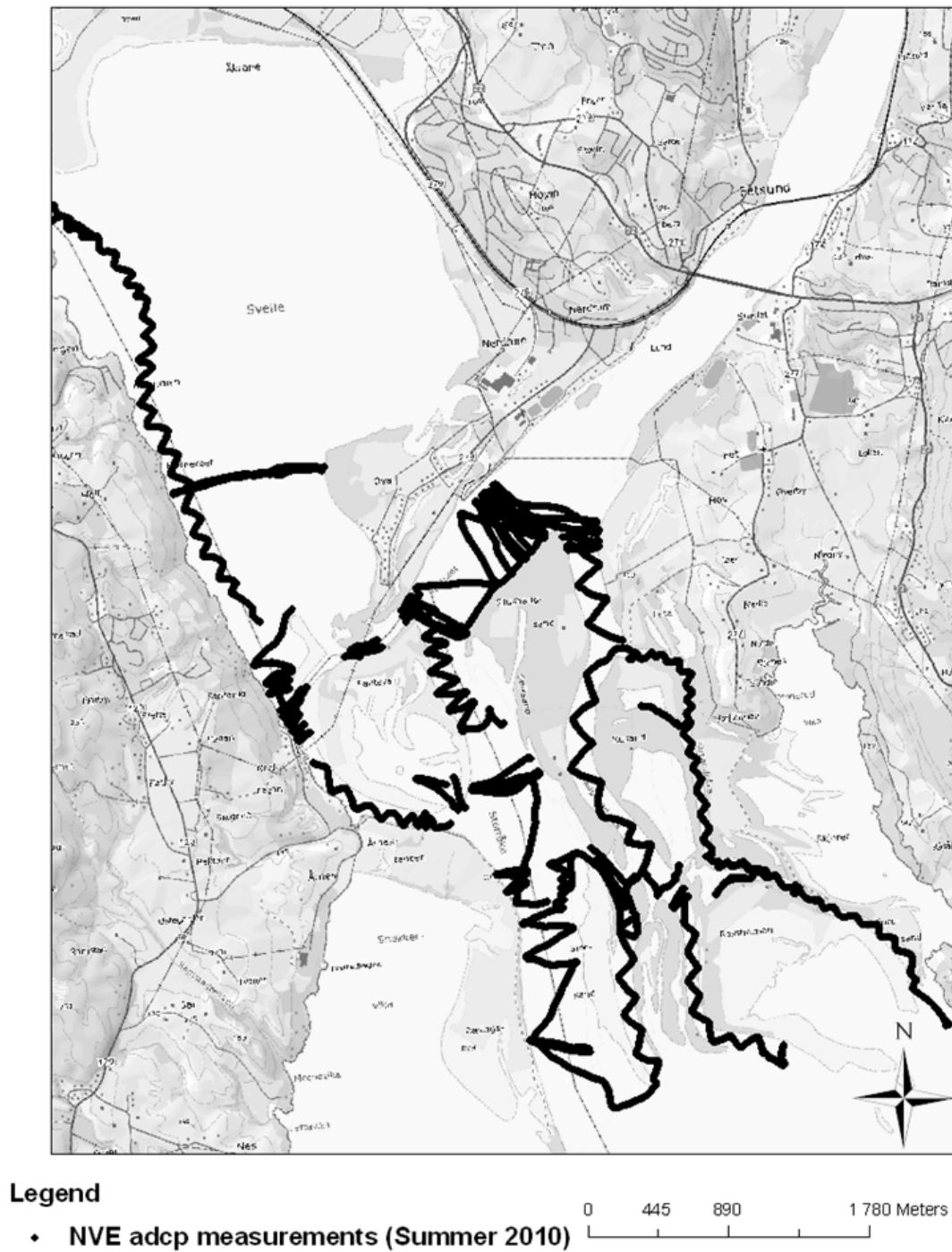


Figure 38. Overview of collected ADCP measurements during the fieldwork conducted by NVE in 2010; Source: Statkart.no (background map).

### 11.3 Flood zone map

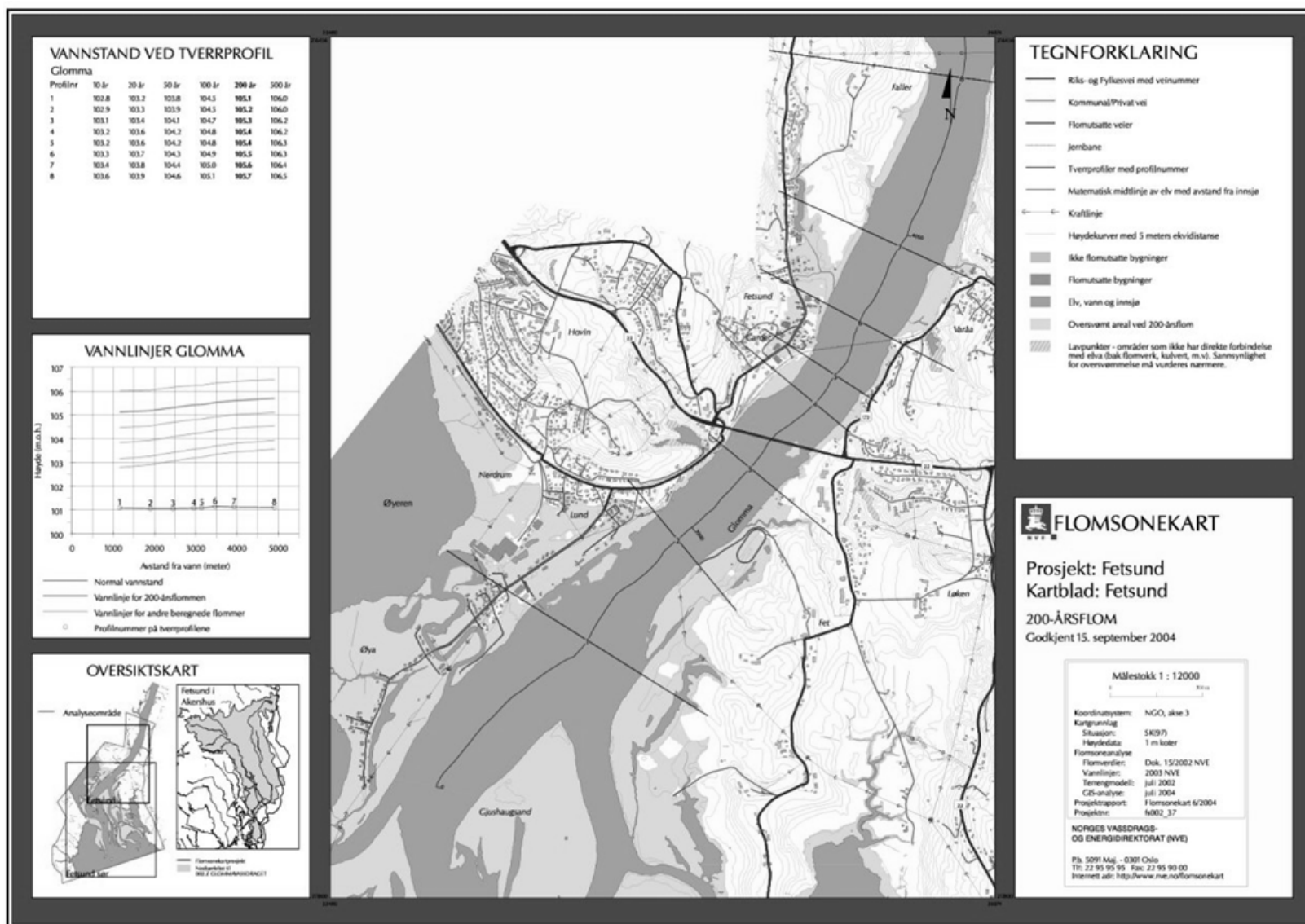


Figure 39. Flood zone map at Fetsund, the gray color corresponds to the 200-year return period inundated area.



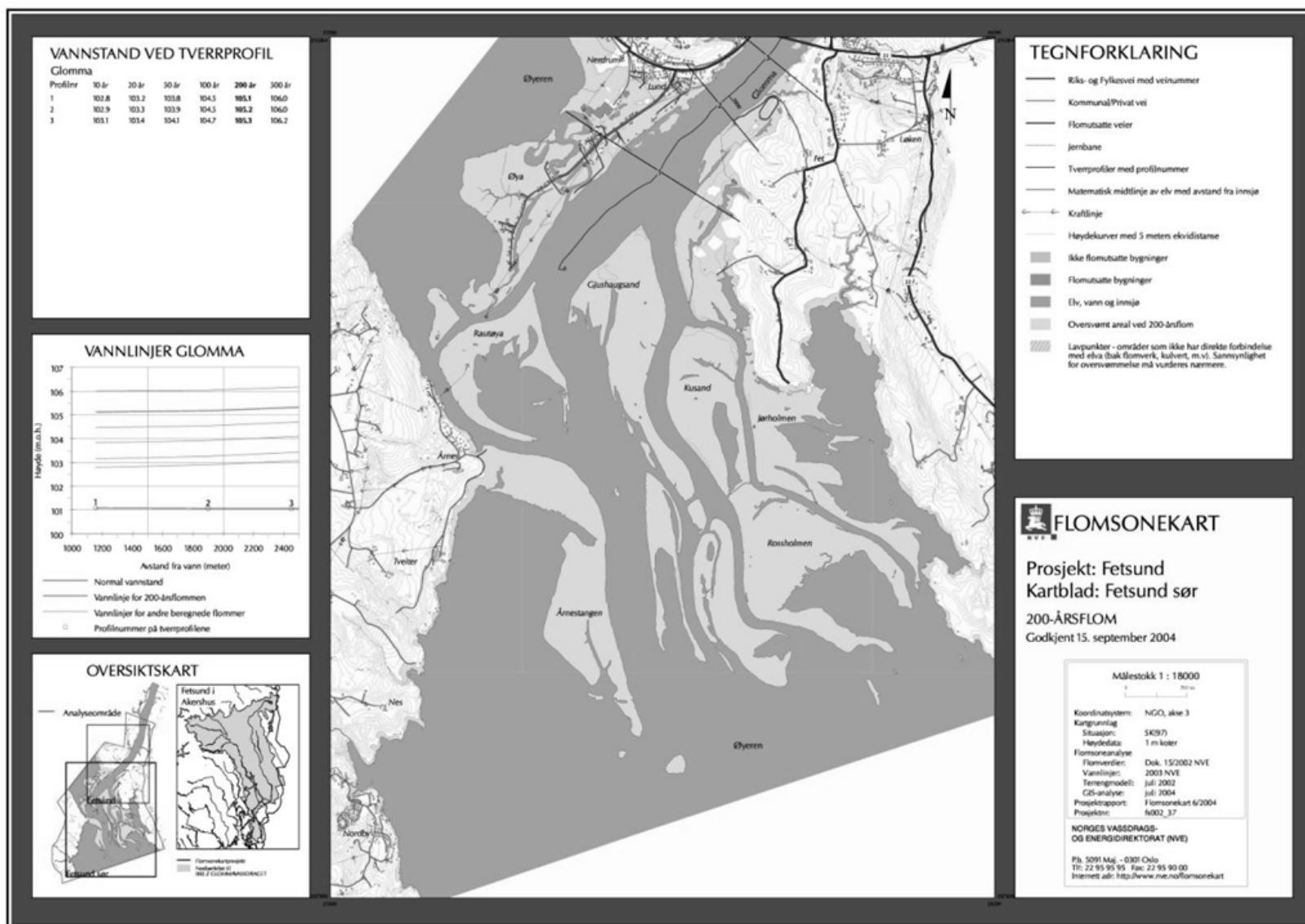


Figure 40. Flood zone map at Øyeren delta, the gray color corresponds to the 200-year return period inundated area.

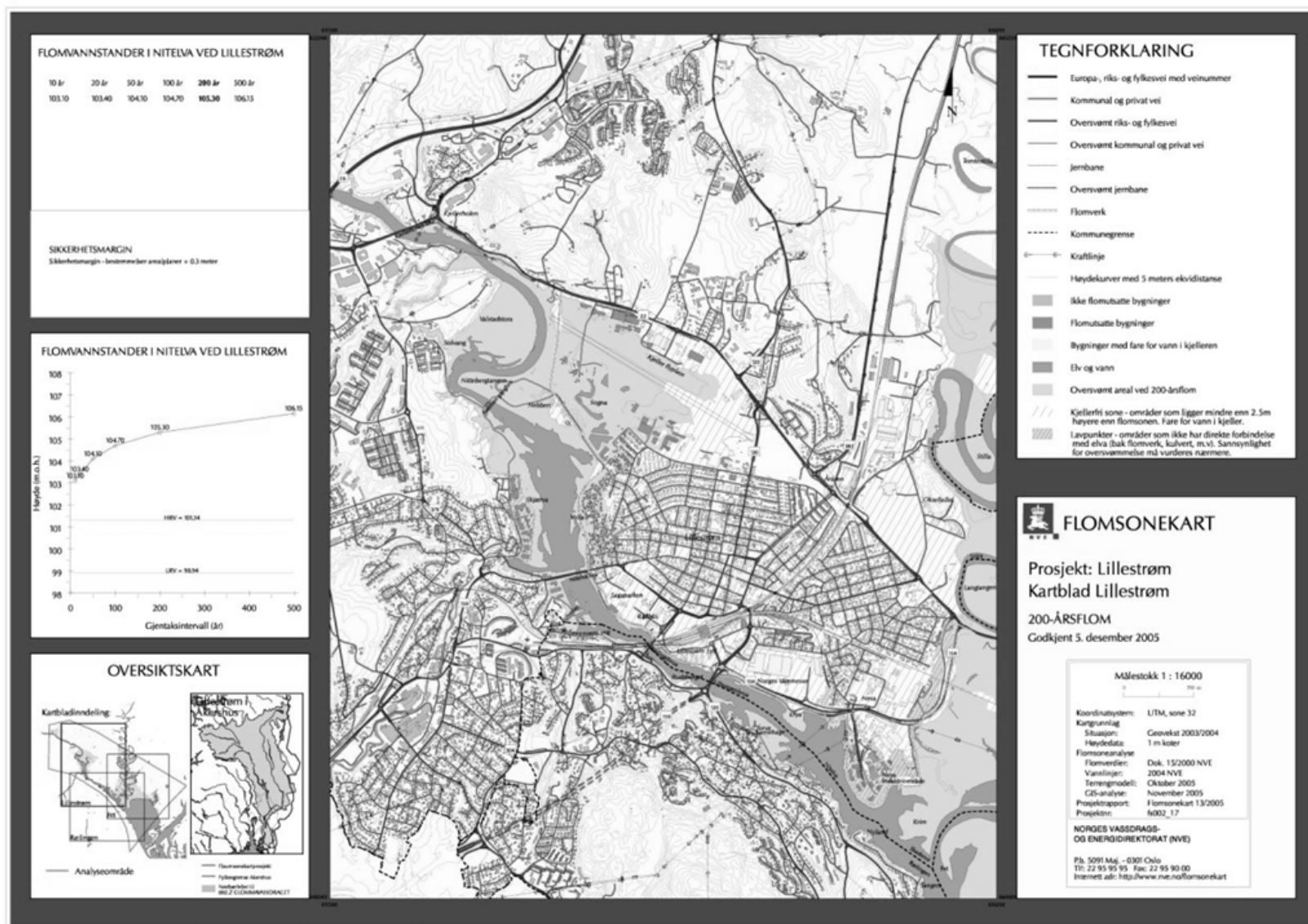


Figure 41. Flood zone map at Lillestrøm, the gray color corresponds to the 200-year return period inundated area.



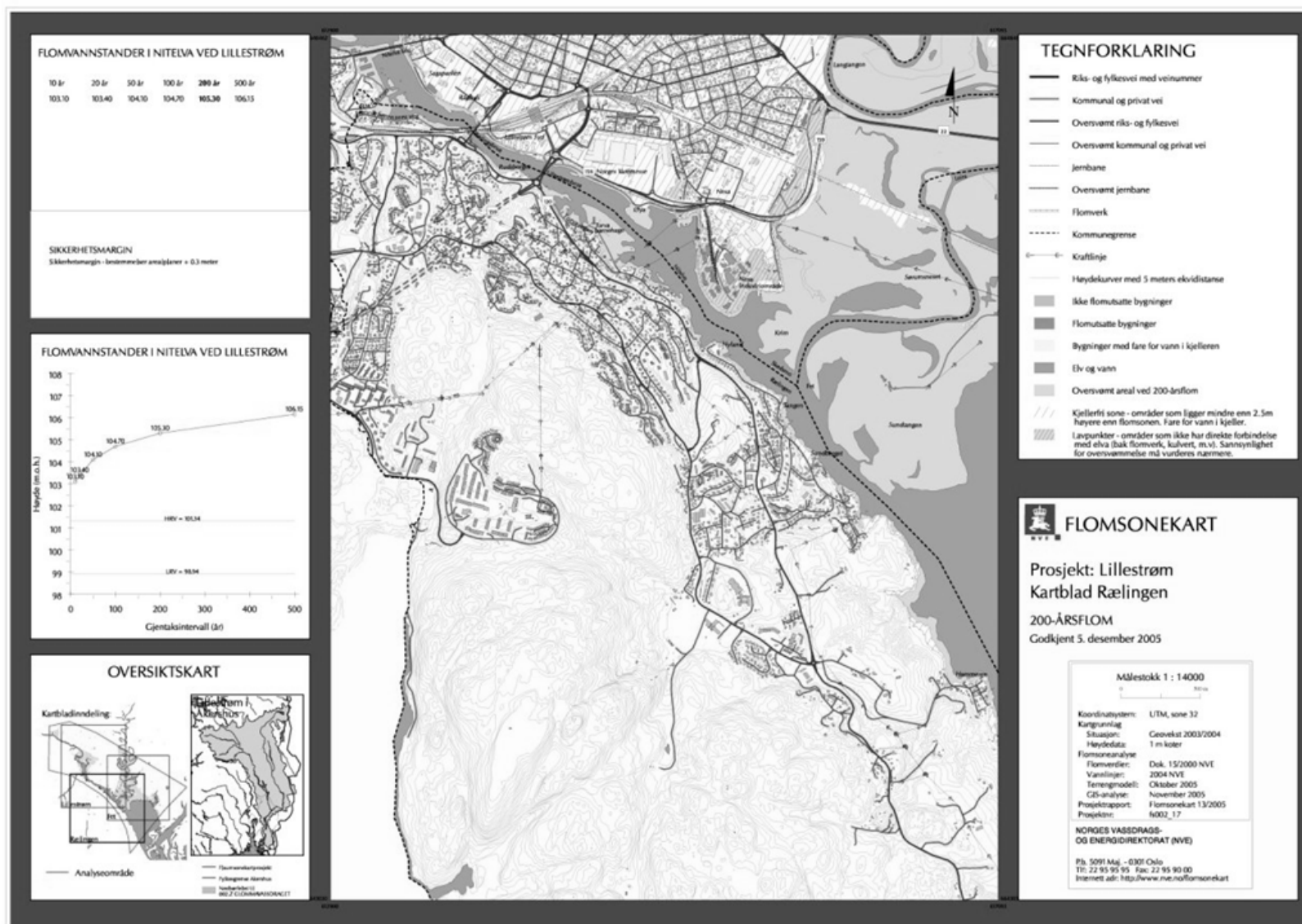


Figure 43. Flood zone map at the meeting point of Leira and Nittelva, the gray color corresponds to the 200-year return period inundated area.

